Stress-dependent Deformations of Concrete using Porous Aggregates

Jóhann Albert Harðarson

Thesis of 60 ECTS credits
Master of Science in Civil Engineering with Specialization in Structural Design and Concrete Technology

January 2015

Stress-dependent Deformations of Concrete using Porous Aggregates

Jóhann Albert Harðarson

Thesis of 60 ECTS credits submitted to the School of Science and Engineering
at Reykjavík University in partial fulfillment
of the requirements for the degree of
Master of Science in Civil Engineering with
Specialization in Structural Design and Concrete Technology

January 2015

Supervisor:

Ólafur H. Wallevik
Professor, Reykjavik University, Iceland

Examiner:

Guðni Jónsson
Civil Engineer, EFLA engineering and consulting firm, Iceland.

Abstract

Stress-dependent deformations of concrete may induce excessive deflections at service loads, which can compromise the performance of a structure. Elastic shortening and the combined effects of creep and shrinkage strains of concrete also cause loss of prestress force applied to prestressed concrete member.

The knowledge of locally obtained materials, used in concrete manufacture, is necessary to effectively model structure's behaviour. Porous basalt rock is the primary source of concrete aggregates in Iceland. Design codes and mathematical models are based on experiments and experience using specific raw materials, not necessarily applying globally. It is therefore essential to validate codes and models to assess their applicability. This thesis is intended to contribute to better understanding of material properties using Icelandic raw minerals.

The focus of the thesis is on the mechanical properties, elastic modulus and creep, and includes: An experiment, using several concrete mixes made from different combination of porous and non-porous aggregates. The elastic modulus was measured and compared with literature and design codes. Numerical evaluations for experimental concrete creep data, made of porous and non-porous aggregates, were carried out, as well as a case study, comparing deflection calculations and prestress losses, using valid codes and calculations based on experimental data.

The results indicate substantial discrepancies in measured elastic modulus for concrete made from limestone aggregates, compared to estimates based on mean concrete cylinder strength according to Eurocode 2 (EC2). A fairly good correlation can be seen between aggregate porosity and elastic modulus of concrete when using basalt aggregate. Experimental results show that the elastic modulus drops well below the EC2 values, using correction factors from Icelandic National Annex to EC2, if the porosity is excessive. Concrete containing porous basalt aggregate shows greater creep than concrete with granite aggregate. Concrete specimens with porous basalt aggregate are still deforming after twelve years under load. The concrete containing basalt aggregates appears to increase its rate of creep after few months. Environmentally friendly self-compacting concrete mixes, containing less cement but higher water-binder ratio, shows greater creep than conventional self-compacting concrete. Addition of air entraining admixture was shown to have limited effect on the specific creep of environmentally friendly self-compacting concrete mixes. Higher cement content, while maintaining constant water-cement ratio, is likely to increase creep-strain. Findings also indicate that concrete with porous basalt aggregate exhibits greater creep than predicted by well accepted mathematical models. A case study, for a post tensioned highway bridge, shows some 10% increase in initial prestress force losses when using experimental results for concrete with porous aggregate, compared to values predicted by EC2. A case study for a slab shows up to 10.3% increase in deflection using experimental results for concrete with porous aggregate, compared to values from EC2.

Keywords: concrete; material science; structural design; elastic modulus; creep; deflections.

Ágrip

Titill á íslensku: Álagsháðar formbreytingar steinsteypu með gleypnum fylliefnum.

Álagsháðar formbreytingar steinsteypu geta valdið óhóflegri svignun í notmarkaástandi sem geta rýrt notagildi mannvirkis. Stytting á fjaðursviði steinsteypu sem og áhrif skriðs og rýrnunar valda einnig spennutapi í forspenntum mannvirkjum.

Þekking á staðbundnu efni er nauðsynleg til að útbúa nothæf reiknimódel. Gleypið ferskt basalt er það fylliefni sem helst er notað við steypuframleiðslu á Íslandi. Hönnunarstaðlar og stærðfræðilíkön eru byggð á rannsóknum og reynslu með tiltekin hráefni í huga og eru ekki nauðsynlega algild. Það er því nauðsynlegt að staðfesta niðurstöður staðla og líkana. Þessu verkefni er ætlað að bæta þekkinguna á efnisfræði steinsteypu með tilliti til íslenskra hráefna.

Aðaláhersla verkefnisins er á efnisfræðiþætti eins og fjaðurstuðul og skrið, og inniheldur: Tilraun með fjölda ólíkra steypublandna, bæði með þéttum og gleypnum fylliefnum. Fjaðurstuðull var mældur og borinn saman við gagnreynda þekkingu og hönnunarstaðla. Samanburð á niðurstöðum skriðmælinga í steinsteypu með þéttum og gleypnum fylliefnum, við gagnreynda þekkingu og staðla. Einnig var gerð tilviksrannsókn, þar sem skoðuð var niðurbeygja og tap í forspennukrafti miðað við hönnunarstaðla og niðurstöður skriðmælinga.

Niðurstöður benda til misræmis á mældum fjaðurstuðli í steinsteypu með fylliefnum úr kalksteini í samanburði við evrópsku þolhönnunarstaðlana, byggðum á meðalþrýstistyrk steinsteypu. Góð fylgni er á milli holrýmd fylliefna og fjaðurstuðuls ef notað er gleypið ferskt basalt. Niðurstöður sýna misræmi á mældum fjaðurstuðli í samanburði við evrópsku þolhönnunarstaðlana, þótt notuð séu lækkunarákvæði úr þjóðarskjali við staðalinn, ef fylliefnin eru áberandi gleypin. Steinsteypa með gleypnu basalti skríður mun meira en steinsteypa með granít fylliefnum. Steinsteypa með gleypnum basalt fylliefnum skríður enn eftir að hafa verið undir álagi í tólf ár. Steinsteypa með gleypnu basalti virðist auka skriðhraða sinn eftir nokkra mánuði. Vistvæn sjálfútleggjandi steinsteypa (Eco-SCC), með skertu sementsmagni og hærra hlutfalli vatns og bindiefnis, skríður meira en hefðbundin sjálfútleggjandi steinsteypa. Loftblendi í vistvænni sjálfútleggjandi steinsteypu (Eco-SCC) hefur takmörkuð áhrif á skrið. Aukið sementsmagn, ef haldið er sama hlutfalli vatns og sements, veldur líklega auknu skriði. Steinsteypa með gleypnum basalt fylliefnum skríður mun meira en reiknilíkön úr hönnunarstöðlum, þar á meðal þeim evrópsku, gefa til kynna. Samanburðarrannsókn á eftirspenntri þjóðvegabrú sýnir 10% aukningu á eftirspennutapi ef notaðar eru niðurstöður mælinga í samanburði við gildi fengin úr evrópska þolhönnunarstaðlinum. Samanburðarrannsókn á slakbentri plötu sýnir um allt að 10.3% meiri svignun ef notaðar eru niðurstöður mælinga í samanburði við gildi fengin úr evrópska þolhönnunarstaðlinum.

Lykilorð: steinsteypa, efnisfræði, burðarþolsfræði, fjaðurstuðull, skrið, formbreytingar.

Stress-dependent Deformations of Concrete using Porous Aggregates

Jóhann Albert Harðarson

60 ECTS thesis submitted to the School of Science and Engineering
at Reykjavík University in partial fulfillment
of the requirements for the degree of
Master of Science in Civil Engineering with
Specialization in Structural Design and Concrete Technology.

January 2015

Student: Jóhann A. Harðarson
Jóhann Albert Harðarson

Supervisor: Ólafur H. Wallevik
Ólafur H. Wallevik

Examiner: Guðni Jónsson
Guðni Jónsson

DEDICATION

To Jóhanna K. Steinsdóttir, for her love and endurance over the years,
which made the writing of this thesis a reality.

Acknowledgements

This project was partially funded by the Concrete Commission in Iceland (Steinsteypunefnd).

The results presented in this thesis are based, in part, on measurements done by Guðni Jónsson, Pálmi Þór Sævarsson, Florian V. Mueller, Jón Guðni Guðmundsson and other researchers at Innovation Center Iceland (ICI). Some laboratory work was done by, and in cooperation with, personal at ICI, in particular Þórður I. Kristjánsson who also designed the concrete for the E-modulus measurements.

I would like to thank ICI for providing me with facilities. The staff at ICI has my appreciation for invaluable assistance and fellowship. Björn Hjartarson, Ófeigur Freysson, Þórður I. Kristjánsson, to name but a few. Helgi Hauksson, a former researcher at ICI, has my thanks for the assistance in creep-strain measurements.

My sister Edda Hrund Harðardóttir and Ásbjörn Jóhannesson, civil engineer at ICI, have my appreciation for proofreading the thesis.

This thesis is inspired by teachers and lecturers at Reykjavik University: Snjólaug Steinarsdóttir and Daníel Viðarsson, preliminary study teachers; Guðbrandur Steinþórsson, emeritus docent; Haraldur Auðunsson, docent; Torfi G. Sigurðsson, part-time lecturer and last but not least my supervisor, Professor Ólafur H. Wallevik.

I would also like to thank fellow students at Reykjavik University for making the past years pleasurable. Ágúst Rúnar Elvarsson, Guðjón Rafnsson, Guðmundur Ingi Hinriksson, Stefán Short, Valgeir Ó. Flosason, Þorsteinn Eggertsson, among others.

Finally, a man without a family is like a bird without wings. To my wife, three sons, daughter and unborn child. Thanks for everything.

Preface

Concrete is used extensively worldwide and has been the main building material in Iceland for decades. Since its redevelopment in the early 19th century [1], there have been gradual advances in concrete technology. The introduction of concrete to Iceland has often been a costly journey. Icelandic concrete has been susceptible to alkali-silica reaction as well as having inadequate frost resistance [2]. More recently there have been reports of excessive deformation in slabs and beams. These costly flaws are due to insufficient knowledge of locally quarried materials and improper implementations of good practices.

My interest in the area of concrete deformation is from BSc courses such as material science and reinforced concrete design. The lecturers kept stating the different behaviour of Icelandic concrete compared to textbooks and codes. I was taught to be conservative in design with respect to Icelandic concrete and recognize the uncertainties in parameters such as elastic modulus, creep, shrinkage and tensile strength.

When Ólafur Wallevik suggested a thesis on deformations of concrete using porous aggregates I immediately became interested. It is my hope that the thesis will contribute to better understanding of concrete material properties using Icelandic raw minerals.

Jóhann Albert Harðarson
Reykjavík, January 2015

Contents

Abstract i
Ágrip ii
Acknowledgements v
Preface vi
List of Tables ix
List of Figures x
List of Symbols xii
List of Abbreviations xv
1 Introduction 1
1.1 Background 1
1.2 Problem Statement 1
1.3 Aim and Objectives 1
1.4 Research Methodology 2
1.5 Outline of the Work 3
2 Literature Review 5
2.1 Elastic Modulus of Concrete 5
2.2 Factors Affecting the Elastic Modulus of Concrete 10
2.3 Shrinkage and Swelling of Concrete 11
2.4 Creep of Concrete 12
2.5 Factors Affecting Concrete Creep 14
2.6 Physical Mechanism of Concrete Creep 15
2.7 The Effects of Concrete Creep 17
2.8 Icelandic Aggregates 18
2.9 Rheological Modelling of Concrete Creep 20
2.10 Eurocode Modelling of Concrete Creep 21
2.11 The fib Model Code 2010 and Concrete Creep 24
2.12 Model B3 and Concrete Creep 24
2.13 ACI 209 Model and Concrete Creep 26
3 Methods 27
3.1 Aggregate Parameters 27
3.2 Parameters of Fresh Concrete 28
3.3 Parameters of Hardened Concrete 30
3.4 Deflection Calculations 32
3.5 Prestress Losses 34
4 Materials 36
4.1 Phase I 36
4.2 Phase II 38
5 Results and Discussion 41

5.1 Phase I 41
5.2 Phase II 44
5.2.1 Elastic Modulus 44
5.2.2 Experimental Results of Creep 46
5.2.3 Comparison between Models and Test Data 58
5.3 Phase III 63
5.3.1 Deflection Calculations 63
5.3.2 Prestress Losses 65
6 Conclusions and Final Remarks 68
6.1 Main Findings 68
6.2 Recommendations for Further Research 69
References 70
Appendix A 74
Appendix B 78
B.1. Obtaining the Final Value of Creep Coefficient According to EC2 78
B.2. Derivation of Equation (2.20) 79
B.3. Derivation of Equation (3.3) 80
B.4. Derivation of K for Simply Supported Beam 81
B.5. Area Moment of Inertia for Bridge Beam 82
Appendix C 83
C.1. MatLab Function that Calculates the Creep Coefficient According to EC2 83
C.2. MatLab Function that Calculates the Creep Coefficient According to fib MC 10 85
C.3. MatLab Function that Calculates the Creep Comp. According to Model B3 87
C.4. MatLab Function, Approximating the Value for $Q(t,t_0)$, Needed for Model B3 89
C.5. MatLab Function that Calculates the Creep Coefficient According to ACI 209 90
Appendix D 92
D.1. Parameters used in the EC2 creep model 92
D.2. Parameters used in the fib MC 10 creep model 93
D.3. Parameters used in the B3 creep model 94
D.4. Parameters used in the ACI 209 creep model 95
Appendix E 96
E.1. Calibration of Strain Gauge 96
E.2. Construction details for post tensioned bridge 97

List of Tables

Table 2-1: Effect of type of aggregates on the modulus of elasticity 9
Table 4-1: Aggregate parameters according to equations 36
Table 4-2: Parameters of fresh concrete, measured prior to casting. 37
Table 4-3: Aggregate parameters 38
Table 4-4: Various measured fresh concrete parameters 39
Table 4-5: Various measured fresh concrete parameters 39
Table 4-6: Various measured fresh concrete parameters 39
Table 4-7: Various measured fresh concrete parameters 40
Table 5-1: Measured parameters of hardened concrete 41
Table 5-2: Evaluated E-modulus values and comparison to fib MC 10 and EC2 models. 45
Table 5-3: Estimated losses of initial prestress force, based on EC2 and INA. 66
Table 5-4: Estimated losses of initial prestress force 67
Table 5-5: Estimated losses of initial prestress force 67
Table B-1: Area Moment of Inertia for Bridge Beam. 82
Table D-1: Parameters used in the EC2 creep model. 92
Table D-2: Parameters used in the fib MC 10 creep model. 93
Table D-3: Parameters used in the B3 creep model. 94
Table D-4: Parameters used in the ACI 209 creep model. 95

List of Figures

Figure 2-1: Propagation of cracks in the transition zone with increased strain. 7
Figure 2-2: Common approaches for evaluation of E-modulus of concrete. 8
Figure 2-3: Secant modulus from Eurocode 2 (EN 1992-1-1:2004). 8
Figure 2-4: Definition of different modulus of elasticity 9
Figure 2-5: Stress-strain curves for compression tests on 150 x 300-mm (6 x 12-in.) 10
Figure 2-6: Constant stress applied at time t_0 13
Figure 2-7: The propagation of strain as a function of time 13
Figure 2-8: Proportional effects of creep and shrinkage of concrete 14
Figure 2-9: Creep and creep recovery of concrete 14
Figure 2-10: Effect of E-modulus of aggregate on relative creep of concrete 15
Figure 2-11: Influence of age at application of load on creep of concrete 15
Figure 2-12: Hydration of pure clinkers as a function of time 17
Figure 2-13: Porous Icelandic aggregate 18
Figure 2-14: Non-porous Icelandic aggregate 18
Figure 2-15: Moisture conditions of aggregate 19
Figure 2-16: Effect of mineralogical character of aggregates on creep 19
Figure 2-17: Some existing rheological models 21
Figure 2-18: Schematic representation of the creep 22
Figure 2-19: Schematic approach to obtain the final creep coefficient 23
Figure 3-1: Schematic representation of EN 1097-6 28
Figure 3-2: Saturated aggregate element 28
Figure 3-3: Deformation of a fluid element 29
Figure 3-4: Flow curve for Newtonian and Bingham fluids 29
Figure 3-5: A strain gauge and equipments to measure creep. 30
Figure 3-6: Spring-loaded creep frame 30
Figure 3-7: Screenshot of a program that logs measurements. 31
Figure 3-8: Satisfactory failure of cylinder specimen 31
Figure 3-9: Stress behaviour in uncracked and cracked beam 33
Figure 3-10: Side view of the highway bridge. 34
Figure 3-11: Load on bridge structure (cross-sectional view) 35
Figure 4-1: Cumulative particle size distribution of mixes containing various aggregates. 37
Figure 4-2: Arbitrary photo of specimens from phase I. 37
Figure 4-3: Arbitrary photo of specimens from phase I. 37
Figure 4-4: Arbitrary photo of creep rig specimens. 40
Figure 4-5: Arbitrary photo of creep rig specimens. 40
Figure 5-1: E-modulus of concrete as a function of aggregate porosity 42
Figure 5-2: E-modulus of concrete, samples containing basalt aggregates 43
Figure 5-3: Mean value of concrete cylinder compressive strength, with basalt aggregates 44
Figure 5-4: Creep compliance for the CVC_1 specimens from 2009 47
Figure 5-5: Specific creep for the CVC_1 specimens from 2009 48

Figure 5-6: Creep compliance for the CVC_2 specimens from 2002 48
Figure 5-7: Specific creep for the CVC_2 specimens from 2002 49
Figure 5-8: Creep compliance for the CVC_3 specimens from 2002 50
Figure 5-9: Specific creep for the CVC_3 specimens from 2002 50
Figure 5-10: Creep compliance for the CVC_4 specimens from 2002 51
Figure 5-11: Specific creep for the CVC_4 specimens from 2002 52
Figure 5-12: Specific creep for CVC_2, CVC_3 and CVC_4 specimens from 2002 53
Figure 5-13: Specific creep for CVC_2, CVC_3 and CVC_4 specimens from 2002 53
Figure 5-14: Specific creep for SCC specimens from 2010 54
Figure 5-15: Creep compliance for specimens from 2004 55
Figure 5-16: Specific creep for specimens from 2004 56
Figure 5-17: Effect of mineralogical character of aggregates on creep 57
Figure 5-18: Measured creep coefficient for the CVC_1 specimens from 2009 58
Figure 5-19: Measured creep coefficient for the CVC_1 specimens from 2009 59
Figure 5-20: Measured creep coefficient for the CVC_1 specimens from 2009 60
Figure 5-21: Measured creep coefficient for the CVC_2 specimens from 2002 60
Figure 5-22: Measured creep coefficient for the CVC_2 specimens from 2002 61
Figure 5-23: Measured creep coefficient for the CVC_4 specimens from 2002 62
Figure 5-24: Measured creep coefficient for the CVC_4 specimens from 2002 62
Figure 5-25: Deflection calculations based on material properties 63
Figure 5-26: Deflection calculations based on the creep compliance 64
Figure 5-27: Deflection calculations based on the creep compliance 65
Figure B-1: Saturated aggregate element (SSD) with total volume equal to 1 80
Figure B-2: Simply supported beam 81
Figure B-3: Bridge Beam. 82
Figure E-1: Construction details at mid-span for post tensioned bridge. 97
Figure E-2: Construction details at mid-span for post tensioned bridge. 97

List of Symbols

Roman upper case letters

A	Cross-sectional area
A_c	Cross-sectional area of concrete
A_s	Cross-sectional area of tension reinforcement
A'_s	Cross-sectional area of compression reinforcement
A_p	Cross-sectional area of tendon
$C(t, t_0)$	Specific creep
E	Modulus of elasticity
E_c	Modulus of elasticity of concrete
E_c	Secant modulus of elasticity of concrete
$E_{c(28)}$	Tangent modulus of elasticity of concrete at a stress of $\sigma_c = 0$ and at 28 days
E_{cd}	Design value of modulus of elasticity of concrete
$E_{c,eff}$	Effective modulus of elasticity calculated using creep coefficient
E_{cm}	Secant modulus of elasticity of concrete
E_{ci}	Initial tangent modulus
E_i	Modulus of elasticity of relevant component
E_s	Modulus of elasticity of steel
E_0	Modulus of modulus of solid material
F	Force
I	Area moment of inertia
I_c	Area moment of inertia for cracked condition
I_u	Area moment of inertia for uncracked condition
$J(t, t_0)$	Creep function or creep compliance
L	Length
ΔL	Elongation
M	Bending moment
M_{cr}	Cracking bending moment
M_{rare}	Design value of bending moment (Rare)
M_{QP}	Design value of bending moment (Quasi-permanent)
P_0	Initial prestress force
RH	Relative humidity
S_c	First moment of area for cracked condition
S_u	First moment of area for uncracked condition

Roman lower case letters

a/c	Aggregate-cement ratio, by mass
c	Cement content of concrete
c_i	Volume percent of component

d	Effective depth of tension reinforcement
d'	Depth to compression reinforcement
e_{av}	Average eccentricity of post-stress tendon
f	Parameter dependent on the grain morphology and pore geometry
f_c	Compressive strength of concrete
$f_c{}'$	Specified compressive strength of concrete
$\overline{f}_c$	Mean value of 28th day cylinder compressive strength
f_{ck}	Characteristic cylinder strength of concrete at 28 days
f_{cm}	Mean value of concrete cylinder compressive strength
$f_{cm}(t_0)$	Mean value of concrete cylinder compressive strength at the time of loading
f_{ctk}	Characteristic axial tensile strength
h	Thickness of slab
h_0	Notional size
k	Wobble factor
k_h	Coefficient depending on the notional size h_0
r	Radius
p	Porosity
p_0	Porosity at which the E-modulus becomes zero
r	Radius
t	Time being considered
t_d	The age of concrete when drying begins
t_0	The age of concrete at the time of loading
u	Parameter of that part of the concrete cross-section which is exposed to drying
w	Water content of concrete
w/c	Water-cement ratio, by mass

Greek letters

α	Angle
α	Deformation parameter
α_e	Modular ratio
α_E	Aggregate coefficient
α_i	Ratio of secant modulus divided by initial tangent modulus
$\alpha_{I,II}$	Uncracked and fully cracked parameters
$\alpha_{1,2,3}$	Coefficients to consider the influence of the concrete strength
β	Parameter for the influence of the duration of loading
$\beta(f_{cm})$	Factor for the effect of concrete strength on the notional creep coefficient (ϕ_0)
$\beta(t_0)$	Factor for the effect of concrete age at loading on the notional creep coeff. (ϕ_0)
$\beta_c(t,t_0)$	Coefficient to describe the development of creep with time after loading
γ_{cE}	Partial factor for modulus of elasticity of concrete
γ_c	Correction factor for creep coefficient if conditions are other than standard
δ_{rare}	Elastic deflection

δ_{tot}	Total deflection
δ_{QP}	Deflection due to creep and shrinkage
ε	Strain
ε_c	Compressive strain in the concrete
ε_{ca}	Autogenous shrinkage strain
ε_{cc}	Compressive strain in the concrete due to creep
ε_{cd}	Drying shrinkage strain
ε_{ci}	Compressive strain in the concrete, initial elastic strain
$\varepsilon_{c\sigma}$	Compressive strain in the concrete, stress-dependent
ε_{c1}	Compressive strain in the concrete at peak stress f_c
ε_{cu1}	Ultimate compressive strain in the concrete
ε_{ca}	Total shrinkage strain
ε_t	Strain at time (t)
ε_0	Initial strain at the time of loading
ζ	Distribution coefficient
ζ_{max}	Maximum distribution coefficient
ζ_{rare}	Distribution coefficient based on total SLS loading
ζ_{QP}	Distribution coefficient based on quasi permanent loading
θ	Angle
μ	Coefficient of friction
σ	Stress
σ_c	Compressive stress in concrete
σ_0	Initial stress at the time of loading
ϕ	Creep coefficient
ϕ_0	Notional creep coefficient
ϕ_{RH}	Factor for the effect of relative humidity on the notional creep coefficient (ϕ_0)
$\phi(t, t_0)$	Creep coefficient, defining creep between times t and t_0
$\phi(\infty, t_0)$	Final value of creep coefficient
$\phi_{bc}(t, t_0)$	Basic creep coefficient
$\phi_{dc}(t, t_0)$	Drying creep coefficient
$\phi_k(\infty, t_0)$	Non-linear final creep coefficient
ϕ_u	Ultimate (final) creep coefficient

List of Abbreviations

ACI	American Concrete Institute
AEA	Air entraining admixture
ASTM	American Society for Testing and Materials
CVC	Conventional vibrated concrete
C-S-H	Calcium-Silicate-Hydrate
EC2	Eurocode 2
EU	European Union
fib	Fédération internationale du béton
ICI	Innovation Center Iceland
INA	Icelandic National Annexes to Eurocodes
MC	Moisture content
MC 10	Model Code 2010
OPC	Ordinary portland cement
SCC	Self-compacting concrete
SCMs	Supplementary cementitious materials
SLS	Service limit state
SSD	Saturated surface dry
TZ	Transition zone
UAE	United Arab Emirates

1 Introduction

1.1 Background

This thesis, which is within the field of material science and structural design, focuses on the material properties of structural concrete with porous aggregate. The main focus is set on the mechanical properties, elastic modulus and creep. Other material properties, such as shrinkage, will be addressed but mainly to clarify and differentiate where the material properties are related.

Design codes and mathematical models are based on experiments and experience using specific raw materials, not necessarily applying globally. It is therefore essential to validate codes and models to assess their applicability. This thesis is intended to contribute to better understanding of material properties using Icelandic concrete aggregates.

1.2 Problem Statement

Stress-dependent deformations of concrete are often responsible for excessive deflections at service loads, which can compromise the performance of a structure. Elastic shortening and the combined effects of creep and shrinkage strains also cause loss of prestress force, applied to prestressed concrete member.

The knowledge of locally obtained materials, used in concrete manufacture, is necessary to effectively model structure's behaviour. Porous basalt rock is the primary source of concrete aggregate in Iceland and concrete made with Icelandic aggregate has been known to exhibit different characteristics.

1.3 Aim and Objectives

The research presented in this thesis is primarily intended to elucidate the effect of porosity in aggregates on the elastic modulus and creep of concrete.

The main objectives of the thesis are in three phases:

I. Study of the elastic modulus of concrete based on an experiment done in the summer of 2014 and presented at the XXII Nordic Concrete Research Symposium, 2014 in Reykjavik.
II. Numerical evaluation on creep experiments, based on available data from Innovation Center Iceland (ICI) and measurements done in the winter of 2014. Comparison of experimental data to codes and known mathematical models.
III. Comparison between deflection calculations and prestress losses, using applicable codes and calculations based on experimental data.

1.4 Research Methodology

Phase I of this thesis is the subject of pure research involving the mechanical properties of concrete. It is intended to elucidate the effect of porosity in aggregates on the elastic modulus of concrete and making comparisons between concrete containing: porous basalt, non-porous granite and limestone aggregate.

This part involves measurements on fresh and hardened concrete parameters. Concrete samples were mixed, casted and measured at ICI according to valid codes and common practices at ICI.

The experimental mechanical properties, i.e. compressive strength and elastic modulus, were discussed and compared with literature and valid design code.

Phase II of this thesis is a numerical evaluation of creep measurements. The aim is to elucidate the effect of porosity in aggregates on the creep of concrete and to make comparisons between concrete containing non-porous granite aggregate. Measurements were also compared to valid design codes, mathematical models, etc.

Innovation Center Iceland (ICI) has been researching creep of concrete from the beginning of the century. An impressive amount of test data has been accumulated over the years. The research methods used to evaluate creep are those proposed by the American Society of Testing and Materials (ASTM) [3].

The oldest creep specimens are from 2002 and contain conventional vibrated concrete (CVC). The specimens were designed to include three strength classes: C40/50, C60/75 and C70/85 and contain aggregates from three Icelandic aggregate suppliers. The characteristic strength of the mixes was however other than intended. The strength of the C40/50 concrete was higher and the strength of the C70/85 concrete was somewhat lower than intended.

In 2004 new specimens were casted. They were intended to elucidate the effect of volume percentage of cement on the creep of concrete. The specimens contain CVC and self-compacting concrete (SCC) with both non-porous granite and porous basalt aggregate. Unfortunately some material parameters have been lost over the years, affecting usage of the test data.

In 2009, specimens were casted containing: CVC, with characteristic strength as C25/30 and with both non-porous granite and porous basalt aggregate.

The newest creep specimens are from 2010 and contain SCC, with and without added air entraining admixture (AEA). The specimens include both conventional SCC and Eco-SCC, which contains less cement and supplementary cementitious materials (SCMs) than conventional SCC.

Phase III of this thesis is a case study, based on deflection calculations for a slab as well as for prestress losses in post-tensioned concrete bridge. It involves calculations in service limit state according to methods and material parameters from valid codes. Deflection and prestress losses are then compared to values obtained by using material parameters from phase I and II.

The deflection calculations relate to a roof slab on a residential house located in the Greater Reykjavík Area. The house is above 100 m elevation and therefore it has higher characteristic snow load than normal in Greater Reykjavík. The slab spans five meters and has additional gravel on top of an insulating layer.

The effects of using material parameters from EC2 instead of experimental results are shown in a case study. Prestress force losses for a post tensioned highway bridge are calculated using material parameters both form EC2 and experimental results. The bridge is a structure common on Icelandic highways. It has a 40.0 m single-span, is 9.0 m wide and located 30.0 m above sea level. The load on the bridge is based on EN 1991-2:2003: Actions on structures - Part 2: Traffic loads on bridges [4]. All calculations are based on EC2 in conjunction with the INA and Reinforced Concrete Design: to Eurocode 2 by W.H. Mosley, J.H. Bungey and R. Hulse [5].

1.5 Outline of the Work

The main body of the thesis comprises six thesis chapters and several chapter sections, with the addition of references and appendices. To maintain clarity, some chapters are split into phase I, II and III according to section 1.3.

The first chapter introduces the project of the thesis and clarifies the aim, objectives and outlines of the work.

Chapter two is a literature review of subjects related to deformations of concrete. It gives a brief overview of literature topics that are important in relation to the content of the thesis, including:

- Elastic Modulus of Concrete
- Factors Affecting the Elastic Modulus of Concrete
- Shrinkage and Swelling of Concrete
- Creep of Concrete
- Factors Affecting Concrete Creep
- Physical Mechanism of Concrete Creep
- The Effects of Concrete Creep
- Icelandic Aggregates
- Rheological Modelling of Concrete Creep
- Eurocode Modelling of Concrete Creep
- The fib Model Code 2010 and Concrete Creep
- Model B3 and Concrete Creep.
- ACI 209 Model and Concrete Creep

Chapter three describes the methodology in obtaining parameters needed for the evaluation of experimental data. Test methods for obtaining: aggregate parameter, parameters for fresh and hardened concrete as well as relevant codes are described in detail. The chapter also contains the methodology used in deflection calculations and prestress losses.

Chapter four gives an overview of the materials used in phase I and II. It also contains tabulated results of measured material parameters, particle size distribution graphs, etc.

Chapter five reports the main findings of the thesis and discusses the results. Since the results and discussion, between the various phases of the thesis, are interlinked; the results and discussion have been merged into one chapter. This has been done for clarity of result and for overall readability.

Chapter six summarizes the main findings of the thesis. It also reflects on unanswered questions that could be the subjects of further researches.

Appendix A contains an article published in the proceedings of the XXII Nordic Concrete Research Symposium, 2014 Reykjavik, Iceland, pp. 179-182.

Appendix B contains various calculations and derivation of equations.

Appendix C contains written MatLab functions used in various calculations.

Appendix D contains the parameters used for creep models.

Appendix E contains additional attachments in Icelandic, intended for clarification.

2 Literature Review

Any material that experiences stress will deform. The quantity of deformation is dependent on material properties. If the material is purely elastic, i.e. where Hook's law applies, the relationship between stress and strain is linear [6]. The slope of the linear relationship between stress and strain is known as elastic modulus (E-modulus).

Hook's law applies or is a good approximation for many structural materials, such as steel, assuming relatively small deformations. Concrete however exhibits a non-linear relationship between stress and strain. Furthermore it will also continue to deform under constant force, a phenomenon known as creep.

The relationship between stress and strain is, strictly speaking, a function of time [7]. For many structural materials, such as steel, the time-dependent influence is negligible and ignored in calculations. Since concrete creeps, i.e. deforms under constant force, it is not possible to ignore the effect of time. When calculating deformations, engineers often define a lowered E-modulus that takes the effect of creep into account. The advantages are that standard deflection equations still apply.

Creep is defined as the increase in strain under a sustained constant stress after taking into account other time-dependent deformations not associated with stress, such as shrinkage, swelling and thermal deformations [7]. To further describe creep, several parameters affecting creep of concrete need to be explained in details e.g. E-modulus of concrete and shrinkage of concrete.

2.1 Elastic Modulus of Concrete

Elastic modulus, often called Young's modulus after the English physicist Thomas Young, is a numerical constant that describes the elastic properties of a solid material undergoing strain in one direction [8]. Elastic modulus is a vital engineering tool and used in deflection calculations. It is best described by its mathematical definition of stress (σ) divided by strain (ε), or by equation (2.1)

$$E \overset{\text{def}}{=} \frac{\sigma}{\varepsilon} = \frac{F/A}{\Delta L/L}, \tag{2.1}$$

where E is the elastic modulus, F is the force exerted, A is the cross-sectional area through which the force is applied, ΔL is the elongation in direction of exerted force and L is the original length.

The elastic modulus (E-modulus) describes a linear relationship between stress and strain i.e. where Hook's law applies [6]. Hook's law applies to many structural materials, such as steel, assuming relatively small deformations. Concrete however exhibits a non-linear relationship between stress and strain. To simplify calculations engineers attempt to define E-modulus for concrete using various models.

Concrete is a composite material consisting of dispersed material and matrix material. The dispersed materials are aggregates (stone and sand) and the matrix material is a paste made from cement or supplementary cementitious materials.

Several well-known theories exist on the E-modulus of composite materials. In 1960 B. Paul wrote a paper predicting E-modulus of multiphase materials. He introduced an upper and lower bound based on the individual properties, seen in eq. (2.2)

$$\left(\sum_{i=1}^{n}\frac{c_i}{E_i}\right)^{-1} \leq E \leq \sum_{i=1}^{n} c_i E_i \;;\quad \sum_{i=1}^{n} c_i = 1\,, \tag{2.2}$$

where c_i is the volume percent of each component and E_i the relevant E-modulus of each component [9].

The derivation of equation (2.2) is based on the assumption that each material has a linear stress and strain relationship. More importantly that continuity of displacement is always maintained at the interface of the two materials. Recent studies show that concrete has an additional component, besides aggregate and paste. There is an interface or transition zone (TZ) between aggregates and paste. The influence of TZ on the elastic properties of concrete depends mainly on volume and modulus of elasticity of the TZ. The volume of TZ is related to the total aggregate surface or the interface surface [10].

The non-linear stress-strain relationship of concrete is likely an influence from the TZ. In normal strength concrete there is an initial nearly linear portion of deformation, lasting up to about 30–40% of the ultimate load. With increasing strain micro-cracks at the paste-aggregate interface or TZ begin to form. As the strain increases the cracks become larger and the E-modulus drops [11] (see Figure 2-1).

In practice, strain is measured at different stresses and empirical equations then fitted to results to obtain the E-modulus of the concrete. Since the stress-strain relationship for concrete is non-linear it is not obvious how to derive E-modulus.

Several approaches for calculating E-modulus are known (see Figure 2-2). An initial tangent modulus measures the tangent to the curve at the origin. It is also possible to find a tangent modulus at any point on the stress-strain curve, but this applies only to very small changes in load above or below the strain at which the tangent modulus is considered. Although rarely used it is possible to measure an unloading modulus. The most common definition of E-modulus is known as secant modulus. Secant modulus is usually measured at stress ranging from 15 to 50% of the peak stress. The secant modulus is dependent on the level of stress and the rate of application. The stress and time taken to apply the stress should always be stated [7].

In the Icelandic Building Regulation there is a clause that states, that a structural designer shall base his calculations on the Eurocode design standards [12].

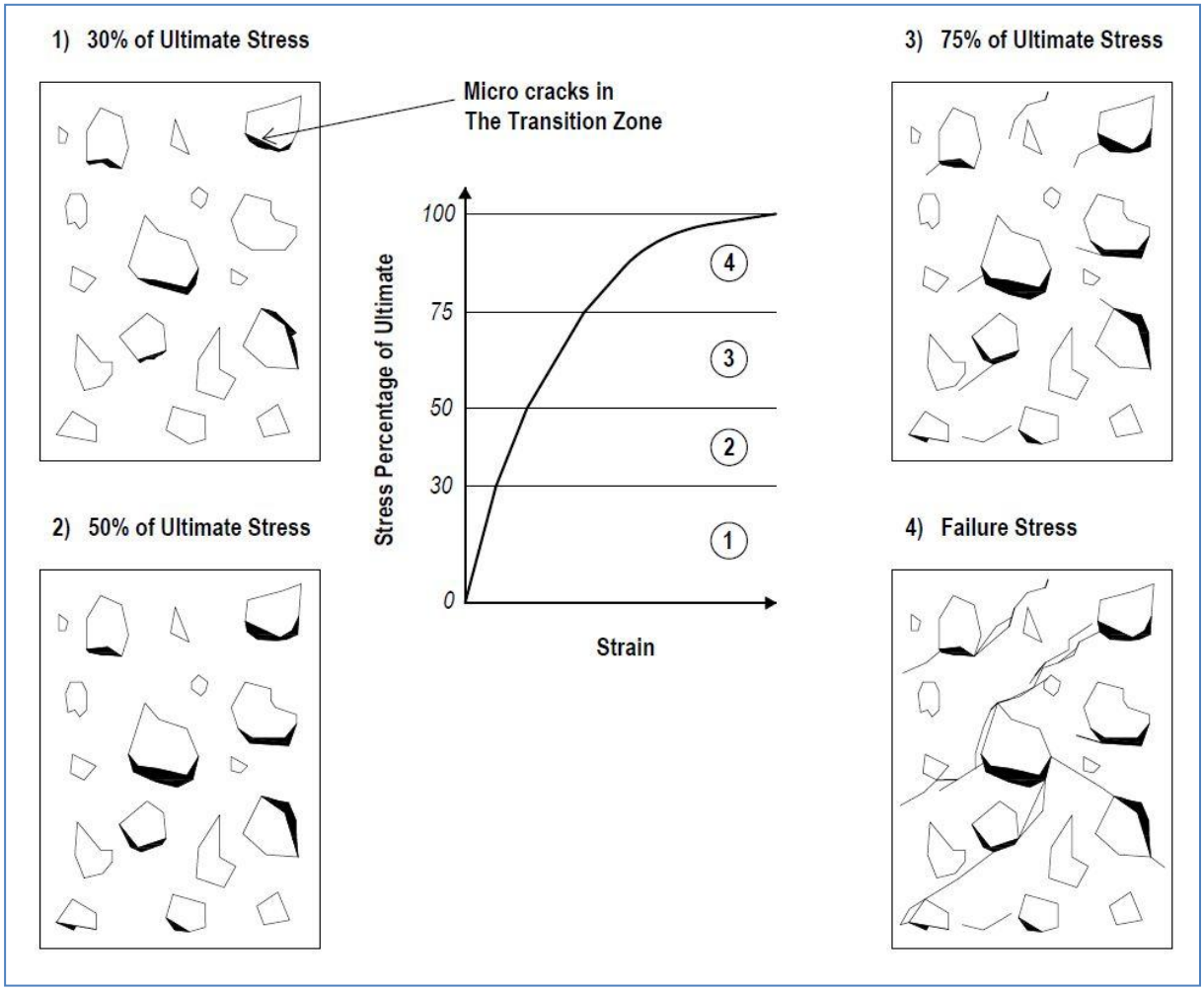

Figure 2-1: Propagation of cracks in the transition zone with increased strain.
Author unknown but the figure is based on J. Weiss, "Stress-Strain Behaviour of Concrete." [11].

Eurocode 2 (EC2) presents an equation to calculate the E-modulus of concrete (E_{cm}) in (GPa) from the average cylinder compressive strength of concrete (f_{cm}) in (MPa), or from eq. (2.3)[1]

$$E_{cm} = 22\left(\frac{f_{cm}}{10}\right)^{0.3}, \tag{2.3}$$

where f_{cm} can by evaluated from eq. (2.4), also from EC2

$$f_{cm} = f_{ck} + 8\ MPa\ , \tag{2.4}$$

where f_{ck} is the characteristic cylinder compressive strength in (MPa). Eq. (2.3) is a secant modulus using 40% of average cylinder compressive strength (see Figure 2-3). EC2 recognizes that E-modulus of concrete is largely based on its composition (especially the aggregates) and eq. (2.3) is valid for quartzite aggregates. For limestone aggregates the value

[1] For ultimate limit state calculations a partial safety factor, γ_{cE}, should be used to determine a design value for the modulus, $E_{cd} = E_{cm}/\gamma_{cE}$ (where γ_{cE} is 1.2) [13].

(E_{cm}) should be reduced by 10% and for sandstone aggregates reduced by 30%. For basalt aggregates it is recommended to increase the value by 20% [14].

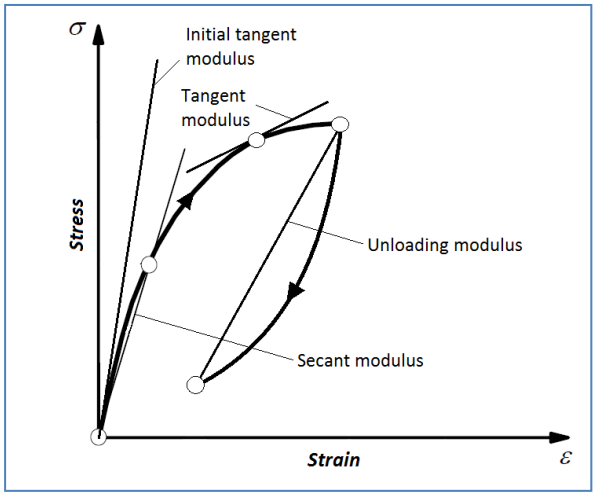

Figure 2-2: Common approaches for evaluation of E-modulus of concrete. Figure based on A. M. Neville and J. J. Brooks, Concrete Technology.

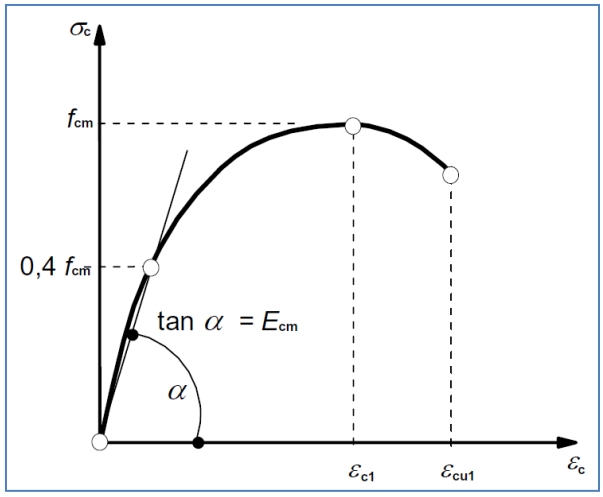

Figure 2-3: Secant modulus from Eurocode 2 (EN 1992-1-1:2004).

There is a known discrepancy between the EC2 model for E-modulus and measured results, using Icelandic aggregates. This is attributed to the prevailing porosity of Icelandic aggregates, moisture content of these in saturated surface dry condition range normally from 3 to 8% [15]. In fact the Icelandic National Annex (INA) to EC2 suggests correction factors to multiply the values obtained from eq. (2.3).

Following values shall be used [16]:

a) 0.9 for non-porous aggregates
b) 0.6 for porous aggregates

The ACI Building Code 318-05 presents an equation (2.5) for calculating E-modulus based on specified compressive strength for normal weight concrete,

$$E_c = 4700\sqrt{f_c'}\,, \tag{2.5}$$

where E_c is the E-modulus of concrete in (MPa) and f_c' is the specified compressive strength of concrete in (MPa). Eq. (2.5) is a secant modulus using 45% of the specified compressive strength. ACI Building Code 318-05 also recognizes that E-modulus is sensitive to variations in the concrete composition. Accordingly, the E-modulus may differ from 120 to 80% of the specified value obtained by eq. (2.5) [17].

Fédération internationale du béton (fib), or The International Federation for Structural Concrete, recently presented the fib Model Code 2010. It is to serve as a basis for future codes and present new developments with regard to concrete structures [18]. The code presents a method for calculating E-modulus which resembles that of EC2. It first introduces eq. (2.6)

that calculates the initial tangent modulus (E_{ci}) which is approximately equal to the slope of the secant of unloading, for rapid unloading (see Figure 2-4)

$$E_{ci} = E_{c0}\,\alpha_E \left(\frac{f_{ck} + 8\ MPa}{10}\right)^{1/3} = E_{c0}\,\alpha_E \left(\frac{f_{cm}}{10}\right)^{1/3}, \qquad (2.6)$$

where $E_{c0} = 21.5 \cdot 10^3\ MPa$ and α_E is an aggregate coefficient found in Table 2-1 [18].

The fib Model Code 2010 also has an equation for the secant modulus.[2] The secant modulus (E_c) should be used if only elastic analysis of concrete structure is carried out, but it accounts for initial plastic strain, causing some irreversible deformations (see Figure 2-4).

$$E_c = \alpha_i\, E_{ci}\,, \qquad (2.7)$$

where α_i is the ratio of secant modulus divided by initial tangent modulus, or

$$\alpha_i = 0.8 + 0.2\,\frac{f_{cm}}{88} \leq 1.0\,. \qquad (2.8)$$

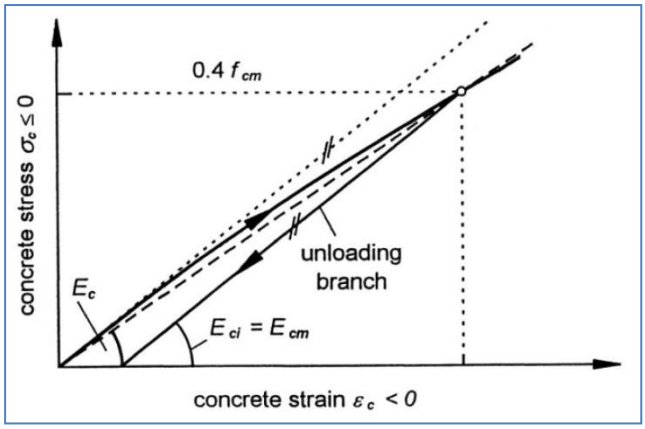

Figure 2-4: Definition of different modulus of elasticity (according to fib Bulletin 42) [18].

From fib Model Code 2010 (Figure 5.1-2). Axes are compressive stress and strain.

Note: E_{cm} is not to be confused with EC2. Here E_{cm} represents average initial tangent modulus but in EC2 it stands for average secant modulus.

Types of aggregate	α_E	$E_{c0}\,\alpha_E$ *[MPa]*
Basalt aggregates	1.2	25800
Dense limestone aggregates	1.2	25800
Quartzite aggregates	1.0	21500
Limestone aggregates	0.9	19400
Sandstone aggregates	0.7	15100

Table 2-1: Effect of type of aggregates on the modulus of elasticity [18].

From fib Model Code 2010 Final draft (Table 5.1-6) and includes coefficients for equation (2.6).

All of the previously described methods are based on linear analysis. It is also possible to derive a stress-strain relationship for non-linear structural analysis. However calculations based on non-linearity are time consuming and require iteration, preferably with computer. EC2 suggests the following non-linear relation between stress (σ_c) and strain (ε_c) in concrete

[2] The fib Model Code 2010 refers to the secant modulus as the reduced modulus.

$$\frac{\sigma_c}{f_{cm}} = \frac{k\eta - \eta^2}{1 + (k-2)\eta} \quad (2.9)$$

$$\eta = \varepsilon_c / \varepsilon_{c1} \quad (2.10)$$

$$k = 1.05\, E_{cm} \cdot |\varepsilon_{c1}| / f_{cm} \quad (2.11)$$

where ε_{c1} is the strain at peak stress according to equation (2.12)

$$\varepsilon_{c1}(^0/_{00}) = 0.7\, {f_{cm}}^{0,31} < 2{,}8. \quad (2.12)$$

Equation (2.9) is valid for

$$0 < |\varepsilon_{c1}| < |\varepsilon_{cu1}| \quad (2.13)$$

where ε_{cu1} is the nominal ultimate strain [14].

2.2 Factors Affecting the Elastic Modulus of Concrete

Equations (2.3) and (2.5) suggest an absolute correlation between compressive strength and E-modulus. However, the factors affecting the E-modulus of concrete are considerably more complex. Among these are factors such as: aggregate type and E-modulus of the TZ (mentioned earlier); moisture; degree of hydration; water-to-cement ratio and the rate of loading affect the E-modulus of concrete.

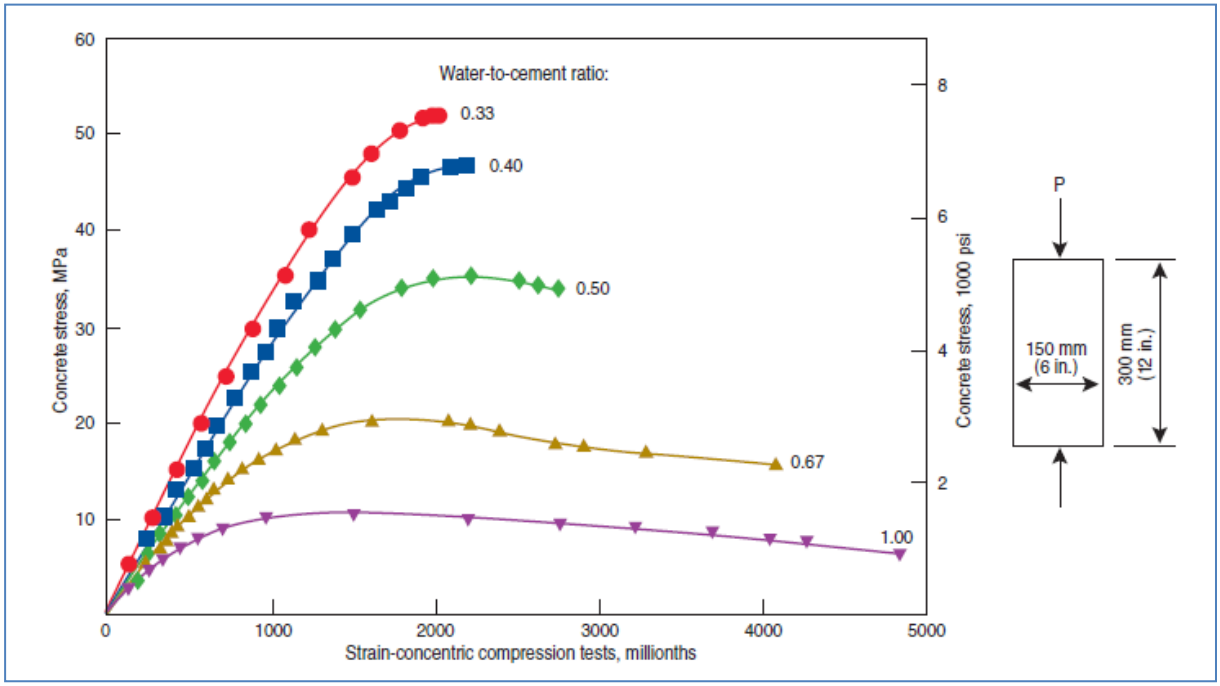

Figure 2-5: Stress-strain curves for compression tests on 150 x 300-mm (6 x 12-in.) concrete cylinders at an age of 28 days (Hognestad, Hanson, and McHenry 1955).

Wet concrete specimen can have E-modulus higher by 3–4 GPa than a dry one [7]. From equation (2.2) it is evident that the volume percent of each concrete component affects the E-modulus. Since fresh paste is plastic, has zero E-modulus, the degree of hydration is also a factor when determining E-modulus of concrete. Figure 2-5 shows the effect of water-to-cement ratio on compressive strength and consequently on E-modulus [19]. Finally, the type of action and the rate of loading affect the E-modulus of concrete. Dynamic E-modulus is not identically the same as the static E-modulus and increased rate of loading yields higher E-modulus [15], [20].

2.3 Shrinkage and Swelling of Concrete

It is well known that concrete exhibits changes in strain with time when no external stress is acting. These changes are simply referred to as shrinkage or swelling. To differentiate between creep deformations and shrinkage or swelling it is necessary to measure, analyze and understand both phenomena. The common practice is to consider the two as additive, i.e. the overall increase in strain is the sum of: elastic deformation, thermal expansion, shrinkage or swelling and creep. This approach has the merit of simplicity and is suitable for many practical applications where creep and shrinkage occur together [21]. Volume changes that are independent of load, excess moisture and temperature changes, are categorized as: plastic shrinkage, chemical shrinkage, drying shrinkage, autogenous shrinkage and carbonation shrinkage [15].

Plastic shrinkage occurs while the concrete is still in its plastic state, i.e. unable to resist tensile stress. It is caused by loss of water by: evaporation from the concrete surface, suction by dry concrete below the surface or loss of water by chemical reaction. This process causes contraction and induction of tensile forces if the concrete is restrained by its non-shrinking inner core or by external restrains [7], [15]. Since plastic shrinkage occurs during setting, or before any external load can be applied to the concrete, it is unimportant with respect to creep.

Chemical shrinkage occurs as long as water hydrates or reacts with cement. The hydration process is fast at first but slows down as hydration products build up. The absolute volume of hydration products, of which the Calcium-Silicate-Hydrate (C-S-H) gel is most abundant, is less than the absolute volume of water and unhydrated cement combined. This decrease in volume causes contraction and it induces tensile forces if the concrete is restrained. Chemical shrinkage is evenly distributed throughout the cross-section and does not propagate from the surface as often is the case with concrete shrinkage [15].

Drying shrinkage is induced by the withdrawal of water from concrete stored in unsaturated air [7]. As water leaves the capillary pores, they experience negative pressure causing the concrete to contract. Drying shrinkage differs from plastic shrinkage because it occurs after strength development has begun. Drying shrinkage is mostly early on but decreases with time,

depending on ambient conditions such as: temperature, wind and relative humidity [15]. It should be noted that only part of the contraction is reversible although the concrete is allowed to submerge in water. For normal concrete the rewetting expansion represents about 40 to 70% of the drying shrinkage [7].

Autogenous shrinkage is a parallel occurrence to chemical shrinkage. As cements hydrates it uses water from the capillary pores and thus causes contraction by the build-up of negative pressure, similar to drying shrinkage. Autogenous shrinkage is independent of ambient relative humidity [15].

Carbonation shrinkage occurs when ambient carbon dioxide (CO_2) reacts with portlandite ($Ca(OH)_2$) in the concrete to form calcium carbonate ($CaCO_3$) and moisture (H_2O), as seen in eq. (2.14) [15].

$$CO_2 + Ca(OH)_2 \rightarrow CaCO_3 + H_2O \quad => shrinkage \tag{2.14}$$

Carbonation shrinkage can, in some instances, be relevant to creep [21] but favourable conditions are needed for the chemical reaction to take place. These conditions are rare but relative humidity of 50% is favourable for carbonation shrinkage as well as permeability and high concentration of carbon dioxide in the ambient medium [7].

Volume changes other than shrinkage include swelling by excess moisture and thermal movement. Like most materials, concrete has positive coefficient of thermal expansion; its value depends both on the concrete composition and moisture condition at the time of temperature change. In order to predict the coefficient of thermal expansion for concrete, a knowledge of the various parameters that govern the two main constituents is needed, e.g. the coefficient of thermal expansion for both cement paste and aggregate, the stiffness ratio of cement paste to aggregate and the volume content of aggregate [7].

2.4 Creep of Concrete

In practice the term creep is often used to denote both the increase in strain under a sustained constant stress and the relaxation of stress [21]. This thesis will mainly focus on time-dependent deformations under constant stress but the relaxation of stress under constant strain is a consequent of the same phenomenon.

Considering concrete specimen, loaded with constant compressive stress (σ_0), at the age (t_0) until some time t ($t > t_0$) (see Figure 2-6). It is assumed that the concrete has been moist cured until age (t_0) and considerations have been made for volume changes other than elastic deformation and creep [7]. At time (t_0), there will be an initial elastic strain (ε_0) according to equation (2.1) and as time passes additional strain will propagate due to the creep behaviour of concrete (see Figure 2-7).

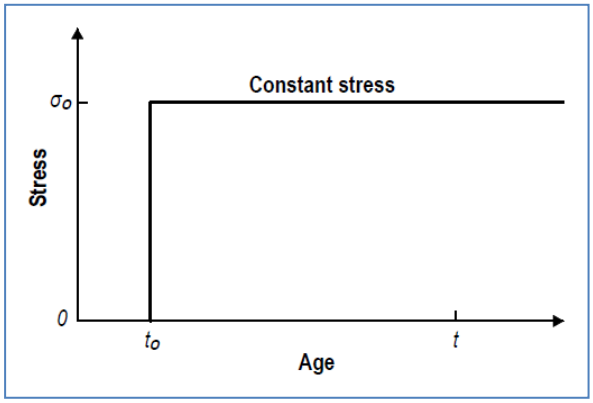

Figure 2-6: Constant stress applied at time t_0. Figure based on A. M. Neville and J. J. Brooks, Concrete Technology.

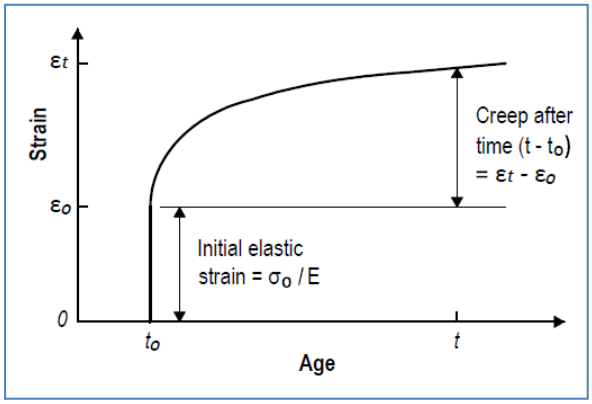

Figure 2-7: The propagation of strain as a function of time. Figure based on A. M. Neville and J. J. Brooks, Concrete Technology.

Creep is generally defined as the increase in strain under static load, after taking into account other time-dependent deformations not associated with stress, such as: shrinkage, swelling, thermal deformations and initial elastic deformations. Creep of concrete is often categorized as: basic creep and drying creep [15].

Basic creep is associated with deformations independent of ambient relative humidity. It is possible to assess basic creep by moist curing or sealing a concrete specimen, keeping it under stress and maintaining constant temperature.

Drying creep is the increase in strain when concrete is stored in unsaturated air. In practice drying creep is a decisive factor in the creep behaviour of concrete. Drying creep is not simply the addition of shrinkage to basic creep but has an extra factor, often referred to as the Pickett effect [15]. The Pickett effect is the excess of creep at drying beyond the sum of shrinkage and basic creep [22] (see Figure 2-8).

Creep is often ill distinguishable from other properties of concrete that often occur simultaneously. If one wants to measure pure creep, it is necessary to exclude other parameters. Let us consider the previous example of concrete loaded to a compressive stress (σ_0) at the age (t_0) (see Figure 2-6). It is evident that concrete is subject to instantaneous strain according to eq. (2.1) or stress divided by E-modulus (see Figure 2-7 & Figure 2-9). Therefore the E-modulus at t_0 needs to be determined and subtracted from measured strain (ε). To exclude shrinkage or swelling from pure creep it is necessary to measure strain (s_h) in a reference concrete sample, not subjected to stress. It is also possible to formulate pure creep strain excluding strain from thermal expansion (s_T). This is best explained in eq. (2.15) [15],

$$c = \varepsilon - \frac{\sigma_0}{E} \pm s_h \pm s_T \,, \qquad (2.15)$$

where c is the creep strain and ε is the measured strain in a sample under constant stress (σ_0).

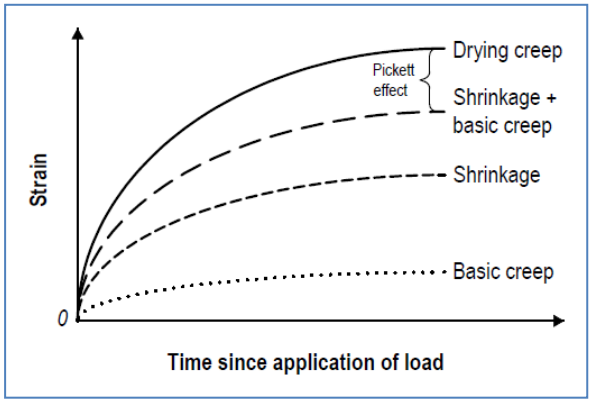

Figure 2-8: Proportional effects of creep and shrinkage of concrete. Figure based on Guðni Jónsson, Formbreytingar í steinsteypu - fjaðurstuðull og skrið - (e. Deformations of Concrete - E-modulus and Creep).

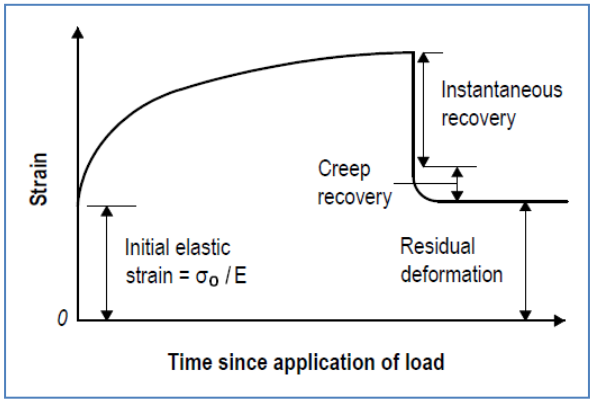

Figure 2-9: Creep and creep recovery of concrete, from initial loading until after stress has been removed. Figure based on A. M. Neville and J. J. Brooks, Concrete Technology.

Figure 2-9, graph based on Concrete Technology by Neville and Brooks, clearly shows the various aspects regarding creep of concrete. The time axis starts at initial loading (t_0) and shows the propagation of creep, as strain increase, until after stress has been removed. Initially the strain will be according to eq. (2.1), i.e. behave in accordance with Hook's Law. As time passes strain increases due to creep but later the load or stress is removed and the concrete is subject to instantaneous strain recovery, proportional to the initial strain. After the instantaneous strain recovery some of the propagated creep will be recovered but what remains is permanent or residual deformation.

2.5 Factors Affecting Concrete Creep

Concrete is a composite material consisting of dispersed material and matrix material. The dispersed materials are aggregates (stone and sand) and the matrix material is a paste made from cement and/or supplementary cementitious materials.

The source of creep is the hardened cement or supplementary cementitious materials but the aggregates are not liable to creep at the level of stress existing in concrete [7]. The aggregates have the tendency to restrain creep in concrete. Hence, stiffer aggregates yield lower creep of concrete (see Figure 2-10).

The water-cement ratio is the main factor influencing the porosity of concrete. The strength of concrete is related to porosity, i.e. strength decreases as porosity increases, since air-voids have no strength. Strength of concrete is often the basis of creep estimations and has a decisive effect on the result, hence also does the porosity of concrete.

The magnitude of creep is dependent on many parameters but one of the most important is the time since application of load. For practical purposes, what is of interest is the creep after several months or years or even the ultimate (or limiting) value of creep [7]. The literature does not agree on when the ultimate value of creep is reached, some say that the increase in creep beyond 20 years is small [7] but others have shown that concrete is still deforming after 30 years [23]. As a guide or a rule of thumb, one can assume that [7]:

about 25% of the 20-year creep occurs in 2 weeks;
about 50% of the 20-year creep occurs in 3 months;
about 75% of the 20-year creep occurs in 1 year.

The time of initial loading (t_0) is also a very important factor in creep quantity. Figure 2-11 shows the benefit in delaying the application initial load with respect to creep. The creep obtained with t_0 equal to 300 days is only about 40% of the creep if t_0 was 7 days. This is not surprising since concrete strength increases with age and consequently creep will decrease with delayed application of initial load.

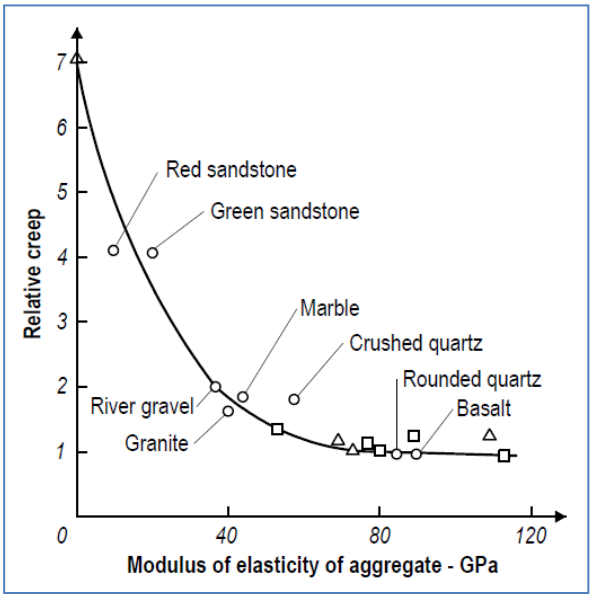

Figure 2-10: Effect of E-modulus of aggregate on relative creep of concrete (equal to 1.0 for an aggregate with a modulus of 69 GPa).

Figure based on A. M. Neville and J. J. Brooks, Concrete Technology. Note: The basalt in this figure is not representative of the basalt found in Icelandic aggregate quarries.

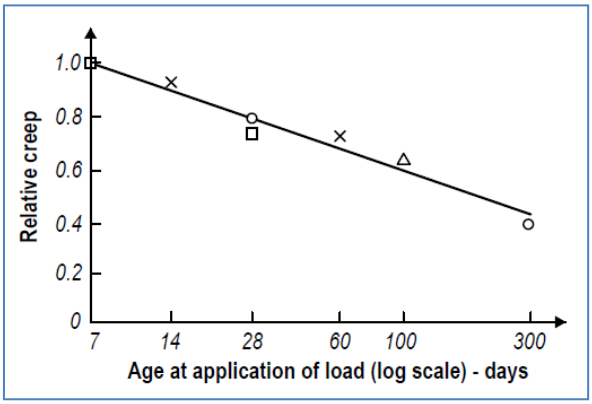

Figure 2-11: Influence of age at application of load on creep of concrete relative to creep of concrete loaded at 7 days, for tests of different investigators: concrete stored at a relative humidity of approximately 75%.

Figure based on A. M. Neville and J. J. Brooks, Concrete Technology. (Originally from: R. L'HERMITE, What do we know about plastic deformation and creep of concrete? RILEM Bulletin, No. 1, pp. 21-25, Paris, March 1959).

Other factors influencing creep of concrete are: relative humidity of ambient air and temperature. But creep of concrete will rapidly increase in excessive temperatures [7]. Generally admixtures have no direct effect on concrete creep [15]. However it is possible to indirectly affect creep by reducing mixing water, using water-reducers, and therefore water-cement ratio. It is also necessary to mention that workmanship affects the properties of concrete and therefore also creep.

2.6 Physical Mechanism of Concrete Creep

There are still debates on the origin of creep of concrete. Generally, creep is considered to be caused by the movement of water between gel pores and capillary pores [15], [24]. Concrete specimen that has been allowed to dry for a long time shows little creep behaviour compared

with specimen with higher degree of hydration or even saturated specimen, provided that the age is the same [15], [24].

Ordinary portland cement (OPC) is made from calcareous materials, such as limestone and chalk, and silica and alumina found as clay or shale. The pure clinkers are composed of the following chemical compounds, using common chemical abbreviations:

- Tricalcium silicate – $3CaO.SiO_2 = C_3S$
- Dicalcium silicate – $2CaO.SiO_2 = C_2S$
- Tricalcium aluminate – $3CaO.Al_2O_3 = C_3A$
- Tetracalcium aluminoferrite – $4CaO.Al_2O_3.Fe_2O_3 = C_4AF$

Note: To control the rate of reaction from C_3A it is necessary to add gypsum ($CaO.SO_3.2H_2O$) = ($C\bar{S}H_2$) to the cement [25].

The hardening of OPC is an exothermic chemical reaction. The hydration process of the most important pure chemical compounds can be seen in eq.: (2.16), (2.17) & (2.18) [26]

$$2C_3S + 6H \rightarrow C_3S_2H_3 + 3CH\ , \tag{2.16}$$

$$2C_2S + 4H \rightarrow C_3S_2H_3 + CH\ , \tag{2.17}$$

$$C_3A + 3C\bar{S}H_2 + 26H \rightarrow C_6A\bar{S}_3H_{32}\ . \tag{2.18}$$

After adding water to the cement, a chemical reaction or hydration starts (see Figure 2-12). Porosity in the concrete decreases but shrinkage begins.

The most important chemical compound in the hydration process is the product of tricalcium silicate (C_3S) and dicalcium silicate (C_2S). C_3S and C_2S, in OPC, begin to react chemically with water, yielding calcium silicate hydrate or (C-S-H). Calcium hydroxide ($Ca(OH)_2$), or portlandite, is considered a by-product. Pozzolan, such as silica fume, is often added into concrete to react with the portlandite to form additional binder, very similar to the C-S-H [25].

C-S-H is often referred to as C-S-H gel since it has very special properties. “In fact, concrete is a heterogeneous visco-elastic material that develops delayed deformations.” [27] The visco-elastic behaviour is, in layman's terms, best described as sponge-like behaviour.

C-S-H gel has solid sheets composition separated by absorbed water [28]. Movement of water is possible, allowing sliding of the solid layers. In the early-ages, when more unhydrated water is present, maximum creep is observed (see Figure 2-7 & Figure 2-9). This hypotheses is supported in the findings by R. L’Hermite (see Figure 2-11), were it is shown that the delayed application of load has a reducing effect on creep.

In mechanism modelling, creep strain for aggregates is considered equal to zero [29]. Since aggregates do not creep they will restrain deformations. Figure 2-10 shows the restraining action of aggregates, stiffer aggregates yield less creep.

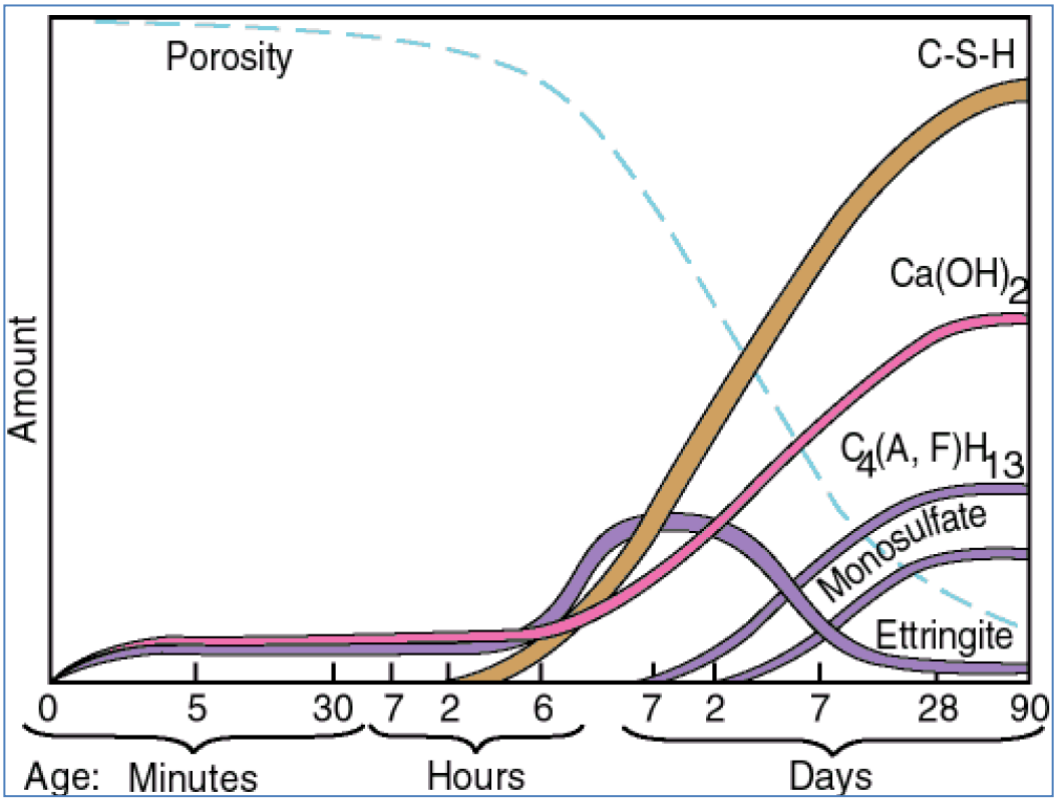

Figure 2-12: Hydration of pure clinkers as a function of time. Figure from lecture presentation on the sustainability of concrete at Reykjavik University.

2.7 The Effects of Concrete Creep

The effect of creep on structures is variable. Creep increases deflection of reinforced concrete beams and slabs. The limits that the Icelandic Building Regulation sets on slab deflections are strict, max 20 mm for residential slabs [12]. This makes creep often a critical design objective.

In reinforced concrete columns, creep results in a gradual transfer of load from the concrete to the reinforcement. Once the steel yields, any increase in load is taken by the concrete, so that the full strength of both the steel and concrete is developed before failure [7].

Creep can be a positive parameter in walls and pavements subject to shrinkage. Stress development, fuelled by drying or autogenous shrinkage, is gradually reduced by creep. In such cases it is preferable to design concrete prone to creep, in order to reduce the effects of other shortcomings, such as shrinkage.

In calculations of post-stressed elements, the effects of creep are known and vital in evaluating the loss in post-stressing force.

Another instance of the adverse effects of creep occurs in tall buildings. Different creep between inner and outer columns, due to different stresses, may cause movement and cracking of partitions [7].

2.8 Icelandic Aggregates

Iceland is a volcanic island, containing mainly basaltic rock types, and geologically it is young [30]. Basalt contains < 52% silicon oxide (SiO_2) [31] and is formed from rapid cooling of exposed lava near the planet's surface. The rapid cooling traps volcanic gases inside the lava and the results are generally rather porous aggregates (see Figure 2-13). Some Icelandic aggregate suppliers offer non-porous aggregates (see Figure 2-14). Icelandic aggregates are quarried from seabed quarries and inland quarries, both gravel and crushed stone.

Figure 2-13: Porous Icelandic aggregate [31].

Figure 2-14: Non-porous Icelandic aggregate [31].

The difference in porosity can be quantitated by the moisture content of aggregates in saturated surface dry (SSD) condition.[3] Moisture content in SSD condition is an indirect way of quantitating porosity by measuring absorption and surface moisture but absorption is related to porosity. "The internal structure of an aggregate particle is made up of solid matter and voids that may or may not contain water [19]." The moisture conditions of aggregates are designated as (see Figure 2-15 & Section 3.1) [19]:

- Oven dry—fully absorbent
- Air dry—dry at the particle surface but containing some interior moisture, thus still somewhat absorbent
- Saturated surface dry (SSD)—neither absorbing water from nor contributing water to the concrete mixture
- Damp or wet—containing an excess of moisture on the surface (free water)

[3] The methods of measuring moisture content in SSD condition are inaccurate. The researcher has to assess visually when the aggregates are SSD. This may lead to fluctuating results between researchers.

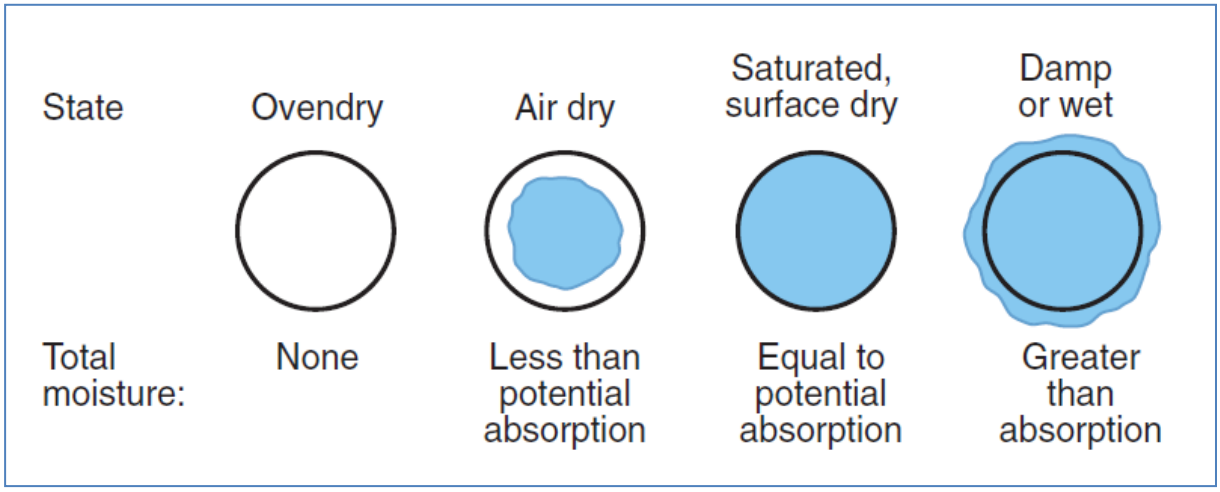

Figure 2-15: Moisture conditions of aggregate [19].

Dry aggregates added to concrete mix will absorb mixing-water. Wet aggregates will however add extra mixing-water. If precautions are not made, and the amount of water not adjusted to the moisture conditions of aggregates, the extra water will increase the water-cement ratio, resulting in: less strength, reduced E-modulus and higher creep coefficient of concrete.

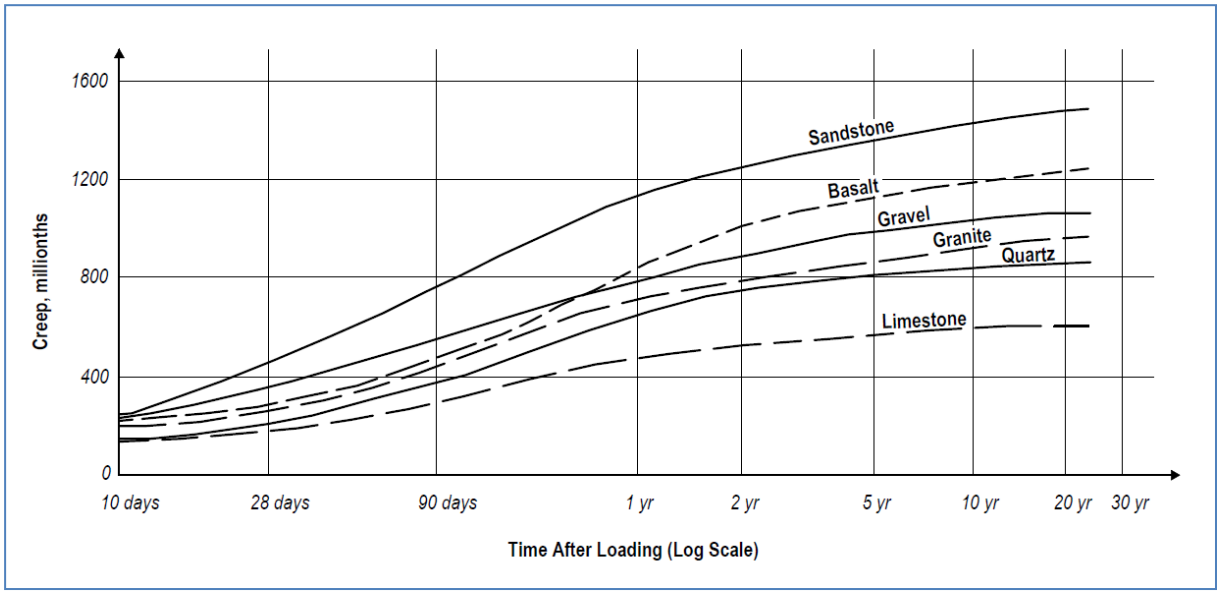

Figure 2-16: Effect of mineralogical character of aggregates on creep. Figure based on G. E. Troxell, J. M. Raphael and R.E. Davis, Long-Time Creep and Shrinkage Tests of Plain and Reinforced Concrete, excluding individual measurements.

Specimens, 4- by 14-in. cylinders. Fineness modulus 5.75, except gravel which had fineness modulus 5.61. Cement type I. Aggregate-cement ratio by weight, 5.67. Water-cement ratio by weight, 0.59. Curing, 28 days in fog at 70 F. Age at loading, 28 days. Sustained compressive stress, 800 psi. Storage after loading, in air at 70 F and 50 per cent relative humidity. Instantaneous deformations in millionths: sandstone, 281; gravel, 275; basalt, 224; limestone, 222; quartz, 212; granite, 205.

Although some Icelandic aggregates are categorized as non-porous, they are all in fact quite porous. Moisture content of 3-8% (by weight) in SSD condition is common in Icelandic aggregates, compared to about 0.5% in neighbouring countries [15].

Figure 2-16 shows the effect of mineralogical character of aggregates upon creep [23]. The concrete containing basalt aggregates increases its rate of creep after about three months, then levels out. It has yet to be seen if the Icelandic aggregate behave similarly.

The aggregate comprises about 70% of concrete volume and is stiffer than the cement paste [13]. In the most general terms, greater volume of aggregate will stiffen the concrete, according to eq. (2.2), and transfer stresses from the binder to the stiffer aggregate. Hence the E-modulus and volume of the aggregate has significant effect on the E-modulus and creep coefficient of concrete.

2.9 Rheological Modelling of Concrete Creep

Rheology is the science of flow and deformation of matter and describes the interrelation between force, deformation and time. The term comes from Greek rheos meaning to flow [32]. It may seem strange to refer to a solid material as concrete as having fluid behaviour. “The idea is that everything flows if you wait long enough, even the mountains.” [33].

Rheological models are used to portray the general deformation behaviour and flow of materials under stress. A model is basically composed of simple elastic springs and ideal dashpots [34]. There are two basic rheological models used to model creep.

The first basic rheological model is the Maxwell model (see Figure 2-17a). It is composed of serially connected elastic spring and ideal dashpot. While load is sustained the deformational response of a Maxwell model is a line, with the y-intercept representing initial elastic deformations. After the load has been removed, instantaneous recovery will occur, equal to the initial elastic deformations and then the deformation will remain constant [21].

The second basic rheological model is the Kelvin model (see Figure 2-17b). It is composed of elastic spring and ideal dashpot, working in parallel. When a load is applied to a Kelvin model it exhibits no instantaneous deformation but the deformation increases with time exponentially. After the removal of load, full recovery will eventually be achieved [21].

The Kelvin and Maxwell models can by combined to build up more complex models. One such model is the Burgers model (see Figure 2-17c). The deformational response of a Burgers model resembles the propagation of strain as a function of time, described in section 2.4 (see Figure 2-7).

Mathematical modelling of concrete creep is based on models, such as the Burgers model, and then experimental data is compared to the models. Some more complex models can be made to represent some material characteristics (see Figure 2-17).

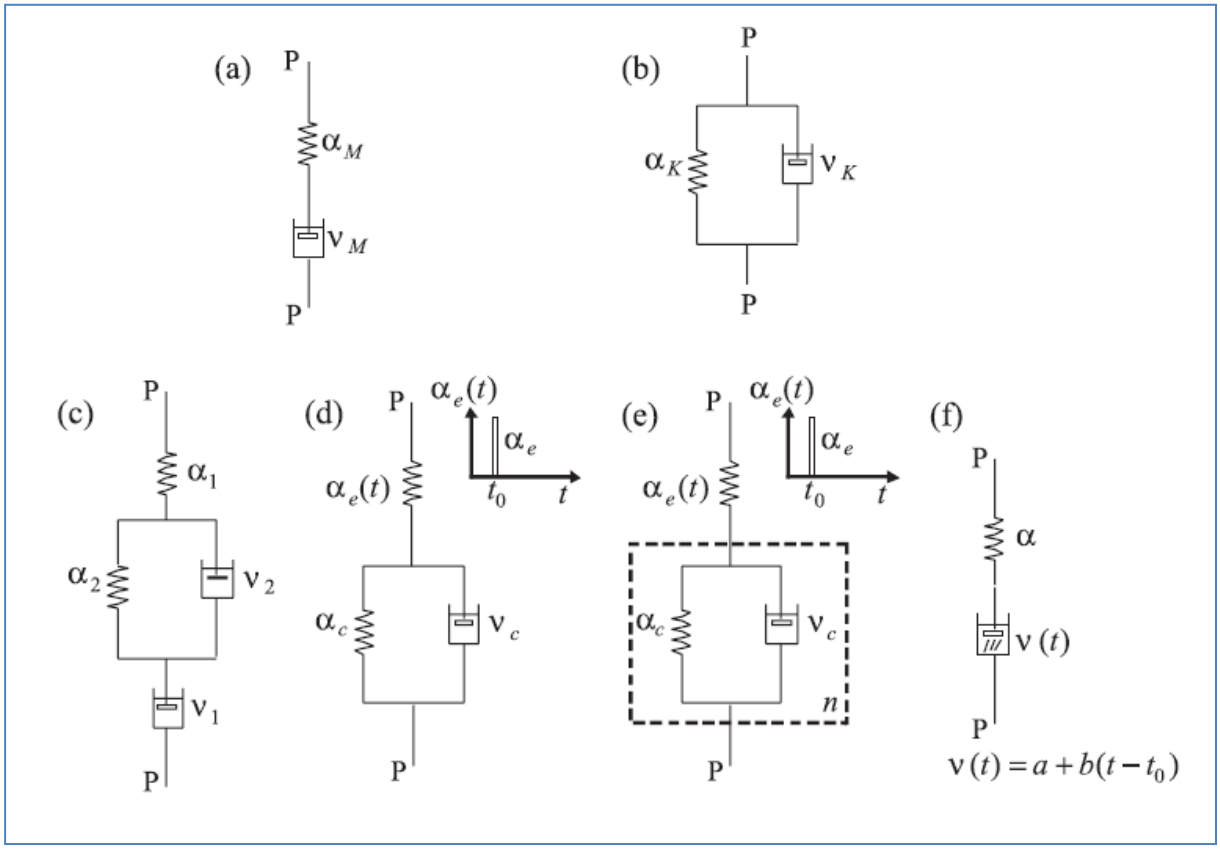

Figure 2-17: Some existing rheological models: (a) Maxwell model, (b) Kelvin Model, (c) Burgers model, (d) Ross model, (e) Feng model and (f) US Bureau of Reclamation model [35].

2.10 Eurocode Modelling of Concrete Creep

The structural Eurocodes are a set European design standards which provide a common approach to structural design across the European Union (EU) [36]. The structural Eurocodes are divided into 10 areas and are made up of 58 parts that have been adopted in full by all EU Member States since April 2010. The area that deals with structural concrete is in four parts and is commonly called Eurocode 2 (EC2). The first part of the code deals with the general rules and when referring to EC2 it is to this part, unless otherwise stated.

Article (2.3.2.2) in EC2 states: "Shrinkage and creep, are time-dependent properties of concrete. Their effects should generally be taken into account for the verification of serviceability limit states". It also states that shrinkage and creep shall be evaluated in ultimate limit state where their effects are significant, e.g. second order effects [14]. EC2 defines creep as a function of two variables, time of consideration (t) and time of initial loading (t_0), it then defines a creep coefficient (ϕ) based on the two variables, i.e. $\phi(t, t_0)$. Often it is of interest to define final creep with the mathematical limit of the formulation or (∞, t_0) [14]. A worked example of obtaining the final value of creep coefficient, i.e. $\phi(\infty, t_0)$, can be found in Appendix B.

The creep coefficient in EC2 is related to the tangent modulus ($E_{c(28)}$) not the secant modulus (E_{cm}). According to the code the tangent modulus may be taken as 1.05 E_{cm} [14]. The creep deformation of concrete is, according to EC2, defined by eq. (2.19)

$$\varepsilon_{cc}(t,t_0) = \phi(t,t_0) \cdot \left(\sigma_c / E_{c(28)}\right) = \phi(t,t_0) \cdot (\sigma_c / 1.05\, E_{cm}), \qquad (2.19)$$

where ε_{cc} is the compressive strain in the concrete due to creep and σ_c is the constant compressive stress in the concrete.

Figure 2-18 shows a schematic representation of the creep coefficient. It shows creep coefficient for 500 x 1000 mm beam, exposed to 80% relative humidity and 250 mm slab, exposed to 50% relative humidity similar to the worked example in Appendix B.

To be able to use standard deflection calculations it is beneficial to define a reduced E-modulus that takes into account the effect of creep. Since the creep coefficient is equal to the ratio of creep strain to elastic strain it is possible to derive eq. (2.20)

$$E_{c,eff} = \frac{E_{c(28)}}{1 + \phi(t,t_0)} = \frac{1.05\, E_{cm}}{1 + \phi(t,t_0)}, \qquad (2.20)$$

where $E_{c,eff}$ is the effective modulus of elasticity. The derivation of equation (2.20) can be seen in Appendix B.

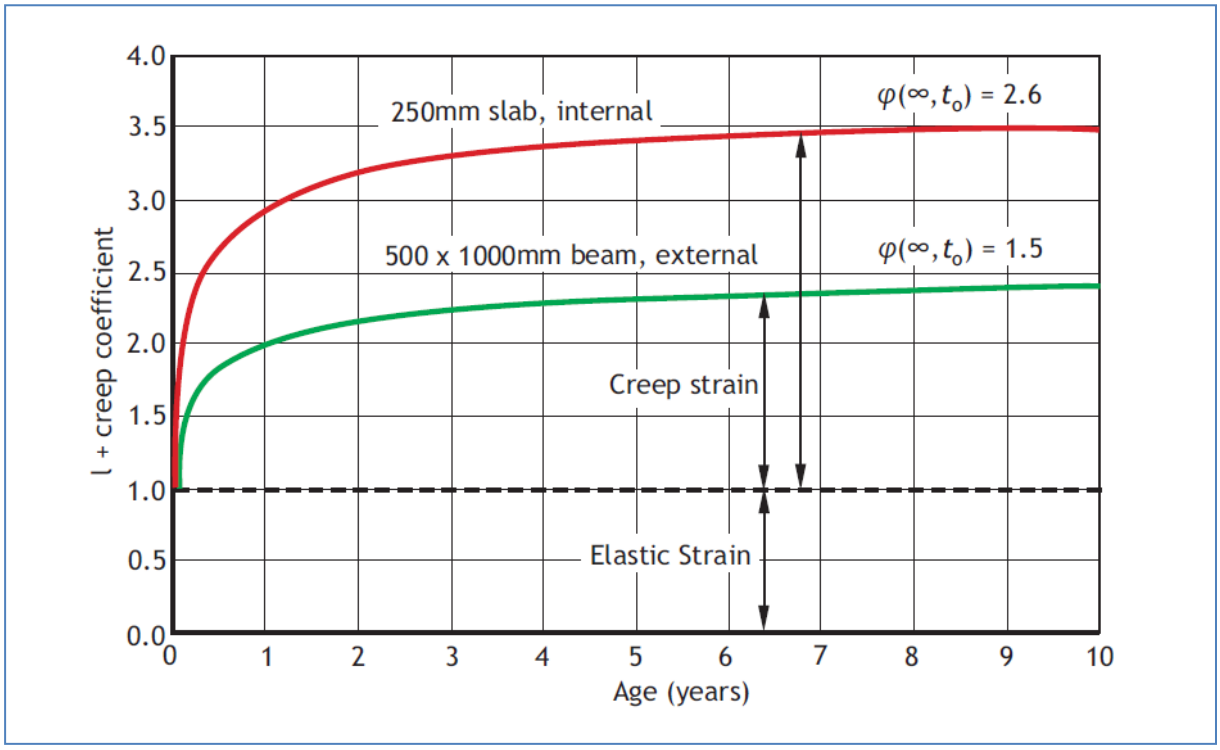

Figure 2-18: Schematic representation of the creep coefficient using two examples [13].

The statement that creep is a function of two variables is incomplete since creep is dependent on many other parameters. If one studies EC2 various parameters, other than time of consideration (t) and time of initial loading (t_0), affect creep. Parameters such as: type of cement, cylinder compressive strength, area of concrete exposed to ambient air, relative humidity of ambient air and ambient temperature, also affect creep.

Where great accuracy is not required, EC2 gives a schematic approach to obtain the final creep coefficient i.e. $\phi(\infty, t_0)$, provided that the concrete is not subjected to a compressive stress greater than $0.45\, f_{ck}$. Figure 2-19 is an example of the schematic approach where two graphs are needed to be read together in order to obtain the final creep coefficient.

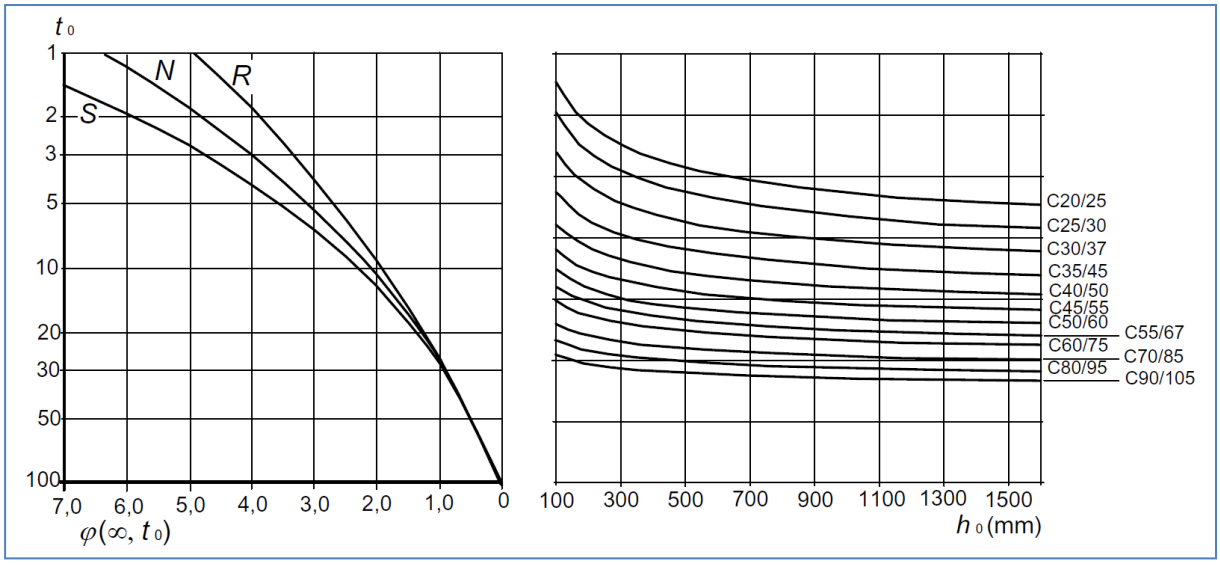

Figure 2-19: Schematic approach to obtain the final creep coefficient if ambient relative humidity is 50% (inside conditions) [14].

$\varphi(\infty, t_0)$	is the final creep coefficient
t_0	is the age of concrete at first loading in days
h_0	is the notional size $2A_c/u$, where A_c is the concrete cross-sectional area and u is the perimeter exposed to drying
S	is for slow hardening cements
N	is for normal hardening cements
R	is for rapid hardening cements

If the compressive stress of the concrete exceeds the value $0.45\, f_{ck}$, or 45% of the characteristic compressive strength, then creep non-linearity should be considered. Such a high stress can occur as a result of pretensioning. In such cases the final creep coefficient should be obtained by eq. (2.21)

$$\phi_k(\infty, t_0) = \phi(\infty, t_0) \exp\left(1.5\left(\sigma_c / f_{cm}(t_0) - 0.45\right)\right), \qquad (2.21)$$

where $\phi_k(\infty, t_0)$ is the non-linear final creep coefficient and $f_{cm}(t_0)$ is the mean concrete compressive strength at the time of loading.

A detailed method of calculating the creep coefficient can be found in Annex B of EC2. The method is time consuming and is better suited to formulate in a computer than writing out on

paper. Appendix C contains a MatLab program that calculates, in details, the creep coefficient, according in EC2. This method should be used if accuracy is required.

2.11 The fib Model Code 2010 and Concrete Creep

Fédération internationale du béton (fib) or The International Federation for Structural Concrete is a pioneering organization in codification. The objectives of the fib Model Code 2010 (MC 10) are to serve as a basis for future codes and present new developments with regard to concrete structures [18].

As with EC2, the fib MC 10 bases creep predictions on the initial tangent modulus of elasticity (see section 2.1). The total strain, a member undergoes, is split into stress-independent strain and stress-dependent strain, creep strain at time $t > t_0$ being part of the latter. Equation (2.22) describes the stress-dependent $(\varepsilon_{c\sigma}(t))$ strain as

$$\varepsilon_{c\sigma}(t,t_0) = \varepsilon_{ci}(t_0) + \varepsilon_{cc}(t) = \frac{\sigma_c(t_0)}{E_{ci}(t_0)} + \frac{\sigma_c(t_0)}{E_{ci}}\phi(t,t_0)\,, \tag{2.22}$$

where $\varepsilon_{ci}(t_0)$ is the initial elastic strain at t_0, $\varepsilon_{cc}(t)$ is the creep strain evaluated at time t, $E_{ci}(t_0)$ is the initial tangent modulus evaluated at t_0, E_{ci} is the initial tangent modulus at 28 days, $\sigma_c(t_0)$ is the constant stress applied at t_0 and $\phi(t,t_0)$ is the creep coefficient [18] [38].

The stress-dependent strain, from eq. (2.22), can by expressed according to eq. (2.23)

$$\varepsilon_{c\sigma}(t,t_0) = \sigma_c(t_0)\left[\frac{1}{E_{ci}(t_0)} + \frac{\phi(t,t_0)}{E_{ci}}\right] = \sigma_c(t_0)\ J(t,t_0)\,, \tag{2.23}$$

where $J(t,t_0)$ is the creep function or creep compliance, representing the total stress-dependent strain per unit stress [18].

Two additions were introduced to fib MC 10 from the older Model Code 1990. The older Model Code lacked asymptotical limit for the function expressing time development of the basic creep [38]. Secondly, new both to the Model Codes and EC2, the fib Model Code 2010 defines the creep coefficient as the sum of basic creep coefficient and drying creep coefficient [18], [38] (see section 2.4) or by eq. (2.24)

$$\phi(t,t_0) = \phi_{bc}(t,t_0) + \phi_{dc}(t,t_0)\,, \tag{2.24}$$

where $\phi_{bc}(t,t_0)$ is the basic creep coefficient and $\phi_{dc}(t,t_0)$ is drying creep coefficient [18].

Appendix C contains a MatLab program that calculates, in details, the creep coefficient, according to the fib Model Code 2010.

2.12 Model B3 and Concrete Creep

Among many models for predicting the creep of concrete, *model B3* by Z. P. Bazant and S. Baweja is the most detailed. It is based on a systematic theoretical formulation of the basic

physical phenomena involved. It is also a statistical optimization with regard to most of the test data that exist in the literature [39].

Model B3 introduces several new parameters for creep prediction [40]. Water-cement ratio by mass (w/c) is a parameter ignored by EC2 and fib MC 2010. The water-cement ratio is the main factor influencing the porosity of concrete (see section 2.5) and as a consequence affecting the compressive strength of concrete. Since creep predictions in EC2 and fib MC 2010 are based on the average cylinder compressive strength (see Appendix C), the two codes indirectly evaluate water-cement ratio.

Another interesting parameter, in model B3, is the aggregate-cement ratio by mass (a/c). Since the aggregate is stiffer than the cement paste, stresses will transfer from the binder to the stiffer aggregate (see section 2.8). Hence less aggregate, more creep.

Model B3 also introduces a parameter for cement content of concrete (c), water content of concrete (w) and the age when drying begins.

The prediction of the model is restricted to Portland cement concrete with the following parameter ranges:

$$0.35 \leq w/c \leq 0.85\,; \quad 2.5 \leq a/c \leq 13.5\,; \tag{2.25}$$

$$17\ MPa \leq \overline{f}_c \leq 70\ MPa\,; \ \ 160\ kg/m^3 \leq c \leq 720\ kg/m^3\,, \tag{2.26}$$

where $\overline{f}_c$ is the mean value of 28th day cylinder compressive strength [40].

The creep compliance, see eq. (2.23), is decomposed, using notation from EC2 and fib MC 2010, as

$$J(t,t_0) = q_1 + C_0(t,t_0) + C_d(t,t_0,t_d)\,, \tag{2.27}$$

where q_1 is the instantaneous strain due to unit stress, $C_0(t,t_0)$ is the compliance function for basic creep, $C_d(t,t_0,t_d)$ is the additional compliance function due to simultaneous drying and t_d is the age when drying begins (only $t_d \leq t_0$ is considered) [40].

By rewriting eq. (2.23), the creep coefficient can by calculated from the creep compliance as

$$\phi(t,t_0) = E_{ci}(t_0)\ J(t,t_0) - 1\,, \tag{2.28}$$

where $E_{ci}(t_0)$ is the initial tangent modulus evaluated at t_0.

Appendix C contains a MatLab program that calculates, in details, the creep compliance, according to model B3.

2.13 ACI 209 Model and Concrete Creep

American Concrete Institute (ACI) committee 209 has published creep and shrinkage prediction model, known as ACI 209R-92.[4] This model was initially developed for the precast- prestressing industry and has been used in design of structures for many years [41].

The ACI 209R-92 method requires the following parameters: the age of concrete at loading, curing method, relative humidity, volume-surface ratio or average thickness, slump, ratio of fine aggregate to total aggregate by mass, air content and cement type.

The model is simple to use with minimal background knowledge but has several disadvantages. It is limited in its accuracy, particularly in the method of accommodating member size [41]. It does not differentiate between basic creep and drying creep as fib MC 10 and model B3. The slump parameter is also questionable. It is meant to represent the composition of concrete but with the use of superplasticizer in concrete, the slump will increase without altering the concrete's composition.

ACI 209R-92 models the creep coefficient according to eq. (2.29)

$$\phi(t, t_0) = \frac{(t - t_0)^{\Psi}}{d + (t - t_0)^{\Psi}} \, \phi_u \, , \tag{2.29}$$

where $(t - t_0)$ is time since application of load, ϕ_u is the ultimate (final) creep coefficient according to eq. (2.30), d and Ψ are constants for a member shape and size. The value of d and Ψ can be determined by use of data obtained from tests performed in accordance to ASTM C 512 [42]. In practice these values are unknown and the recommended values of 10 and 0.6 for d and Ψ are used.

The ultimate creep coefficient is as follows

$$\phi_u = 2.35 \, \gamma_c = 2.35 \, \gamma_{c,to} \, \gamma_{c,RH} \, \gamma_{c,vs} \, \gamma_{c,s} \, \gamma_{c,\psi} \, \gamma_{c,sh,\alpha} \, , \tag{2.30}$$

where γ_c is a correction factor for other than standard conditions and composed of six factors, depending on particular conditions.

Appendix C contains a MatLab program that details individual factors for particular conditions and calculates the creep coefficient, according to ACI 209R-92.

[4] The ACI209R-92 model has been reapproved in 1997 and 2008.

3 Methods

This chapter describes the methodology in obtaining parameters needed for the evaluation of experimental data. Test methods for obtaining: aggregate parameter, parameters for fresh and hardened concrete as well as relevant codes are described in detail. The chapter also contains the methodology used in deflection calculations and prestress losses.

3.1 Aggregate Parameters

Water absorption or moisture content (MC), as a percentage of dry mass after immersion for 24 hours (WA_{24}), is calculated according to the European standard EN 1097-6 (see Figure 3-1), or eq. (3.1)

$$WA_{24} = \frac{M_1 - M_4}{M_4} \cdot 100\% \,, \tag{3.1}$$

where M_1 is the mass of the SSD aggregate in the air and M_4 is the mass of the oven-dried test portion in air [37].

It is also possible to quantify porosity as a measure of the void in the aggregate, but first another aggregate parameter needs to be defined. Particle density on a SSD basis (ρ_{ssd}) is calculated according to the same standard as the water absorption, EN 1097-6 (see Figure 3-1 for pycnometer method), or eq. (3.2)

$$\rho_{ssd} = \rho_w \frac{M_1}{M_1 - (M_2 - M_3)} \,, \tag{3.2}$$

where M_1 is the mass of the SSD aggregate in the air, M_2 is the mass of the pycnometer containing sample of saturated aggregate, M_3 is the mass of the pycnometer filled with water only and ρ_w is the density of water at the temperature recorded when M_2 was determined [37].

Porosity is the ratio of voids by volume by the total volume [43]. Figure 3-2 shows a saturated aggregate element in SSD condition with total volume equal to 1. By using common approaches from geotechnical engineering, eq. (3.3) for porosity can be derived

$$n = \frac{(WA_{24}/100\%)}{\left(1 + (WA_{24}/100\%)\right)} \frac{\rho_{ssd}}{\rho_w} \,. \tag{3.3}$$

The derivation of equation (3.3) can be seen in Appendix B.

Cumulative particle size distribution was conducted in accordance with EN 933-1:1997. The aggregate is sieved into particle size categories (see Figure 4-1) [44]. Before sieving, samples were divided and reduced in accordance with EN 932-2:1999 [45].

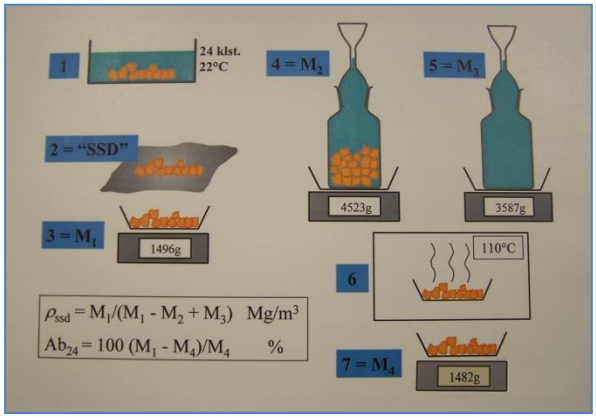

Figure 3-1: Schematic representation of EN 1097-6 from the geotechnical laboratory at the Innovation Center Iceland.

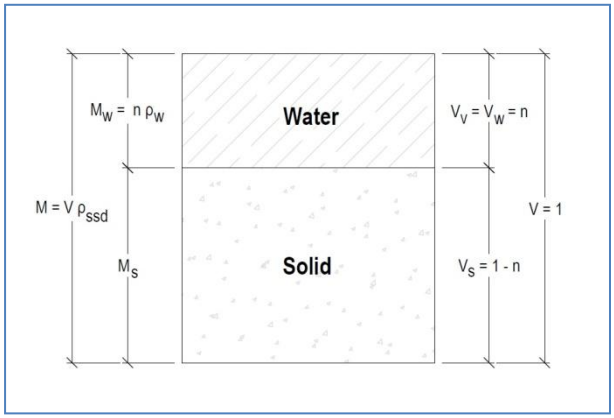

Figure 3-2: Saturated aggregate element (SSD) with total volume equal to 1 [43]. Mass to the left and volume to the right.

3.2 Parameters of Fresh Concrete

Traditional slump test is carried out, according to EN 12350-2:2000, using a mould known as slump cone. The cone is placed on a hard surface and filled in three stages, each time tamped using a rod. At the end of the third stage, concrete is struck off flush to the top of the mould. The mould is carefully lifted and the concrete subsides. The subsidence is measured and the measured value is known as slump value [46].

The slump test is suitable for concrete in "normal" workability ranges or for mixes that yield slump value between 5 and 260 mm. It fails to determine the difference in very stiff mixes and "wet" mixes or collapsing slumps [47]. Despite its shortcomings the slump test is appropriate in the proper range and in "normal" circumstances e.g. conventional vibrated concrete (CVC).

An alternative way of measuring slump is known as the slump flow test. It is preferable when dealing with concrete mixes with collapsing slumps. The slump flow test is simply the measurement of the diameter of the concrete after it has collapsed in conventional slump test [48].

The slump test has been criticized since it fails to fully describe the rheological properties of fresh concrete. The slump test, both the traditional slump test and the slump flow test, gives only a single value, namely the slump value. Concrete with the same slump value can have different rheological properties [49] and therefore it is not adequate when evaluating self-compacting concrete (SCC).

As an alternative to the slump test is a measurement of the fundamental rheological properties of concrete. Figure 3-3 shows a fluid element under shear stress (τ) and the deformation angle (γ). In fact it is the derivative with respect to time or rate of shear ($\dot{\gamma}$) that is of interest. The relationship between shear stress and rate of shear is dependent on the properties of the fluid in question and is given by the eq. (3.4)

$$\tau = \eta(\dot{\gamma})\,\dot{\gamma}\,, \tag{3.4}$$

where $\eta(\dot{\gamma})$, sometimes referred to as apparent viscosity, is a function of the rate of shear and is dependant on fluid properties [50].

If the apparent viscosity is constant the fluid is said to be Newtonian fluid. Water is an example of Newtonian fluid but concrete is an example of a non-Newtonian fluid.

Concrete can often be regarded as a Bingham fluid where the relationship between shear stress and rate of shear can by described by eq. (3.5) and (3.6)

$$\eta(\dot{\gamma}) = \mu + \tau_0/\dot{\gamma}\ ,\tau \geq \tau_0\,, \tag{3.5}$$

$$\dot{\gamma} = 0\,,\tau < \tau_0\,, \tag{3.6}$$

where τ_0 is the yield value and μ the plastic viscosity [50].

If equations (3.4) and (3.5) are combined, the result is

$$\tau = \mu\,\dot{\gamma} + \tau_0\,,\tau \geq \tau_0\,. \tag{3.7}$$

This relationship can best be illustrated graphically, where shear stress is plotted as a function of the rate of shear (see Figure 3-4). It can be seen that the plastic viscosity is the slope of the straight line from equation (3.7) and the line intercept, if present, the material yield value.

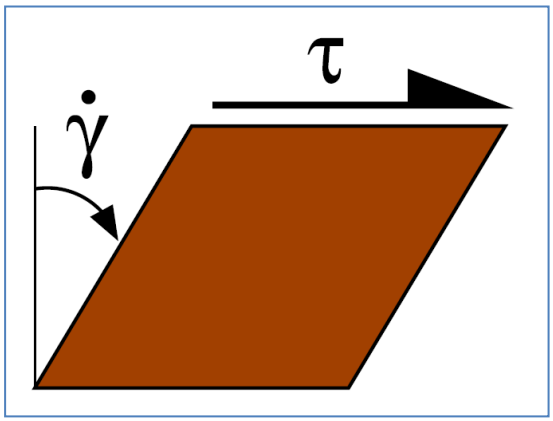

Figure 3-3: Deformation of a fluid element [50].

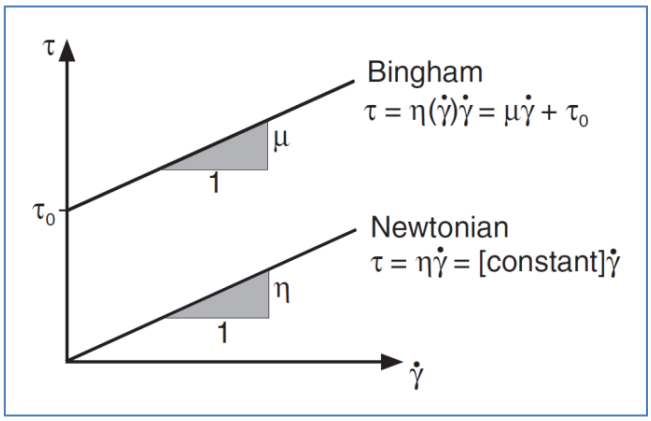

Figure 3-4: Flow curve for Newtonian and Bingham fluids [50].

The yield value can therefore be described as the shear stress that the material can resist before it starts to flow. The plastic viscosity is on the other hand a property that describes the materials resistance to increasing rate of shear.

Some measurements were done using a portable rheometer that gives the yield value as so called G-yield value in amperes (A) and the plastic viscosity as H-plastic viscosity in ampere-seconds (A·s). There is a fairly good correlation between the fundamental rheological properties and G-yield value & H-plastic viscosity [51].

Determination of air and density for fresh concrete was carried out according to EN 12350-7:2000. Air and density was measured using the same concrete sample, first weighing a known volume for density then using air pressure to measure air content [52].

3.3 Parameters of Hardened Concrete

Determination of static modulus of elasticity in compression was carried out according to ISO 1920-10:2010. A basic stress of 0.5 MPa was applied to a test specimen and the stress was steadily increased at a constant rate within the range 0.20 to 0.60 MPa/s until it was equal to one-third of the cylinder strength. The modulus of elasticity was when calculated by dividing the difference between the basic stress and the upper stress by the difference between the corresponding strains [53]. The measurements were done on two moulded cylinder test specimens, 150 mm in diameter and 300 mm in height.

Determination of creep of concrete in compression was carried out according to ASTM C512 / C512M – 10. Strain measurements were done with a strain gauge that measures length changes using 200 mm as a control length (see Figure 3-5). Figure 3-6 shows the equipment setup but the spring was replaced by a jack and screw threads, adjusted regularly to maintain constant force.

Figure 3-5: A strain gauge and equipments to measure creep.

The strain gauge used to measure creep is old but accurate equipment. To convert the readings to millimetres it necessary to multiply by 0.156 (see Appendix E).

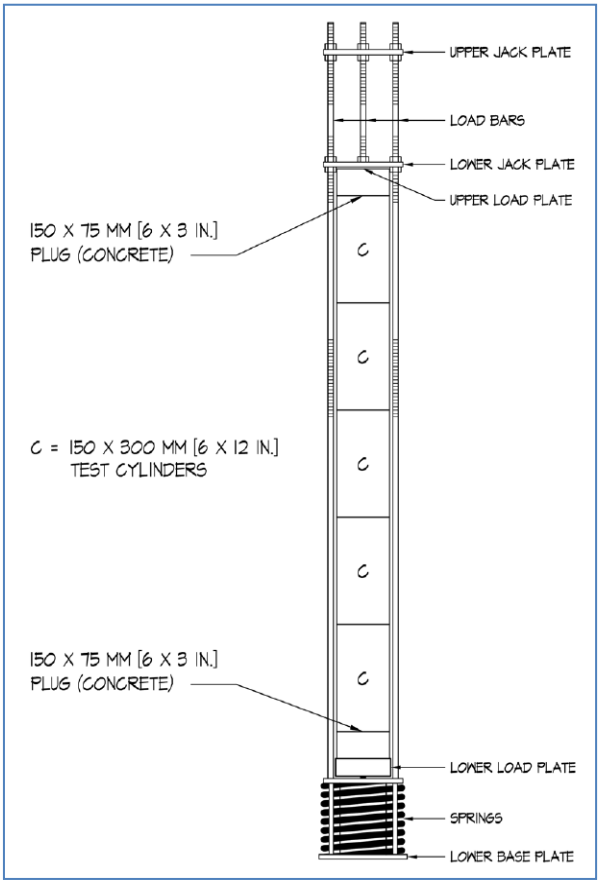

Figure 3-6: Spring-loaded creep frame [3].

Concrete creep is proportional to stress as long as stress is within 0 to 40 % of concrete compressive strength [3]. Accordingly the stresses need to be kept within these limits and compensated for the loss of stress due to relaxation. In the experiments both 0.3 f_{ck} and 0.4 f_{ck} were used as constant stress.

After 28 days of curing, load is applied and thenceforward the specimens are stored at temperature of 23.0 ± 1.0 °C and relative humidity of 50 ± 4%. Environmental conditions as well as load are monitored (see Figure 3-7). The specimen diameters are 150 ± 1.5 mm and the length shall be at least 290 mm. Before strain readings, load is measured and adjusted if the load varies more than 2 % from the correct value [3]. Strains readings on control specimens, under no load and kept in the same conditions, are made to account for shrinkage.

Determination of compressive strength of test specimens was carried out according to EN 12390-3:2009. Specimens were tested with the constant rate of loading within the range 0.6 ± 0.2 MPa/s. The specimens need to show a satisfactory type of failure (see Figure 3-8). The compressive strength is the maximum load at failure divided by the cross-sectional area of the specimen on which the compressive force acts, calculated from the average of six diameter measurements [54].

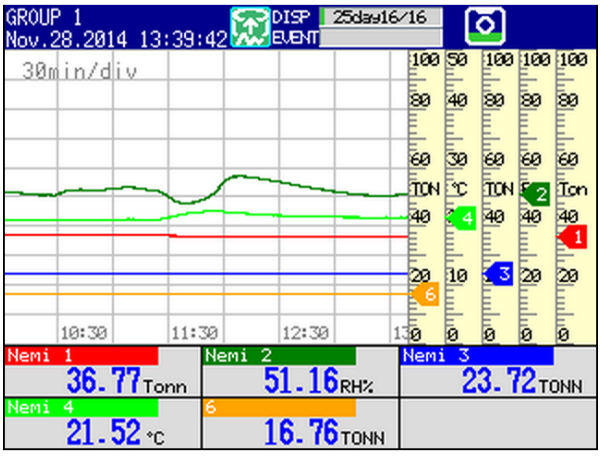

Figure 3-7: Screenshot of a program that logs measurements.

Tonn means metric ton and the fluctuations in RH and °C are due to exposure during measurements.

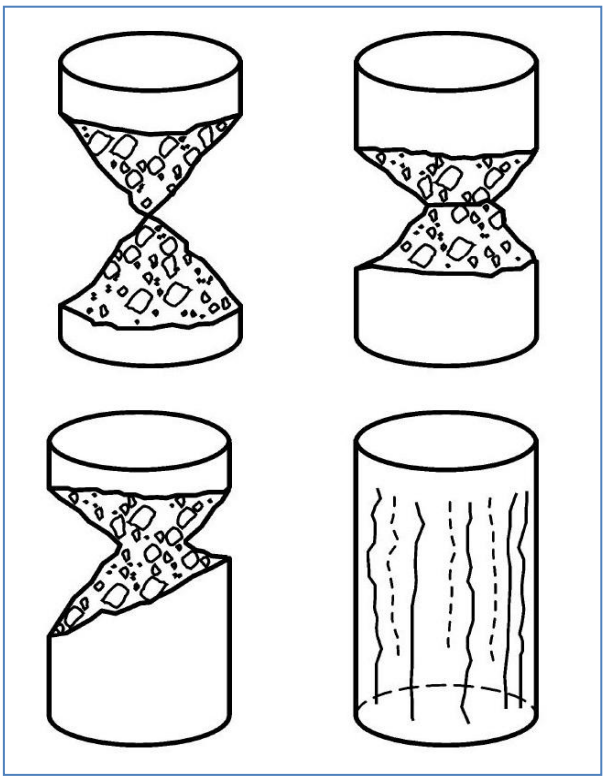

Figure 3-8: Satisfactory failure of cylinder specimen [54].

When determining the compressive strength, an average of three 100 x 200 mm cylinders was used.[5] When measuring the static modulus of elasticity, according to ISO 1920-10:2010, a test was first carried out on a 100 x 200 mm cylinder to estimate compressive strength. E-modulus was then measured using 150 x 300 mm cylinder and stress proportional to the ultimate strength, based on the estimation. Finally the 150 x 300 mm cylinder was used to access the compressive strength.

3.4 Deflection Calculations

Deflection calculations are based on the Euler-Bernoulli beam theory. The assumption is that the cross section is perpendicular to the bending line. The alternative would be the Timoshenko beam theory where rotation between the cross section and the bending is allowed. This rotation is caused by shear force, which is not included in the Euler-Bernoulli theory [57]. Euler-Bernoulli beam is therefore stiffer. However, if the ratio between length and height is large enough the discrepancy between models is relatively small.

All deflection calculations are based on linear elastic assumption. Creep deformations are allowed for by reduction in E-modulus, according to eq. (2.20).

Deflection calculations are based on service limit state (SLS) according to EN 1990 - Basis of structural design [58] and actions are according to EN 1991 - Actions on structures [59].

Structural members which are expected to crack under loading, but may not be fully cracked, will behave in a manner intermediate between the uncracked and fully cracked conditions. To take an advantage of the stiffer sections where the members are uncracked, eq. (3.8) is used

$$\alpha = \zeta \alpha_{II} + (1 - \zeta)\alpha_{I}\,, \tag{3.8}$$

where α is the deformation parameter considered which may be, for example, a strain, a curvature, or rotation. α_I and α_{II} are the values of the parameter calculated for uncracked and fully cracked conditions [14]. ζ is a distribution coefficient according to eq. (3.9) (see Figure 3-9)

$$\zeta = 1 - \beta \left(\frac{\sigma_{sr}}{\sigma_s}\right)^2, \tag{3.9}$$

where β is a coefficient taking account of the influence of the duration of loading or of repeated loading on the average strain (1,0 for a single short-term loading and 0,5 for sustained loads or many cycles of repeated loading). σ_s is the stress in the tension

[5] **Note:** According to EN 206-1:2000, the compressive strength of concrete is classified with respect to 150 x 300 mm cylinders [55]. It is the common practice at ICI to reduce the results from 100 x 200 mm cylinders by 5%. This is due to the tendency of smaller specimens showing greater strength. The 5% deduction has been difficult to confirm but the previously described tendency can be verified here [56].

reinforcement calculated on the basis of a cracked section and σ_{sr} is the stress in the tension reinforcement calculated on the basis of a cracked section under the loading conditions causing first cracking [14].[6]

Appendix B contains further derivation of equations, used in deflection calculations.

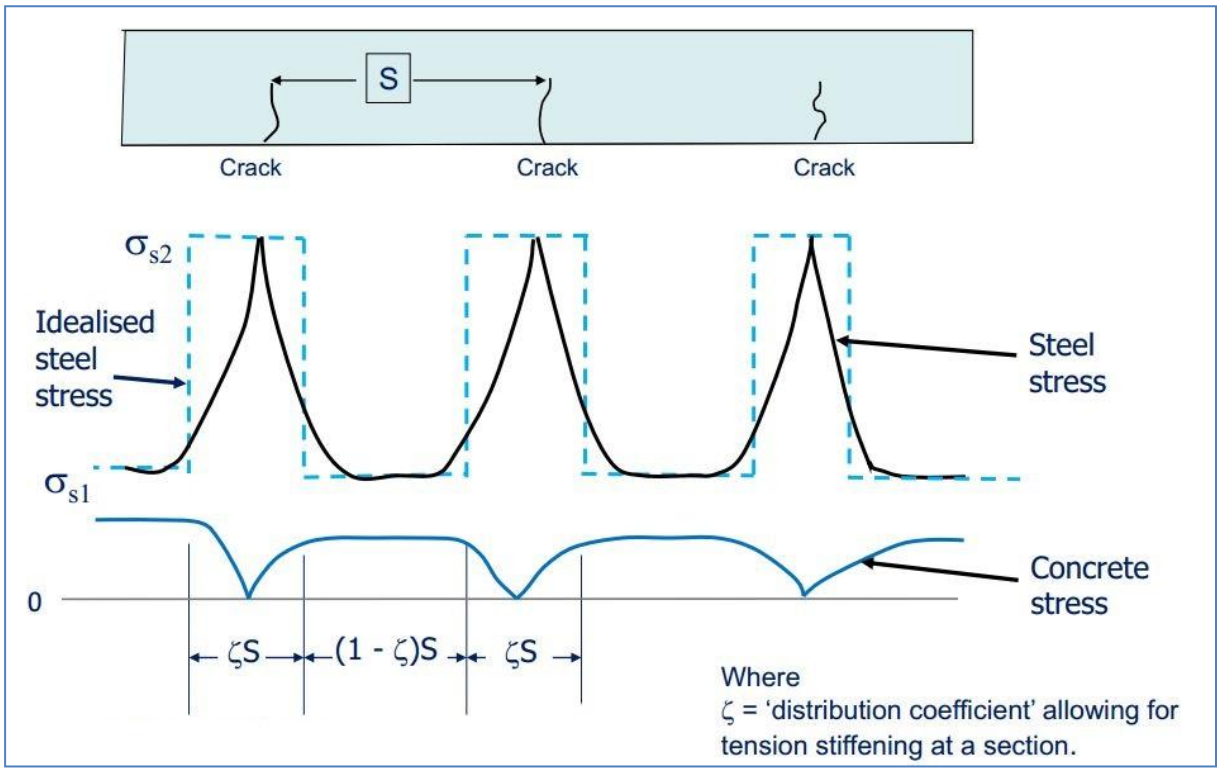

Figure 3-9: Stress behaviour in uncracked and cracked beam [60].

It is common practice to use the mean values of E-modulus and tensile strength as bases for deflection calculations [60]. It is, however, the opinion of the author that basing calculations on average tensile strength is not warranted. This is due to lack of case studies where tensile strength of concrete with porous aggregate is compared with values from EC2. It is possible that the tensile strength might by lower, when using porous aggregate, since it is strongly dependant on the interfacial transition zone (see section 2.1). It is therefore considered conservative to use the characteristic axial tensile strength (f_{ctk}) (5% fractile) as flexural strength.

The deflection calculations are for a roof slab on a residential house located in the Greater Reykjavík Area. The house is above 100 m elevation and therefore it has higher characteristic snow load than normal in Greater Reykjavík. The slab spans five meters and has additional gravel on top of insulating layer.

[6] **Note:** σ_{sr}/σ_s may be replaced by M_{cr}/M for flexure or N_{cr}/N for pure tension, where M_{cr} is the cracking moment and N_{cr} is the cracking force [14].

See section 3.5, eq. (3.10), for evaluating creep coefficient based on different conditions for drying creep.

3.5 Prestress Losses

The prestress force applied to prestressed concrete member continuously decreases during the lifetime of the structure. Immediately after release of the strands, the initial prestress force decreases due to the elastic shortening of the concrete. From then on, it continues to decrease due to the combined effects of creep and shrinkage strains of the concrete and relaxation of the steel [61].

The effects of using material parameters from EC2 instead of experimental results are shown in a case study. Prestress force losses for a post tensioned highway bridge (see Figure 3-10) are calculated using material parameters both form EC2 and experimental results (see Appendix E for construction details).

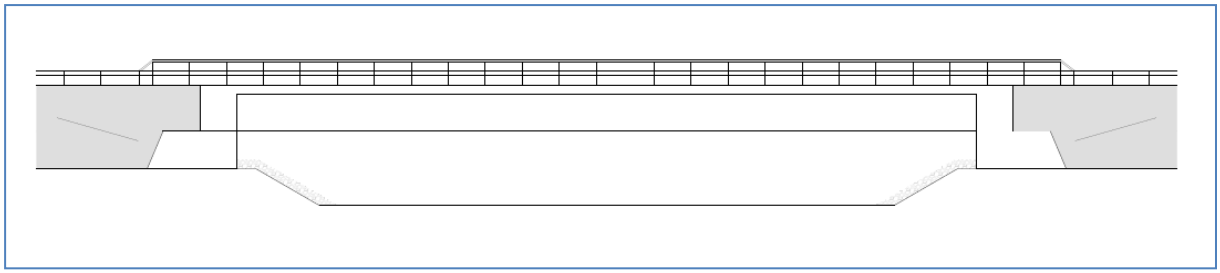

Figure 3-10: Side view of the highway bridge.

The structure is common on Icelandic highways. It has a 40.0 m single-span, is 9.0 m wide and located 30.0 m above sea level. The load on the bridge is based on EN 1991-2:2003: Actions on structures - Part 2: Traffic loads on bridges [4] (see Figure 3-11). All calculations are based on EC2 in conjunction with the INA and Reinforced Concrete Design: to Eurocode 2 by W.H. Mosley, J.H. Bungey and R. Hulse [5].

The experimental data is based on specimens exposed to 50% relative humidity and relatively large surface exposed to drying (see section 3.3). The conditions for drying creep are consequently different for the bridge deck, exposed to outdoor conditions, 80% relative humidity, and relatively small surface exposed to drying. The described differences affect the creep coefficient and need to be accounted for. Equation (3.10) is based on the assumption that the relative difference between EC2 value for creep coefficient and creep coefficient from experimental results is the same for both exposure conditions.

$$\frac{\phi_{m,1}}{\phi_{EC2,1}} = \frac{\phi_{m,2}}{\phi_{EC2,2}}, \tag{3.10}$$

where $\phi_{m,1}$ is the measured creep coefficient for condition no. 1, $\phi_{m,2}$ is the measured creep coefficient for condition no. 2, $\phi_{EC2,1}$ is the creep coefficient from EC2 for condition no. 1 and $\phi_{EC2,2}$ is the creep coefficient from EC2 for condition no. 2.

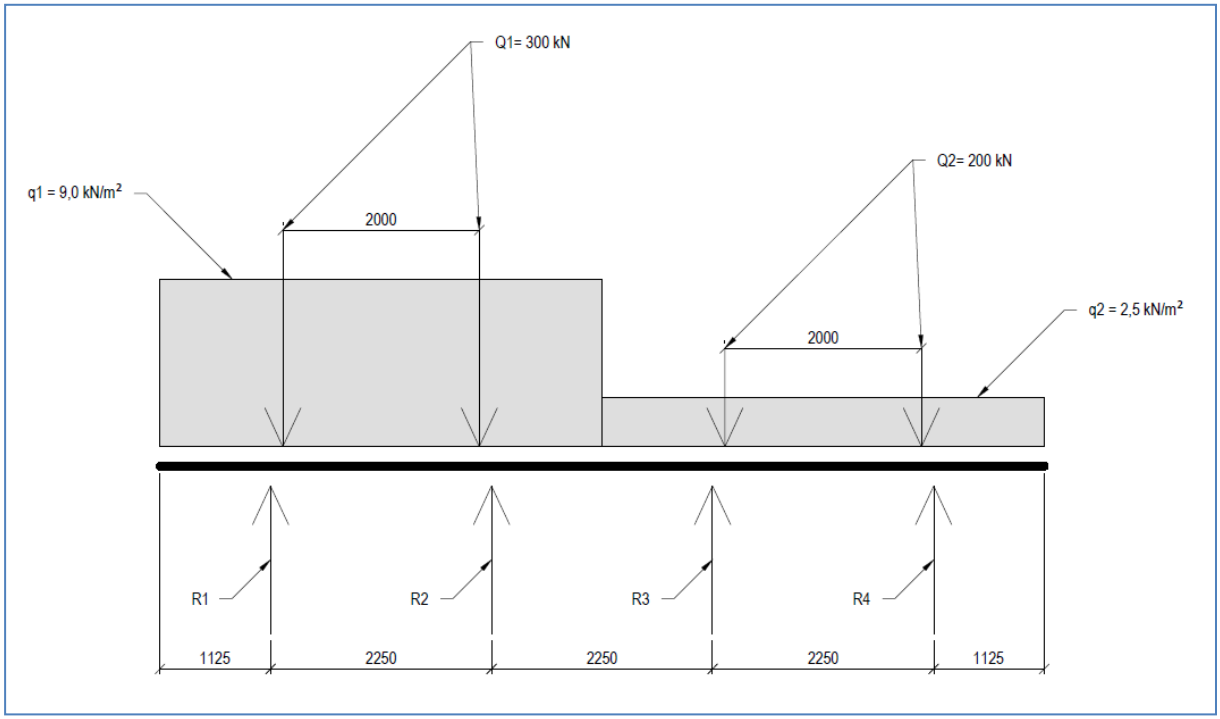

Figure 3-11: Load on bridge structure (cross-sectional view), the vectors R_1, R_2, R_3 & R_4 are the four bridge beams.

4 Materials

This chapter gives an overview of the materials used in phase I and II. It also contains tabulated results of measured material parameters, particle size distribution graphs, etc.

4.1 Phase I

Phase I of the thesis is a study of the elastic modulus of concrete. It is based on an experiment done in the summer of 2014 and presented at the XXII Nordic Concrete Research Symposium, 2014 in Reykjavik.

Six concrete mixes were made using different combination of aggregates. The mass-ratio of fine aggregates (< 4.0 mm) was the same in all mixes, 47% of total aggregates. This made the accumulative particle size distribution fairly homogeneous, except maybe for the basalt mix no. 4 (see Figure 4-1). Abbreviations and aggregate composition is as follows:

Granite:	Norwegian granite aggregates.
Limestone:	Dune sand and limestone aggregates from Abu Dhabi, UAE.
Basalt no. 1:	Basalt aggregates from Harðikambur, Icelandic inland quarry.
Basalt no. 2:	Basalt from Björgun, Icelandic seabed quarry and sand from Rauðimelur, Icelandic inland quarry.
Basalt no. 3:	Basalt aggregates from Björgun, Icelandic seabed quarry.
Basalt no. 4:	Basalt aggregates from Vatnsskarð, Icelandic inland quarry.

Particle density and porosity, expressed as moisture content (MC) in saturated surface dry (SSD) condition and the ratio of voids by volume, can be seen in Table 4-1.

Required mass content was calculated for the six mixes by maintaining a constant volume of 30 litres. Cement content in all the mixes was 315 kg/m^3 and water content 174 kg/m^3, maintaining a water-to-cement ratio of 0.55 and a paste volume of 27.7%. Cement from the Danish Aalborg Portland was used (CEM I 52.5 N), ρ = 3130 kg/m^3, tricalcium silicate (C_3S): 55%, dicalcium silicate (C_2S): 18%, tricalcium aluminate (C_3A): 8%, tetracalcium aluminoferrite (C_4AF): 12%. Blain (particle size): 423 m^2/kg. Water demand: 27%.

	MC in SSD condition (%)	*Particle density SSD basis (kg/m^3)*	*Porosity (%)*
Granite	0.3	2730	0.8
Limestone	0.6	2630	1.6
Basalt no. 1	1.7	2790	4.6
Basalt no. 2	2.9	2790	7.9
Basalt no. 3	3.0	2770	8.2
Basalt no. 4	4.8	2710	12.5

Table 4-1: Aggregate parameters according to equations: (3.1), (3.2) & (3.3) and based on weighted average.

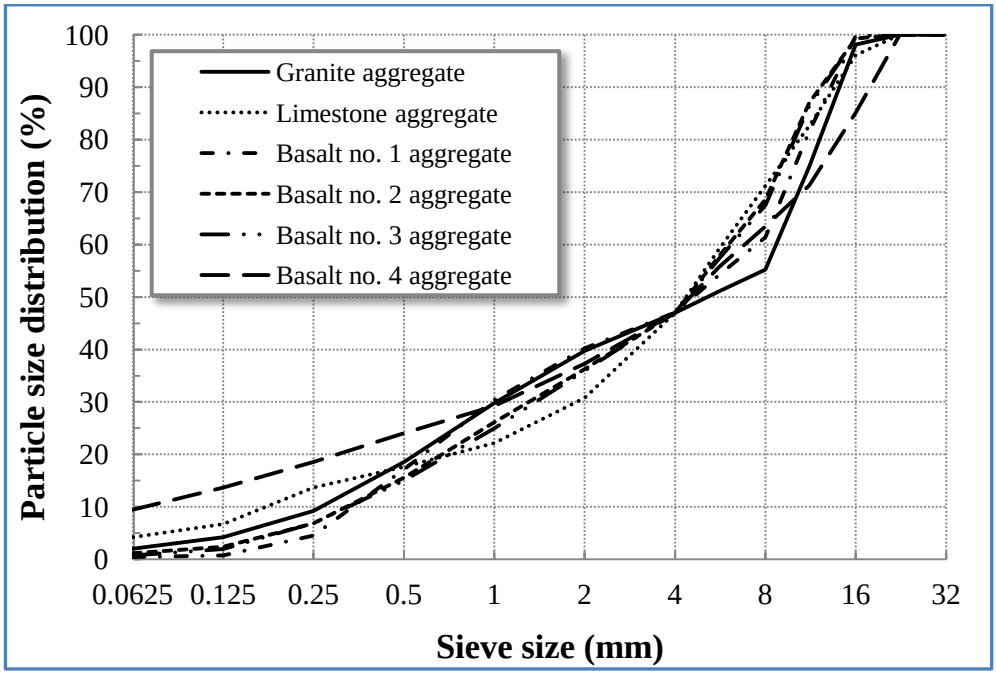

Figure 4-1: Cumulative particle size distribution of mixes containing various aggregates. Particle size distribution by Þórður I. Kristjánsson.

The amount of superplasticizer in each mix was arrived at with acceptable workability in mind. Additives: Omnicon SPC-25 (polycarboxylic ether) ρ = 1100 kg/m^3, dry content 39.3%. Additional information for mixes can be seen in Table 4-2.

	SPC-25 * *(kg/m^3)*	*Air (%)*	*Slump (mm)*	*G-yield value (A)*	*H-plastic viscosity (A•s)*
Granite	1.0	4.1	215	0.68	1.87
Limestone	1.5	3.3	190	0.73	2.10
Basalt no. 1	1.0	4.3	235	0.64	1.50
Basalt no. 2	2.2	5.5	185	-	-
Basalt no. 3	2.0	4.2	185	-	-
Basalt no. 4	1.9	3.2	170	0.92	5.21

* Omnicon SPC 25 (polycarboxylic ether)

Table 4-2: Parameters of fresh concrete, measured prior to casting.

Figure 4-2: Arbitrary photo of specimens from phase I.

Figure 4-3: Arbitrary photo of specimens from phase I.

4.2 Phase II

Phase II of the thesis is a study of the creep of concrete. It is based on an experimental data recorded, for over twelve years, at ICI. Some material parameters have been lost over the years. In the case of missing material parameter, tables will indicate a dash symbol (-).

The aggregate used in creep test specimens are from three Icelandic quarries and imported aggregate from Norway. Abbreviations and aggregate composition is as follows:

Granite quarry:	(GQ)	Norwegian granite aggregates.
Basalt quarry no. 1:	(BQ1)	Basalt aggregates from Björgun, Icelandic seabed quarry.
Basalt quarry no. 2:	(BQ2)	Basalt aggregates from Vatnsskarð, Icelandic inland quarry.
Basalt quarry no. 3:	(BQ3)	Basalt aggregates from Seljadalur, Icelandic inland quarry.

	Sieve size range (mm)	*MC in SSD condition (%)*	*Particle density SSD basis (kg/m^3)*	*Porosity (%)*
Granite quarry:	-	0.3	2650	0.8
Granite quarry:	0-8	0.3	2660	0.8
Granite quarry:	0-8	0.6	2650	1.7
Granite quarry:	8-16	0.5	2650	1.3
Granite quarry:	8-16	0.6	2700	1.6
Granite quarry:	8-16	0.7	2660	1.8
Basalt quarry no. 1:	0-8	3.3	2660	8.4
Basalt quarry no. 1:	0-8	3.3	2750	8.7
Basalt quarry no. 1:	0-8	4.2	2680	10.8
Basalt quarry no. 1:	0-8	4.8	2610	12.0
Basalt quarry no. 1:	8-16	2.0	2830	5.5
Basalt quarry no. 1:	8-16	2.4	2850	6.6
Basalt quarry no. 1:	8-16	2.6	2820	7.1
Basalt quarry no. 1:	8-16	3.0	2800	8.2
Basalt quarry no. 2:	0-8	6.1	2670	15.4
Basalt quarry no. 2:	8-19	7.2	2530	17.0
Basalt quarry no. 2:	8-22	7.0	2620	17.1
Basalt quarry no. 3:	8-12	2.3	2930	6.6
Basalt quarry no. 3:	12-16	1.7	2960	4.9

Table 4-3: Aggregate parameters according to equations: (3.1), (3.2) & (3.3).

In all test specimens but those in the last creep rig, blended silica fume cement from an Icelandic cement producer (Sementsverksmiðjan) was used, classified as CEM II/A-M 42.5 R, and containing 6% silica fume and 3% rhyolite [62], Blain (particle size) 4600 cm^2/g. The

test specimens in the last creep rig contains Danish Aalborg Portland cement (CEM I 52.5 N),[7] 6.7% silica fume was added to the EcoSCC mixes and 26.7% fly ash to the SCC mix.

Table 4-4 shows various measured fresh concrete properties for the test specimens in creep rigs from 2002.

Creep rig	*Quarry*	*Water-cement (-)*	*Cement content (kg/m^3)*	*Air (%)*	*Slump (mm)*	*Density (kg/m^3)*	*Paste volume (%)*
CVC_2 2002	BQ1	0.374	440	7.1	210	2270	31.0
	BQ2	0.373	452	8.0	130	2230	31.8
	BQ3	0.372	454	6.0	190	2370	31.9
CVC_3 2002	BQ1	0.312	512	4.7	80	2410	33.0
	BQ2	0.313	505	6.2	100	2270	32.5
	BQ3	0.310	513	4.7	90	2440	32.9
CVC_4 2002	BQ1	0.291	549	4.0	60	2470	34.2
	BQ2	0.290	539	6.6	170	2310	33.5
	BQ3	0.292	555	3.8	160	2520	34.7

Table 4-4: Various measured fresh concrete parameters for the specimens in the CVC creep rigs from 2002.

Table 4-5 shows various measured fresh concrete properties for the specimens in the CVC creep rig from 2004. Measurements on test specimens in the SSC creep rig are not displayed, since the available data is not considered reliable.

Creep rig	*Quarry*	*Water-cement (-)*	*Cement content (kg/m^3)*	*Air (%)*	*Slump (mm)*	*Density (kg/m^3)*	*Paste volume (%)*
CVC_0 2004	GQ	0.380	440	8.4	190	2230	31.4
	GQ	0.384	360	5.3	140	2330	25.7
	BQ1	0.394	359	3.5	30	2430	26.0

Table 4-5: Various measured fresh concrete parameters for the specimens in the CVC creep rig from 2004.

Table 4-6 shows various measured fresh concrete properties for the specimens in the CVC creep rig from 2009.

Creep rig	*Quarry*	*Water-cement (-)*	*Cement content (kg/m^3)*	*Air (%)*	*Slump (mm)*	*Density (kg/m^3)*	*Paste volume (%)*
CVC_1 2009	BQ1	0.550	321	5.6	110	2350	28.1
	BQ2	0.510	317	5.5	130	2300	26.4
	GQ	0.550	322	4.9	150	2300	28.2

Table 4-6: Various measured fresh concrete parameters for the specimens in the CVC creep rig from 2009.

[7] **Note:** Cement is classified according to EN 197-1:2000 where only two classes for early strength is used, i.e. N and R [63]. This classification is not to be confused with EC2 where both CEM II/A-M 42.5R and CEM I 52.5N are, according to article 3.1.2 (6), classified as R [14].

Table 4-7 shows various measured fresh concrete properties for the specimens in the SCC creep rig from 2010. The supplementary cementitious material (SCM) used in the SCC AEA mix was fly ash and in the Eco-SCC mix, silica fume was used. Slump measurements are excluded from the table since the measurements were above 260 mm and therefore fail to determine the difference in consistency (see section 3.2). The difference in consistency for SCC mixes should be quantitated by the slump flow test or preferably by measuring the fundamental rheological properties (see section 3.2).

Creep rig	*Quarry*	*Water-binder ratio (-)*	*Cement content (kg/m^3)*	*SCMs content (kg/m^3)*	*Air content (%)*	*Density of con. (kg/m^3)*	*Paste volume (%)*
SCC AEA	GQ	0.336	402	146	7.2	2180	45.3
Eco-SCC	GQ	0.604	295	21	1.3	2340	30.8
Eco-SCC AEA	GQ	0.576	295	21	5.7	2250	34.4

Table 4-7: Various measured fresh concrete parameters for the specimens in the SCC creep rig from 2010.

Figure 4-4: Arbitrary photo of creep rig specimens.

Figure 4-5: Arbitrary photo of creep rig specimens.

5 Results and Discussion

This chapter reports the main findings of the thesis and discusses the results. Since the results and discussion, between the various phases of the thesis, are interlinked; the results and discussion have been merged into one chapter. This has been done for clarity of results and over all readability.

5.1 Phase I

This section contains an extended version of results presented at the XXII Nordic Concrete Research Symposium, 2014 in Reykjavik, involving the elastic modulus of concrete.

Table 5-1 shows results from both 7th and 28th day compressive strength as well as 7th and 28th day E-modulus; calculated values, using eq. (2.3) from EC2, based on 28th day compressive strength and the ratio of measured 28th day E-modulus to EC2 E-modulus.

	7th day Comp. st. (MPa) *	*7th day E-mod. (GPa)*	*28th day Comp. st. (MPa)* *	*28th day E-mod. (GPa)*	*E-mod. from EC2 (GPa)* **	*Ratio of E_{28} to E_{EC2} (-)*
Granite	30.9	29.4	40.5	29.4	33.5	0.88
Limestone	31.4	35.9	41.7	39.4	33.8	1.17
Basalt no. 1	31.5	28.9	42.0	30.8	33.8	0.91
Basalt no. 2	37.9	27.9	47.0	28.3	35.0	0.81
Basalt no. 3	38.8	27.8	51.0	29.6	35.9	0.83
Basalt no. 4	41.8	19.2	54.6	22.3	36.6	0.61

* Mean value of concrete cylinder compressive strength.
** Value calculated according to equation (2.3) and without modification factor.

Table 5-1: Measured parameters of hardened concrete and compared to EC2 values for E-modulus. The specimens are listed in the order of increasing porosity.

Article 3.1.3, in EC2 states that eq. (2.3) is valid for quartzite aggregates, but the outcome should be reduced by 10% for limestone and increased by 20% for basalt [14]. There is a known discrepancy between EC2 values for E-modulus and measured results, using Icelandic aggregates. This is attributed to the prevailing porosity of Icelandic aggregates, MC in SSD condition from 3 to 8% [15]. In fact the Icelandic National Annex (INA) to EC2 suggests a correction factor to multiply the values obtained from eq. (2.3); 0.9 for non-porous aggregates and 0.6 for porous aggregates [16] (see section 2.1).

Due to the inherent stiffness and large volume fraction that the aggregates occupy in concrete, it exerts major influence on the E-modulus of concrete [64]. The E-modulus of quartzite aggregate is higher than that of granite aggregate [65] (see also Figure 2-10) and therefore it is not surprising that the E-modulus of the concrete mix with granite is lower than the EC2 value, since the aggregates have the tendency to restrain creep in concrete (see section 2.5).

This tendency can by validated in literature [64] but as for the precise value of 88% reduction from EC2, it is more difficult to validate.

The result for the mix containing limestone aggregate, above the EC2 value, was unexpected, especially since EC2 recommends 10% reduction. The codification society has however seemed to realize their error by adding a clause into the new fib MC 10. Table 2-1, from fib MC 10 final draft, recommends an aggregate coefficient for dense limestone, that increases calculated values by 20%. The clause from fib MC 10 was unknown to the author prior to the experiment.

Figure 5-1 shows the measured E-modulus plotted as a function of MC in SSD condition. If the values obtained from granite and limestone aggregates (values with low MC) are ignored, a fairly good linear correlation emerges between porosity and E-modulus.

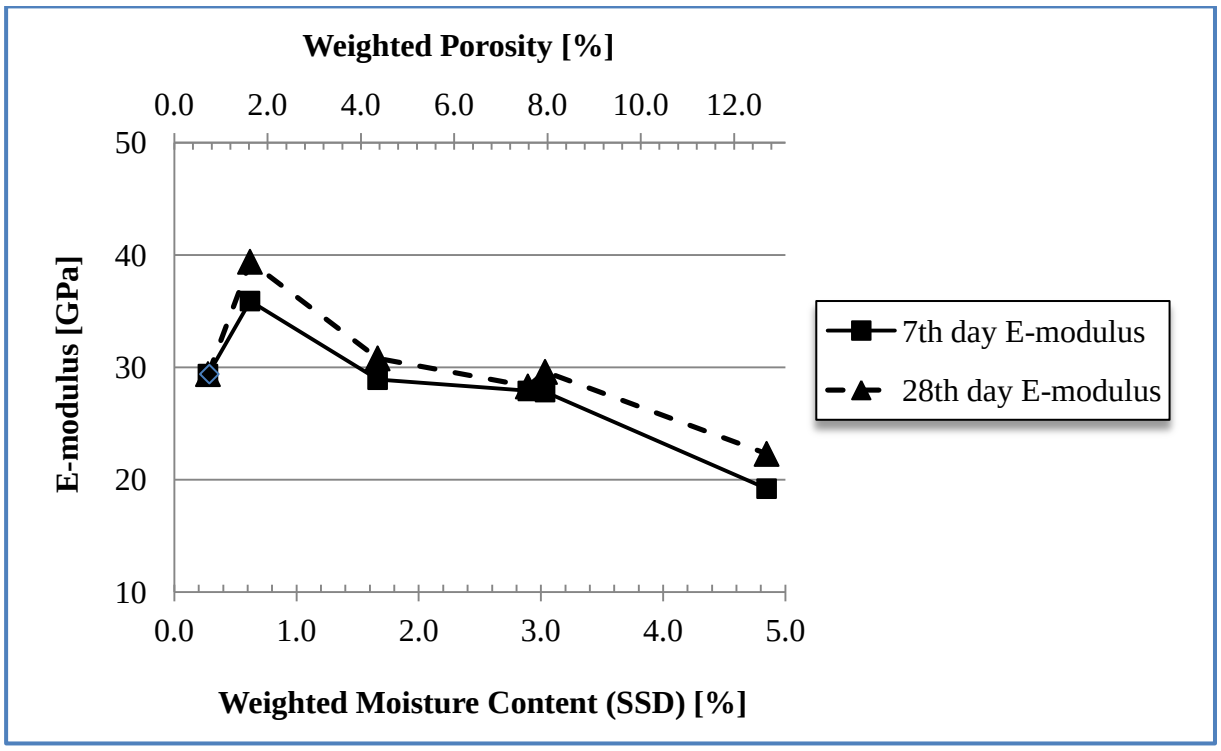

Figure 5-1: E-modulus of concrete as a function of aggregate porosity and MC in SSD condition.

The measured results, for basalt 1-4, agree fairly with the EC2 model if the correction factors from INA are used. It is however interesting to exclude the granite and limestone aggregates and plot the E-modulus of concrete, with basalt aggregates, as a function of aggregate porosity (see Figure 5-2).

It is not good practice to extrapolate a fitted line outside the range of data, since the linear relationship may not hold there [66]. But with the given statistical reservation, it is however interesting to predict the E-modulus for higher aggregate porosity. The MC in SSD condition for Icelandic aggregate can be as high as 8% [15]. By using the linear regression (arrived at in

Figure 5-2), the equation predicts the E-modulus of basalt with MC of 8% at SDD condition to 14.4 GPa. This value is likely to be outside the reduction suggested by INA.

Measuring the E-modulus of concrete is a rather simple task for concrete manufacturers, especially since it can be done using the same specimens as for the compressive strength test. It is the author's opinion, that basing the E-modulus of concrete on a single parameter such as the compressive strength is not acceptable. The E-modulus of concrete is a vital parameter in design and should be listed by the manufacturer, just as the characteristic compressive strength.

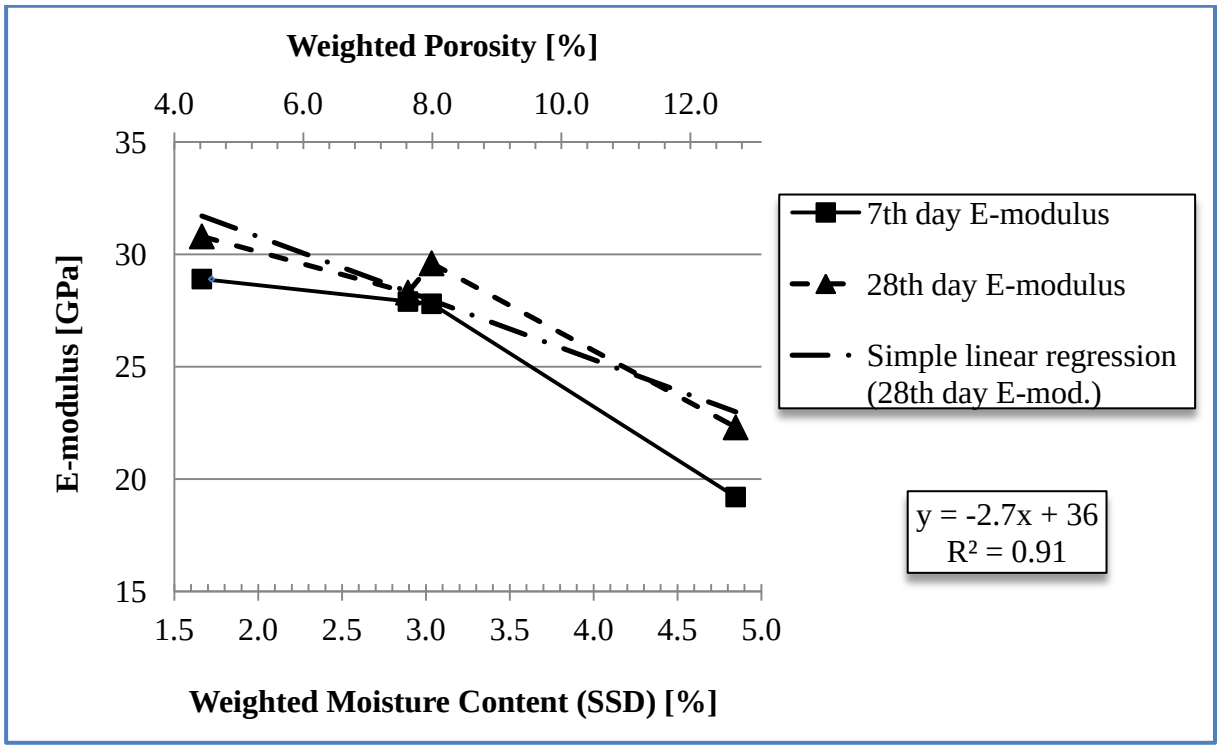

Figure 5-2: E-modulus of concrete, samples containing basalt aggregates, as a function of aggregate porosity and MC in SSD condition.

Another observation that can be made from table 5-1 is the compressive strength. Figure 5-3 shows the mean value of concrete cylinder compressive strength, with basalt aggregates, as a function of aggregate porosity and MC in SSD condition. It shows a fairly good correlation between porosity and compressive strength, where the compressive strength increases with increased porosity. This is likely due to the failure mechanism of concrete, where the cement paste-aggregate bond plays a major part. Aggregate surface texture is one of the most important factors affecting bond strength; rough surfaces usually offer better bond than sawn surfaces [67].

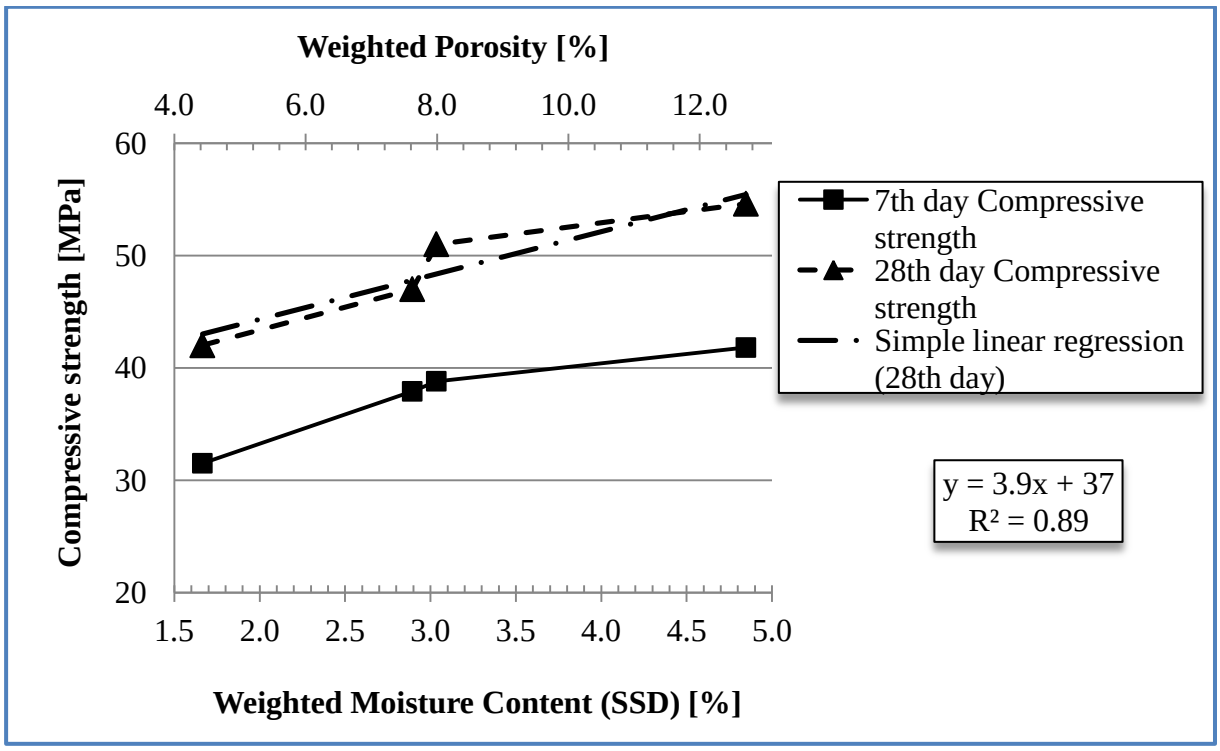

Figure 5-3: Mean value of concrete cylinder compressive strength, with basalt aggregates, as a function of aggregate porosity and MC in SSD condition.

5.2 Phase II

5.2.1 Elastic Modulus

In order to fully elucidate the test data on creep strain, it is first necessary to evaluate the E-modulus for various mixes. Table 5-2 shows the 28th day E-modulus obtained from strain readings in creep rigs (see Figure 4-4 & Figure 4-5), immediately after loading and by using eq. (2.1). Although the E-modulus is not obtained by standardized method, as in phase I, it is never the less reasonably obtained data.

Columns five and six in table 5-2 contain values obtained with eq. (2.3) from EC2 and eq. (2.7) from fib MC 10. The difference between the values from the two equations is from 1 to 11%.

Column seven in table 5-2 contains the ratio of the measured E-modulus by the E-modulus obtained with eq. (2.3) from EC2. This is in fact the necessary correction factor to obtain the correct value, using the equation from EC2. The Icelandic National Annex (INA) to EC2 suggests a correction factor to multiply the values obtained from eq. (2.3); 0.9 for non-porous aggregates and 0.6 for porous aggregates [16] (see section 2.1). The measured E-modulus for four mixes (highlighted values) is lower than the values obtained through the correction factor recommended by the INA.

The ratio of the measured E-modulus by the calculated E-modulus in the SCC specimens is somewhat lower than in other granite specimens (see row 1, column 6 in Table 5-1 and row 12, column 6 in Table 5-2). There are several possible reasons for this. The paste volume is higher in the SCC specimens containing AEA (air entraining admixture) and from equation (2.2) it is evident that the volume percent of each concrete component affects the E-modulus. The ratio of fine aggregate to total aggregate by mass is a possible factor. The Eco-SCC specimens contain fine basalt filler and thus increasing the total aggregate surface. The volume of the transition zone (TZ) is related to the total aggregate surface or the interface surface [10] and the TZ influences the elastic properties of concrete (see section 2.1). The water-to-cement or water-to-binder ratio can be a factor in the Eco-SCC specimens but it affects the E-modulus of concrete (see section 2.2 and Figure 2-5).

The tendency, encountered in from table 5-1, where the compressive strength increases with increased porosity (see Figure 5-2) does not hold for table 5-2. The relationship seems only to be relevant for mixes with the lower characteristic compressive strength (f_{ck}). This is likely due to the higher cement content in the stronger mixes.

	Aggregate Quarry	$f_{ck} = f_{cm} - 8$ *(MPa)*	28^{th} *day E-mod. (GPa)*	*E-mod.* * *from MC10 (GPa)*	*E-mod.* * *from EC2 (GPa)*	*Ratio of* E_{28} *to* E_{EC2} *(-)*
CVC_2 2002	BQ1	51.3	27.3	36.4	37.5	0.73
	BQ2	54.4	17.9	37.3	38.1	**0.47**
	BQ3	48.4	28.3	35.5	37.0	0.76
CVC_3 2002	BQ1	69.5	34.1	41.5	40.7	0.84
	BQ2	62.4	19.9	39.6	39.5	**0.50**
	BQ3	68.0	32.9	41.1	40.4	0.81
CVC_4 2002	BQ1	68.9	37.4	41.4	40.6	0.92
	BQ2	65.5	22.4	40.4	40.0	**0.56**
	BQ3	83.4	37.9	45.0	42.7	0.89
CVC_1 2009	BQ1	26.1	22.6	28.4	31.8	0.71
	BQ2	30.4	18.2	29.9	32.9	**0.55**
	GQ	28.0	26.4	29.1	32.3	0.82
SCC AEA	GQ	49.6	24.7	35.9	37.2	0.66
Eco-SCC	GQ	50.0	26.0	36.0	37.3	0.70
Eco-SCC AEA	GQ	40.4	27.3	33.1	35.3	0.77

* Values calculated according to eq. (2.3) & (2.7) and without modification factor.

Table 5-2: Evaluated E-modulus values and comparison to fib MC 10 and EC2 models.

5.2.2 Experimental Results of Creep

Experimental results from creep data is best illustrated graphically. The creep compliance from eq. (2.23) can be plotted as a function of time. Note that, the creep compliance is often incorrectly referred to as specific creep. Specific creep is the creep strain divided by the constant stress, excluding the elastic strain. Or as a continuation from eq. (2.23), the creep compliance can be written as eq. (5.1)

$$J(t,t_0) = \frac{1}{E_{ci}(t_0)} + \frac{\phi(t,t_0)}{E_{ci}} = \frac{1}{E_{ci}(t_0)} + C(t,t_0)\,, \tag{5.1}$$

where $C(t,t_0)$ is the specific creep [68] [69].

Figure 5-4 shows the creep compliance for a creep rig, known as CVC_1 from 2009. All the specimens have characteristic compressive strength of about 25 MPa, similar fresh concrete parameters (see Table 4-6) and contain three different aggregates. The BQ1 specimens have a weighted average MC of 3.7% in SSD condition, the BQ2 specimens 6.4% and the GQ specimens 0.45%. In the beginning the BQ1 specimens deform less than the BQ2 specimens but then gradually exceed the BQ2 specimens. The GQ specimens deform much less than the BQ specimens.

The fact that the less porous BQ1 aggregate specimens deform more than the BQ2 specimens is contrary to the established theories. Section 2.6 describes the physical mechanism of concrete creep. The creep strain for aggregates is considered equal to zero. Since aggregates do not creep they will restrain deformations. Figure 2-10 shows the restraining action of aggregates, stiffer aggregates yield less creep.

The question remains, are porous aggregate stiffer then less porous aggregate. The elastic properties of porous materials can be described by the empirical relationship of Phani and Niyogi or eq. (5.2) [70]

$$E = E_0\left(1 - \frac{p}{p_c}\right)^f\,, \tag{5.2}$$

where E is the elastic modulus of porous material with porosity p, E_0 is the elastic modulus of solid material, p_c is the porosity at which the elastic modulus becomes zero and f is a parameter dependent on the grain morphology and pore geometry of porous material. The value of f is a positive number and since the outcome inside the bracket is less than one, elastic modulus decreases with increasing porosity.

All the specimens are still deforming after five years.

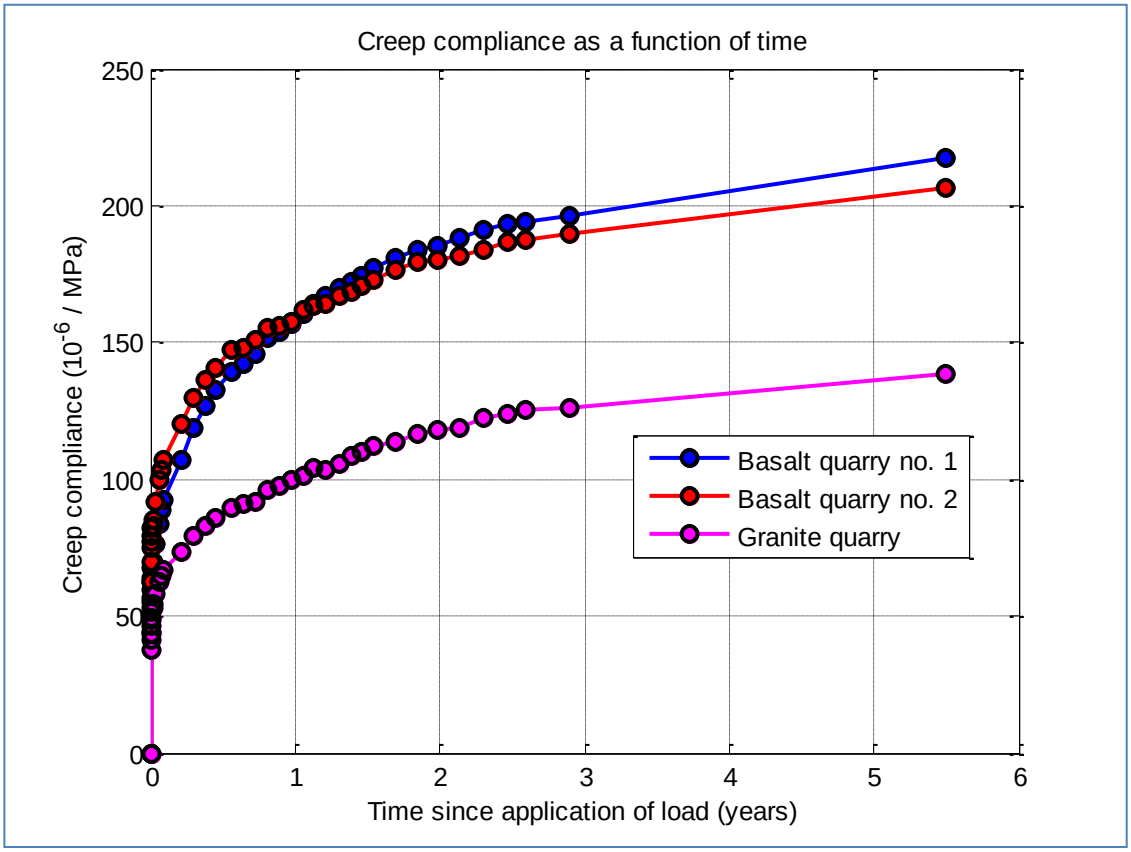

Figure 5-4: Creep compliance for the CVC_1 specimens from 2009, comprising three different mixes (BQ1, BQ2 and GQ).

Figure 5-5 excludes the elastic strain and shows that the difference between the BQ1 and BQ2 specimens is increasing. The physical mechanism of this behaviour cannot be verified in literature and a proper hypothesis is difficult to establish.

In a monograph by Guðni Jónsson, publish by the Icelandic Building Research Institute, a result bearing similarity is shown [15]. Creep specimens, containing C25/30 concrete with both porous and non-porous aggregate, were tested for a year. The result shows the same specific creep independent of aggregate porosity. This was however, only true for C25/30 concrete specimens, not for C35/45; C50/60 and C70/85.

Figure 5-6 shows the creep compliance for one of the oldest creep rigs, known as CVC_2 from 2002. All the specimens have characteristic compressive strength of about 50 MPa, similar fresh concrete properties (see Table 4-4) and contain three different aggregates. The BQ1 specimens have a weighted average MC of 3.5% in SSD condition, the BQ2 specimens have 6.2% and the BQ3 specimens have 3.4%. There is almost no difference in creep compliance between the BQ1 and BQ3 specimens but the BQ2 specimens deform more.

Figure 5-6 also shows that the specimens are still deforming after twelve years. This is congruent with literature, where it has been shown that concrete is still deforming after thirty years [23].

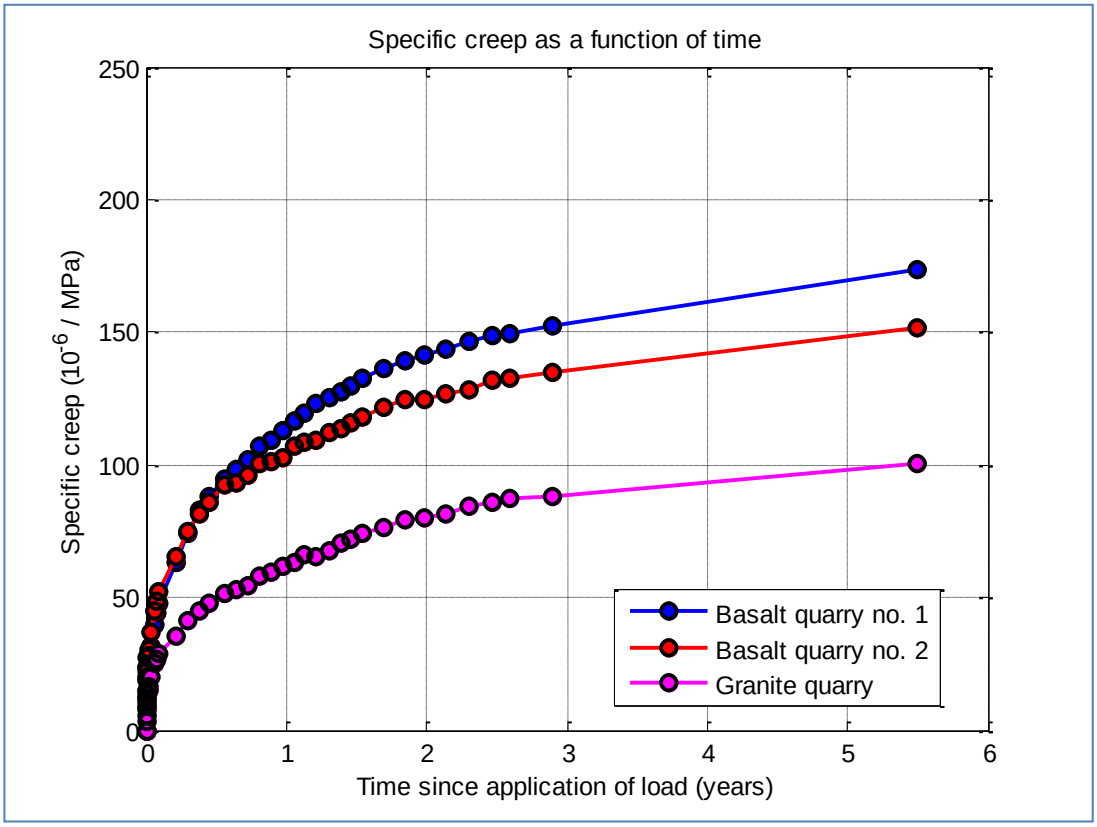

Figure 5-5: Specific creep for the CVC_1 specimens from 2009, comprising three mixes (BQ1, BQ2 and GQ).

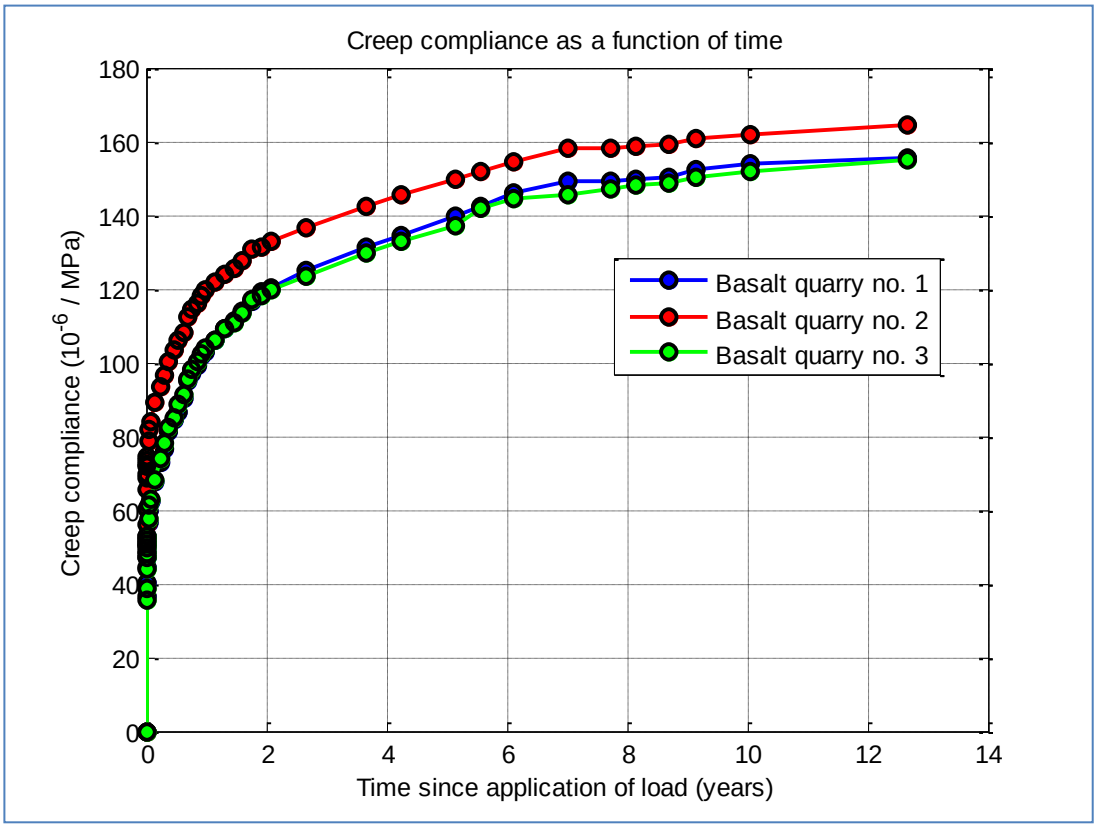

Figure 5-6: Creep compliance for the CVC_2 specimens from 2002, comprising three different mixes (BQ1, BQ2 and BQ3).

Table 5-2 shows that the BQ2 specimens have much lower E-modulus than the BQ1 & BQ3 specimens. If the specific creep is plotted, excluding the elastic strain, interesting results emerge (see Figure 5-7). The BQ2 specimens, containing aggregate with higher porosity, deform less than the BQ1 & BQ3 specimens. These results bear similarity to earlier tendency (see Figure 5-5).

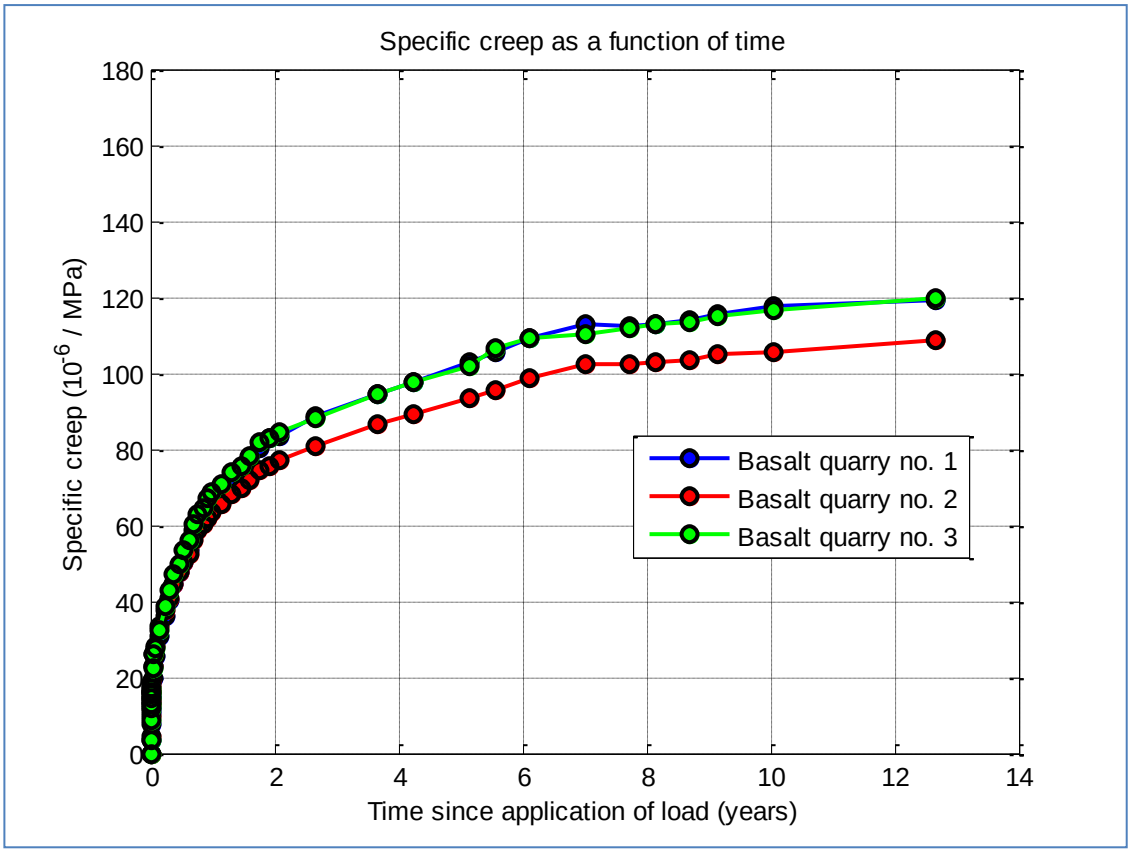

Figure 5-7: Specific creep for the CVC_2 specimens from 2002, comprising three different mixes (BQ1, BQ2 and BQ3).

Figure 5-8 shows the creep compliance for creep rig, known as CVC_3, from 2002. The specimens have characteristic compressive strength ranging from 62.4 to 69.5 MPa (see Table 5-2), similar fresh concrete properties (see Table 4-4) and contain three different aggregates. The BQ1 specimens have a weighted average MC of 3.5% in SSD condition, the BQ2 specimens 6.2% and the BQ3 specimens 3.4%. There is little difference in creep compliance between the BQ1 and BQ3 specimens but the BQ2 specimens deform more.

Figure 5-9 shows higher specific creep for the BQ2 specimens than BQ1 and BQ3. These results are in agreement with literature, where stiffer aggregate restrain deformations (see section 2.6).

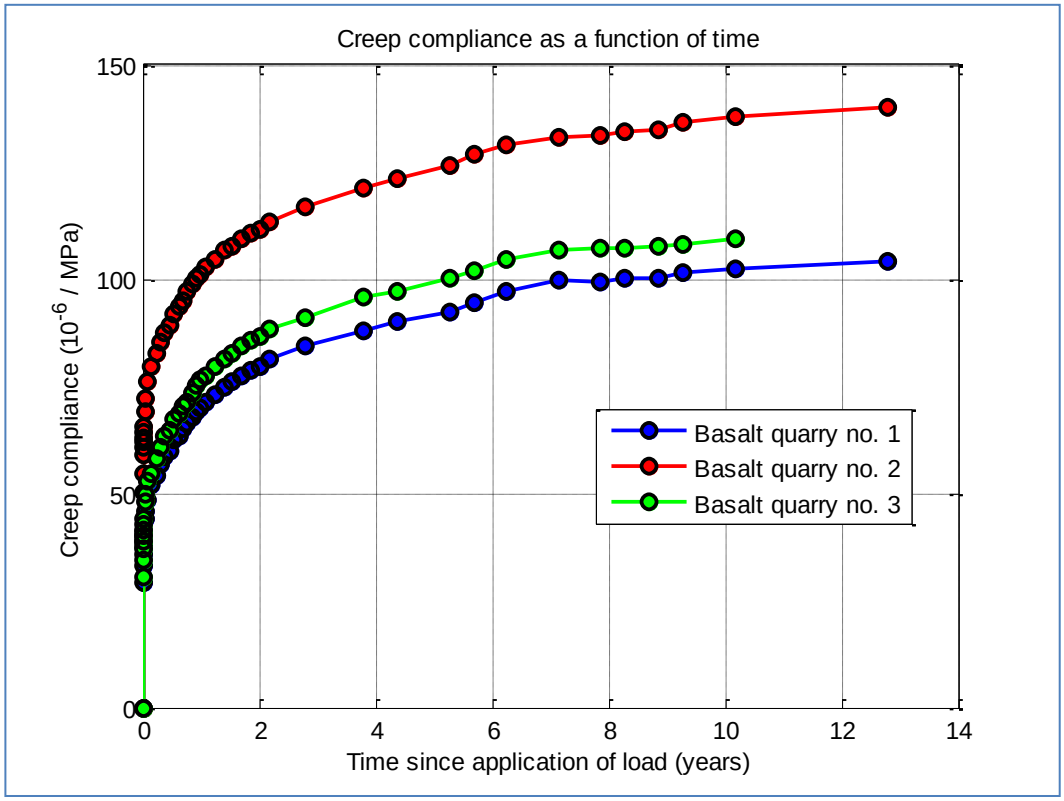

Figure 5-8: Creep compliance for the CVC_3 specimens from 2002, comprising three mixes (BQ1, BQ2 and BQ3). Note: It was impossible to get an accurate strain reading for the last BQ3 measurement.

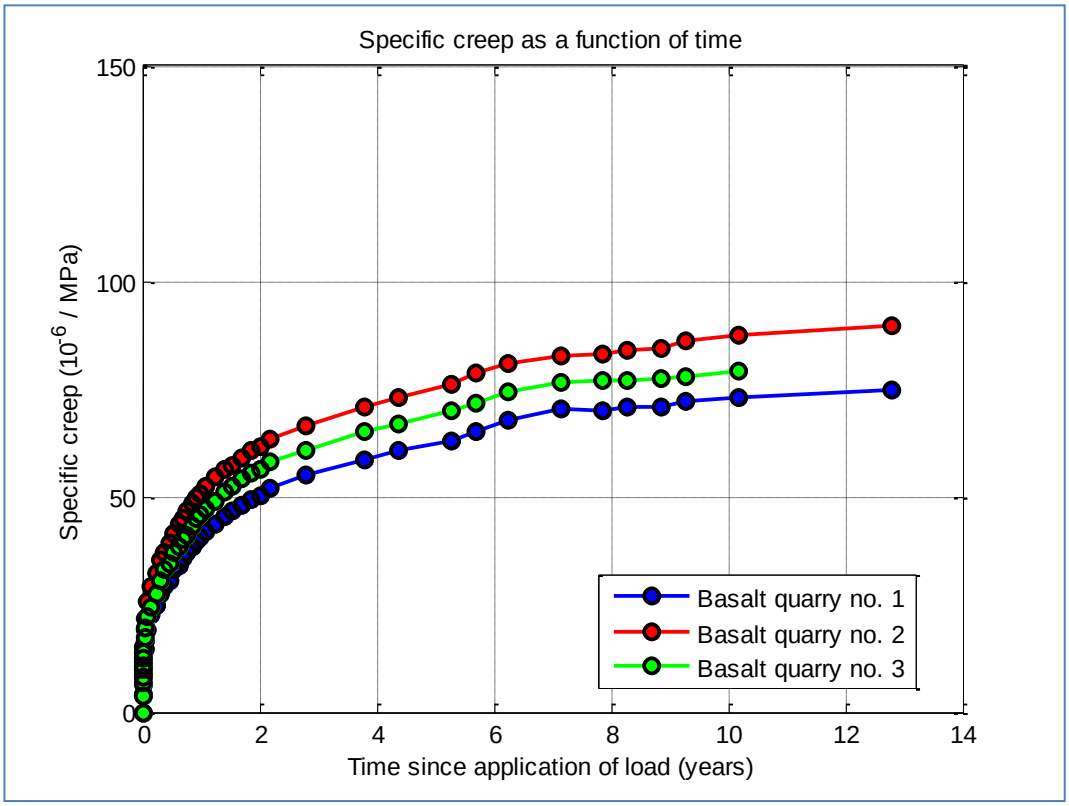

Figure 5-9: Specific creep for the CVC_3 specimens from 2002, comp three mixes (BQ1, BQ2 and BQ3). Note: It was impossible to get an accurate strain reading for the last BQ3 measurement.

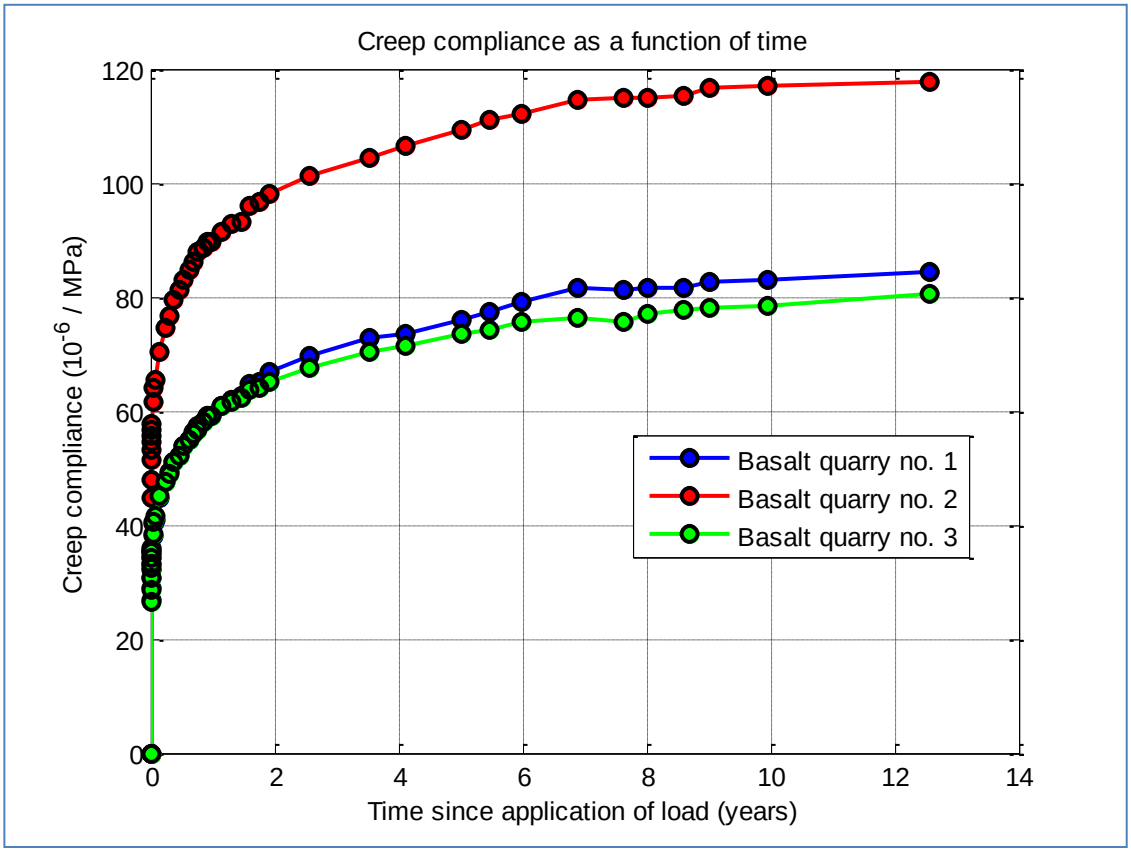

Figure 5-10: Creep compliance for the CVC_4 specimens from 2002, comprising three different mixes (BQ1, BQ2 and BQ3).

Figure 5-10 shows the creep compliance for one of the oldest creep rigs, known as CVC_4 from 2002. The specimens have characteristic compressive strength ranging from 65.5 to 83.4 MPa (see Table 5-2), similar fresh concrete properties (see Table 4-4) and contain three different aggregates. The BQ1 specimens have a weighted average MC of 2.7% in SSD condition, the BQ2 specimens 5.5% and the BQ3 specimens 2.7%. There is little difference in creep compliance between the BQ1 and BQ3 specimens but the BQ2 specimens deform much more.

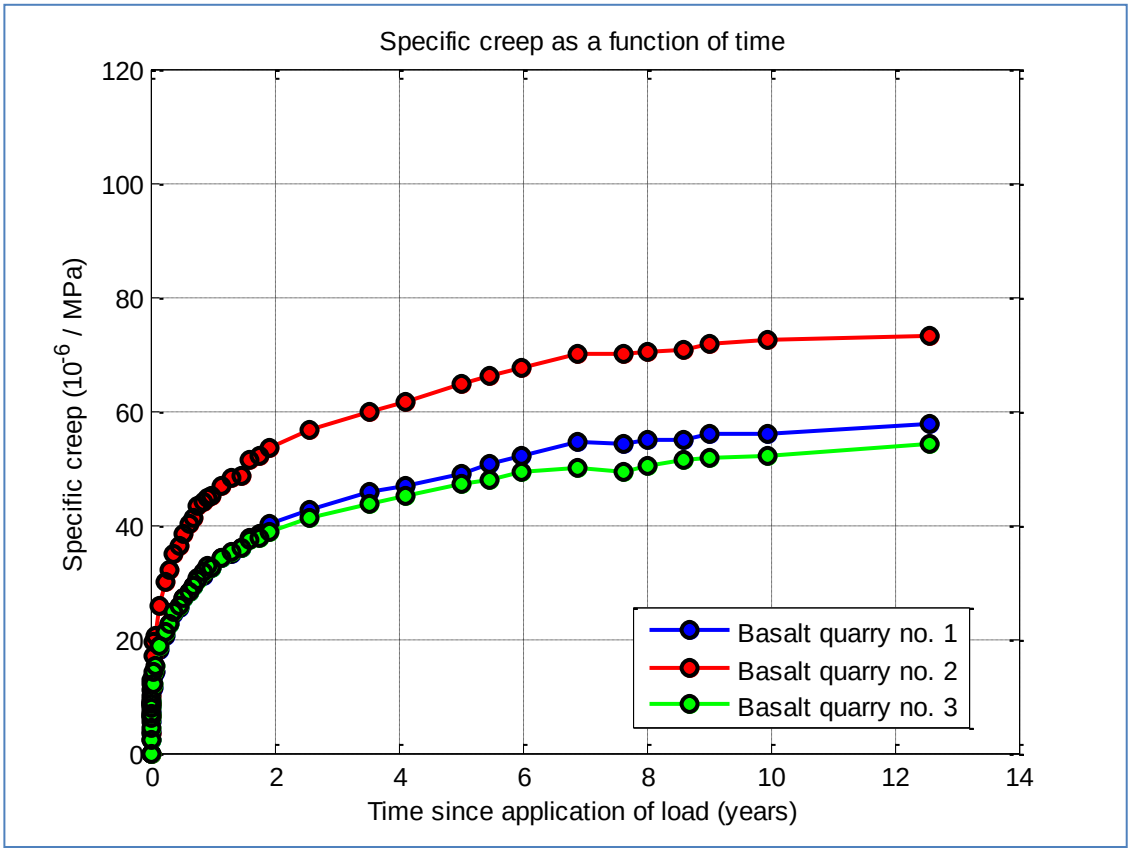

Figure 5-11: Specific creep for the CVC_4 specimens from 2002, comprising three different mixes (BQ1, BQ2 and BQ3).

Figure 5-11 shows higher specific creep for the BQ2 specimens than BQ1 and BQ3 and is therefore also in agreement with literature. The difference in specific creep seems to be dependent on concrete strength, i.e. cement content and water-cement ratio. It has been difficult to formulate a proper hypothesis for these findings and it must be a subject of further research.

It should be noted that the main difference between BQ1 and BQ3 aggregates is its shape. The BQ1 aggregate is rounded from seabed quarry and BQ3 is crushed aggregate from inland quarry. The aggregate shape appears to have little effect on the specific creep (see Figure 5-7, Figure 5-9 and Figure 5-11).

Figure 5-12 shows the specific creep for different strength classes all comprised of BQ1 aggregate and Figure 5-13 shows the specific creep for the same strength classes all comprised of BQ2 aggregate. The graphs show that specific creep is dependent on the compressive strength of concrete. These results are not surprising since it is the water-cement ratio that mainly governs the compressive strength of concrete by influencing the amount of capillary pores. The water-cement ratio then affects the creep of concrete, but the origin of creep is considered to be caused by the movement of water between gel pores and capillary pores [15], [24] (see section 2.6).

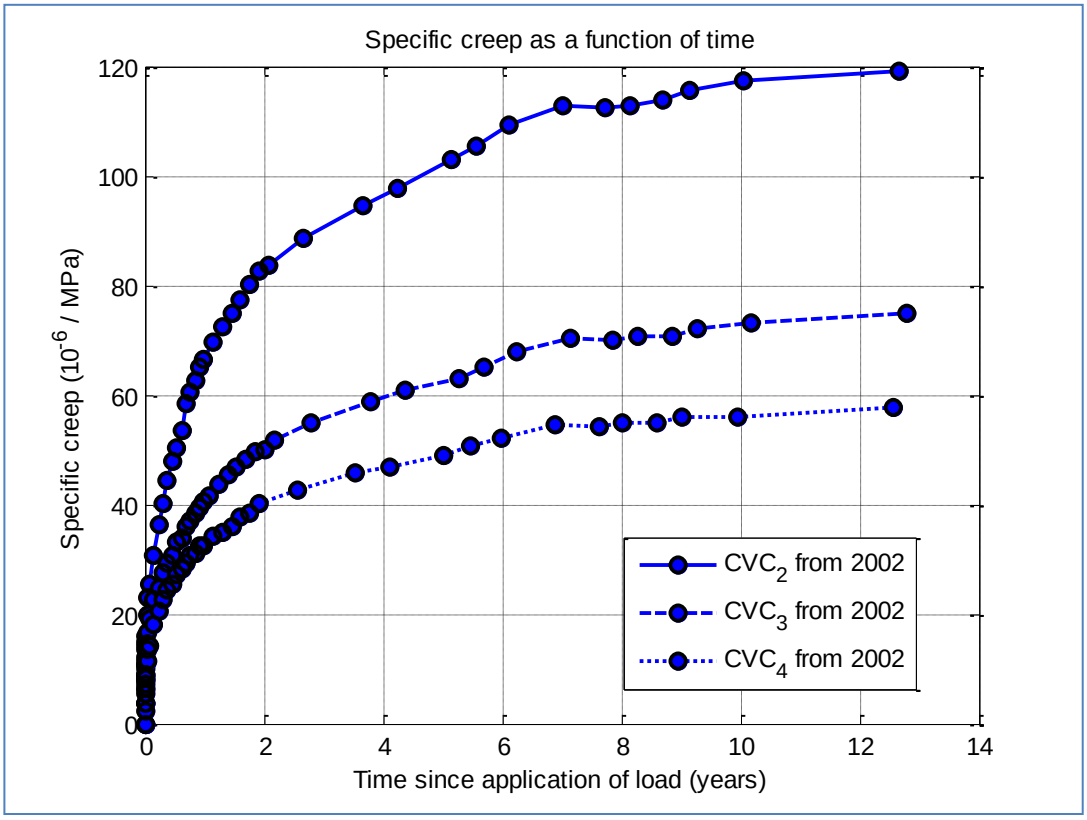

Figure 5-12: Specific creep for CVC_2, CVC_3 and CVC_4 specimens from 2002, all the specimens are comprised of BQ1 aggregates.

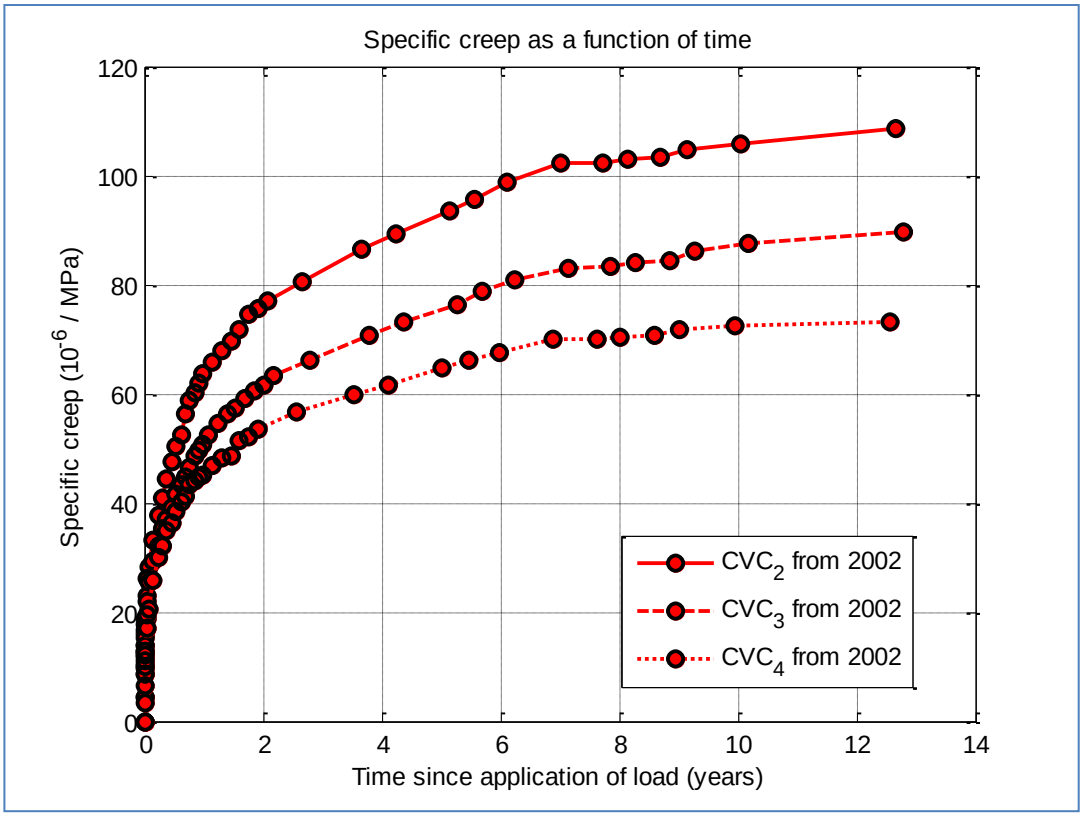

Figure 5-13: Specific creep for CVC_2, CVC_3 and CVC_4 specimens from 2002, all the specimens are comprised of BQ2 aggregates.

Figure 5-14 shows the specific creep for SCC specimens from 2010. All the specimens contain granite aggregate and have characteristic compressive strength from 40.4 to 50.0 MPa (Table 5-2). Table 4-7 shows the differences between the three mixes but in general they are: SCC rich in cement and supplementary cementitious materials (SCMs) using air entraining admixture (AEA). Two mixes named Eco-SCC, contain less cement and SCMs, one with and the other without AEA.

The experimental data shows that, in spite of less cement content, the Eco-SCC creeps more. This is likely due to the higher water-binder ratio in the Eco-SCC mixes. This result can be supported by literature (see section 2.6) but the origin of creep is generally considered to be caused by the movement of water between gel pores and capillary pores [15], [24].

The addition of AEA seems to have limited effect on Eco-SCC mixes, with respect to creep. There is no consensus in literature on the effect of AEA on creep, although some literature may suggest an increase in creep when adding AEA [15], [71]. Air void represent aggregate with zero E-modulus so that the resistance to creep deformation should be less in air entrained concrete. AEA generally improves the workability of concrete and allows the use of lower water-cement ratio, but creep decreases with lower water-cement ratio [23]. For practical conditions air entrainment is not considered an important factor in creep [21].

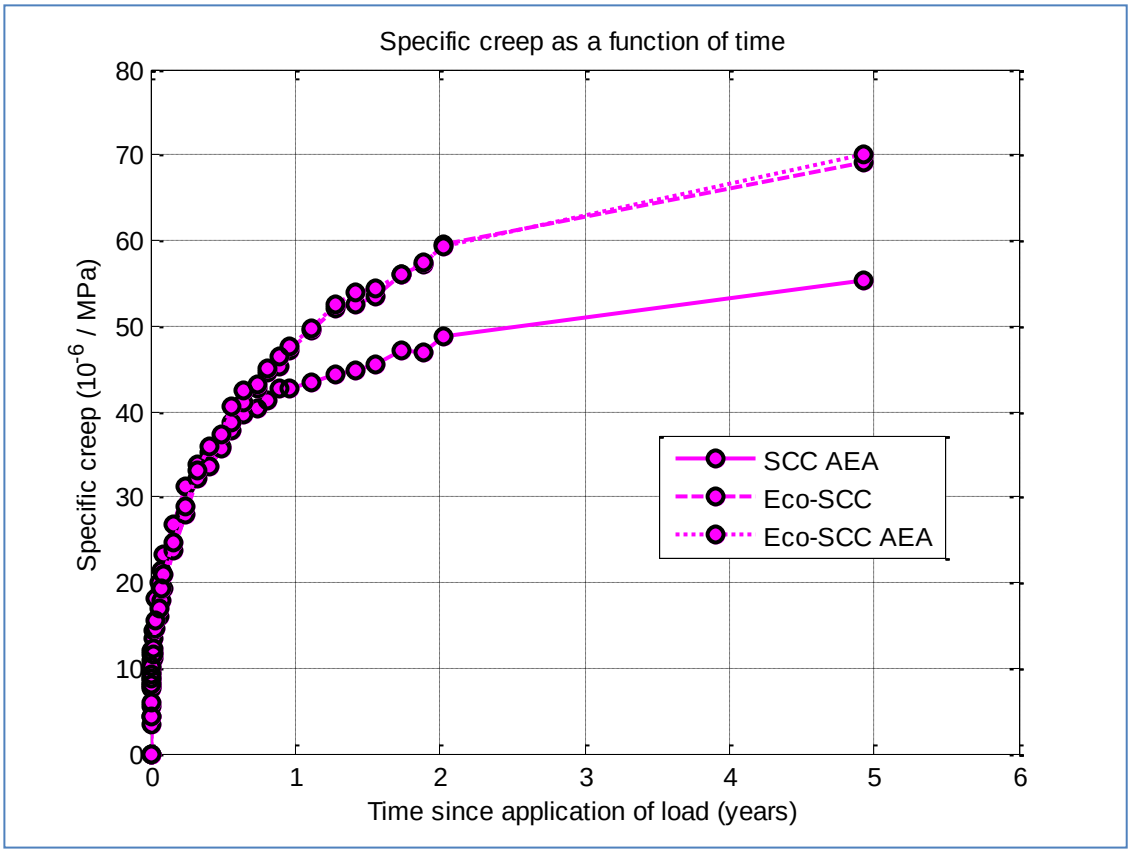

Figure 5-14: Specific creep for SCC specimens from 2010, comprising three granite specimens (SCC AEA, Eco-SCC and Eco-SCC AEA).

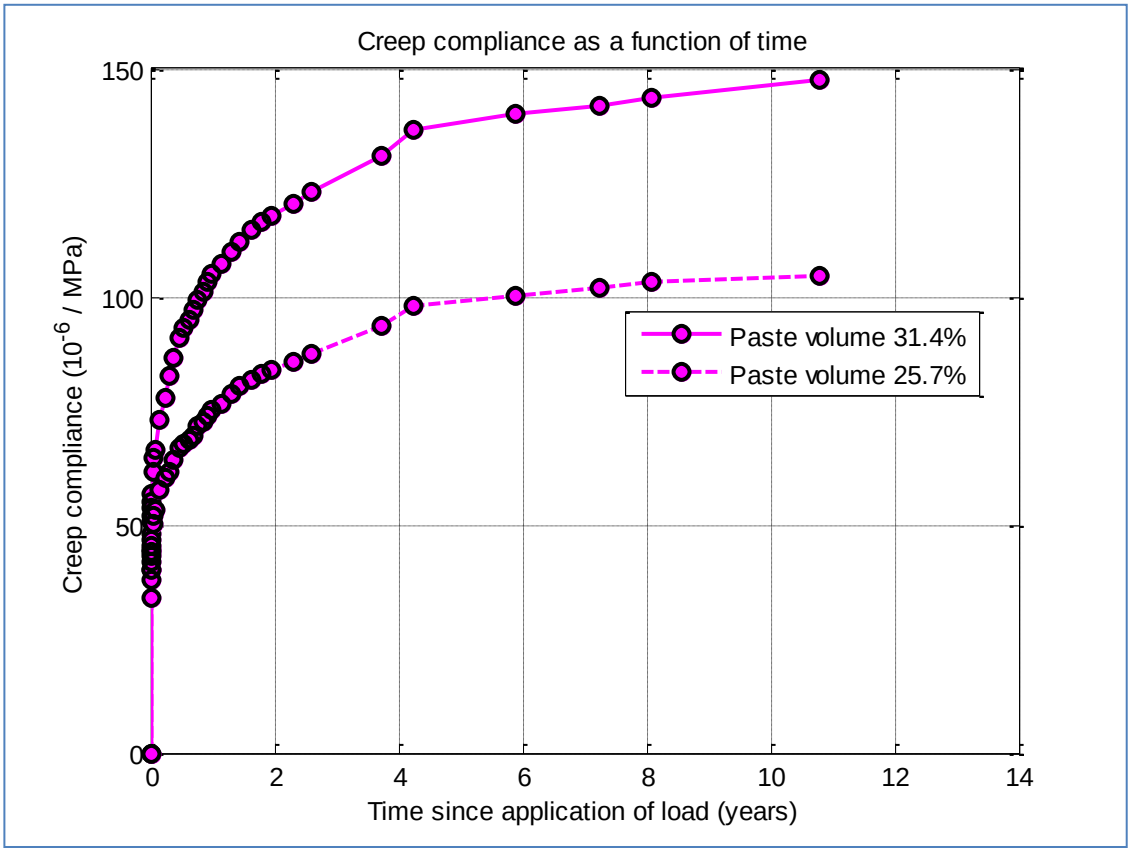

Figure 5-15: Creep compliance for specimens from 2004, comprising two granite mixes with paste volume of 31.4 and 27.7%.

Although some parameters concerning the specimens from 2004 are lost, at least some test data can be used. Figure 5-15 shows the creep compliance for two granite mixes with paste volume of 31.4 and 27.7%. The specimens with 31.4% paste volume have 440 kg/m^3 cement content and 8.4% air but the 25.7% paste volume specimens have 360 kg/m^3 cement content and 5.3% air. In both mixes the water to cement ratio and aggregate composition is the same.

The E-modulus for the specimens with 31.4% paste volume is 24.8 GPa and 29.4 GPa for the 25.7% paste volume specimens. This finding is in agreement with literature (see section 2.1), where the volume percentage of hydrated cement is replaced with the stiffer aggregate, thus increasing the E-modulus. The higher air content in the specimens with 31.4% paste volume is also a possible factor, since addition of air decreases the compressive strength and consequently the E-modulus.

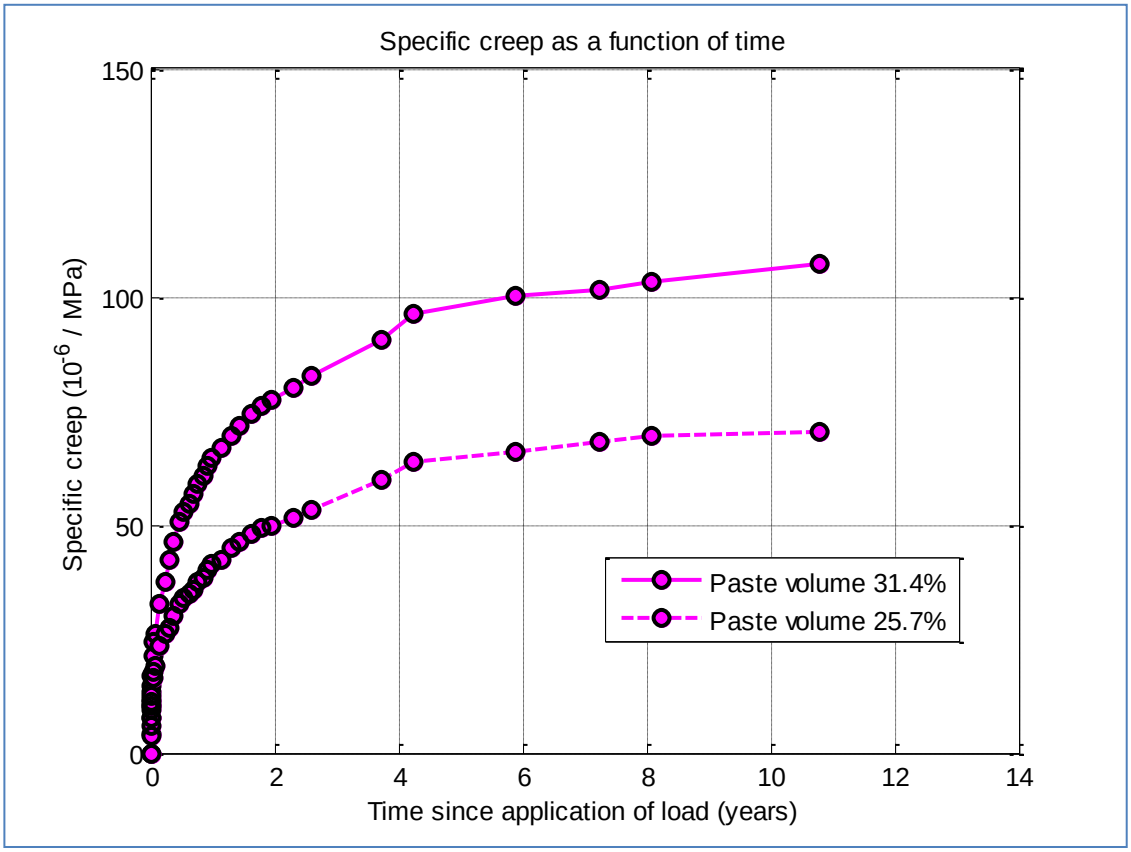

Figure 5-16: Specific creep for specimens from 2004, comprising two granite mixes with paste volume of 31.4 and 27.7%.

Figure 5-16 shows the specific creep for the two granite mixes from 2004. The specimens containing 31.4% paste volume creeps significantly more than the 25.7% paste volume specimens. It is difficult to identify a single cause for the increased creep, it might have been affected by air or cement content. The difference in specific creep is however so great ($36.9 \cdot 10^{-6}$ / MPa) that both these factors are likely the cause for higher creep-strain.

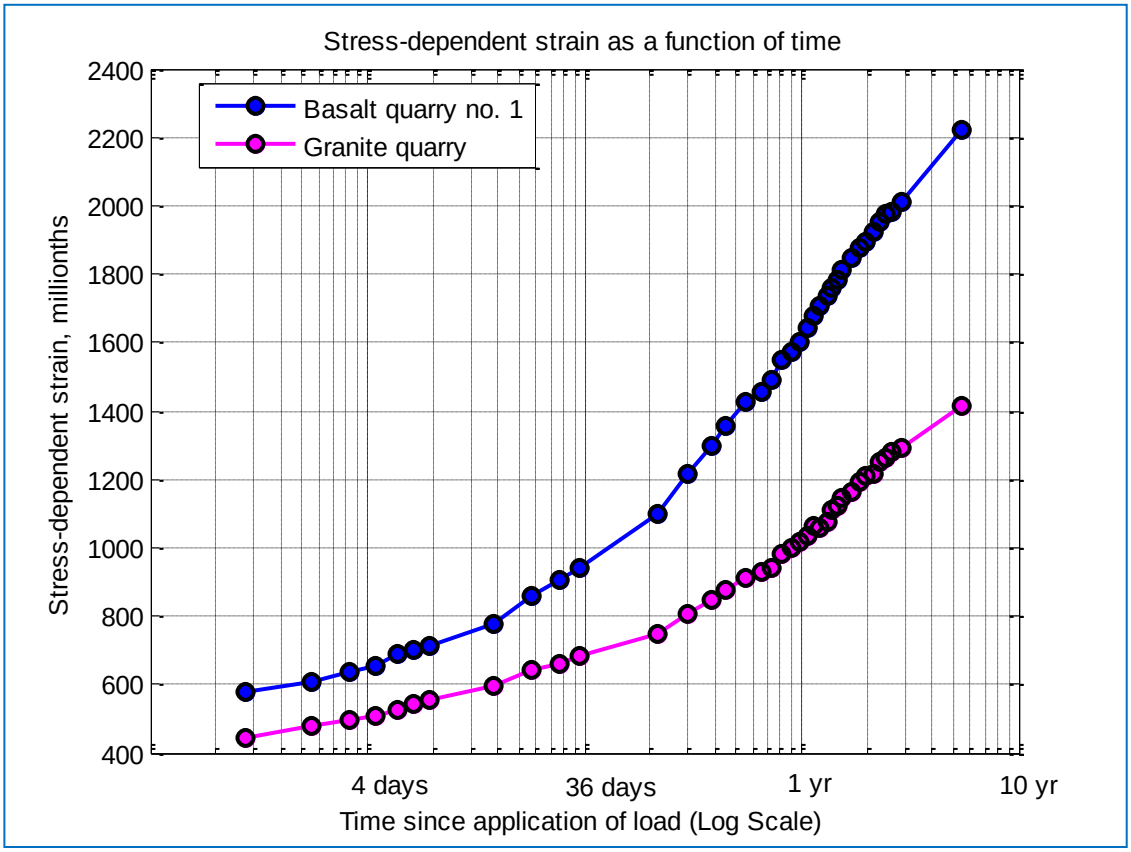

Figure 5-17: Effect of mineralogical character of aggregates on creep, CVC_1 specimens from 2009 and BQ1 containing GQ aggregate.

Figure 5-17 shows the stress-dependent strain for specimens from 2009, in logarithmic scale. All the specimens have characteristic compressive strength of about 25 MPa, similar fresh concrete properties (see Table 4-6) but contain aggregates from two quarries. The BQ1 specimens have a weighted average MC of 3.7% in SSD condition and the GQ specimens 0.45%. The results confirm the effect of mineralogical characteristics of aggregates upon creep; from section 2.8 (see Figure 2-16). The rate of creep for concrete containing basalt aggregates exceeds the concrete containing granite after a few months.

5.2.3 Comparison between Models and Test Data

In order to best compare test data on creep strain to mathematical models, all the model parameters need to be unambiguous. This is not the case when using the EC2 model in conjunction with the corresponding INA. The INA to EC2 suggests two reduction factors for E-modulus, based on aggregate porosity, but gives no guidance for which porosity range each reduction factor belongs to. Due to this ambiguity, the comparison between models and experimental results will be based on creep coefficient and thus excluding the E-modulus as a model parameter.

Figure 5-18 shows experimental development of creep coefficient for CVC_1 and aggregate from BQ1 in comparison with four mathematical creep models. Early on EC2; fib MC 10 and Model B3 overestimate the creep development but as time passes the data vastly overtake the models.

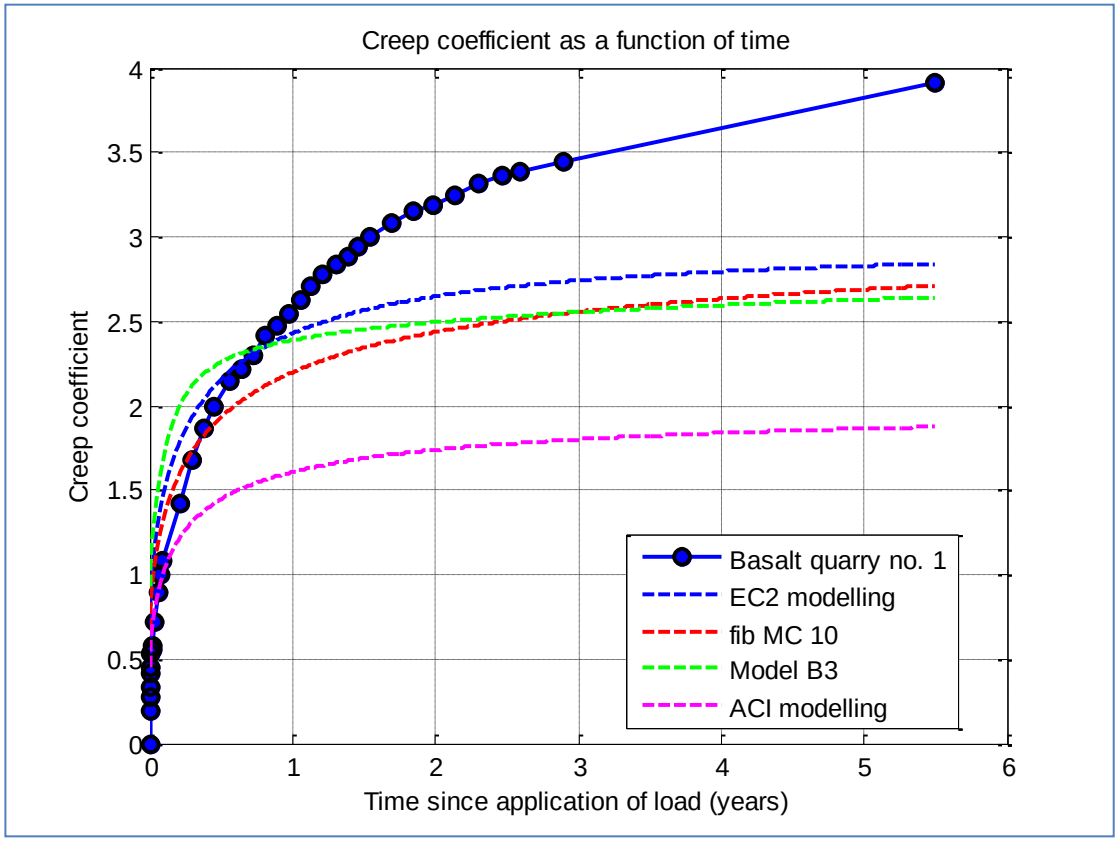

Figure 5-18: Measured creep coefficient for the CVC_1 specimens from 2009, comprising BQ1 aggregate and comparison to four creep models.

Figure 5-19 shows experimental development of creep coefficient for CVC_1 and aggregate from BQ2 in comparison with four mathematical creep models. The difference between experimental results and models is not as much as shown using BQ1 aggregate. The smaller difference is both due to less creep development in the BQ2 specimens as well as larger characteristic compressive strength that affect the models. Note: The rate of creep in the experimental results appears constant while the creep rate in the models seems to be levelling out.

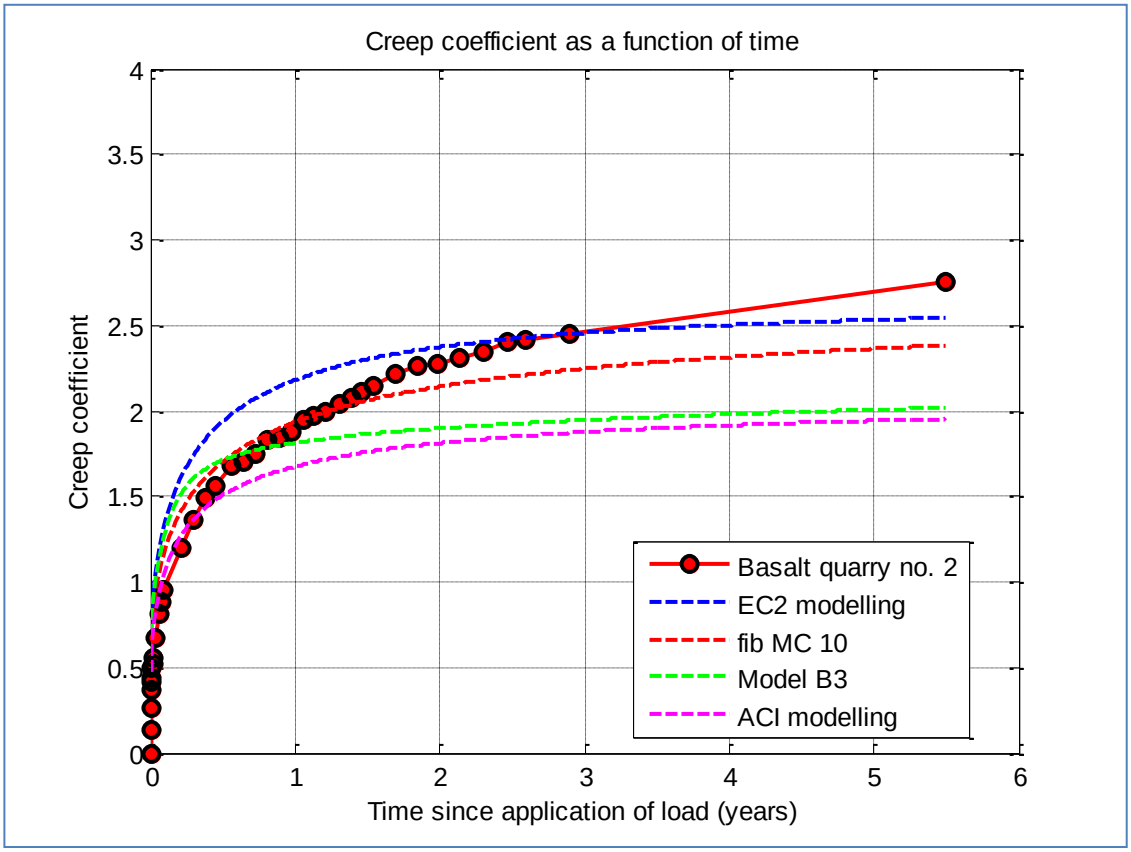

Figure 5-19: Measured creep coefficient for the CVC_1 specimens from 2009, comprising BQ2 aggregate and comparison to four creep models.

Figure 5-20 shows experimental development of creep coefficient for CVC_1 and GQ aggregate in comparison with four mathematical creep models. The EC2 and Model B3 overestimate the creep development, ACI model underestimates creep development and fib model code best describes the creep development.

When comparing Figure 5-19 and Figure 5-20 the creep coefficient, after little over 5 years, is almost the same for concrete containing different aggregate. It should be noted that the specific creep is the creep coefficient divided by the E-modulus, see eq. (5.1). Since the E-modulus for the concrete with GQ aggregate is higher than concrete with BQ2 aggregate, the specific creep for concrete with GQ aggregate is lower.

Figure 5-21 shows experimental development of creep coefficient for CVC_2 and aggregate from BQ1 in comparison with four mathematical creep models. The difference between experimental results and EC2 and fib MC 10 models is sizeable but not as much compared to Model B3 and ACI modelling.

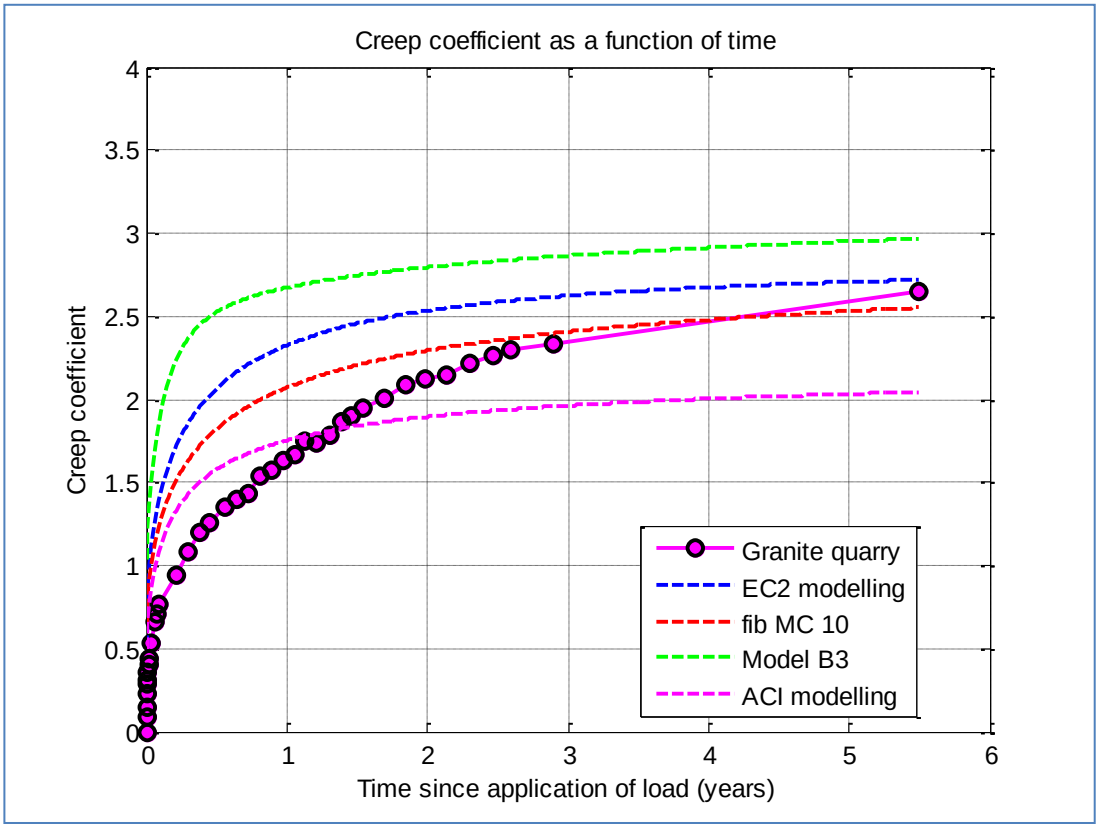

Figure 5-20: Measured creep coefficient for the CVC_1 specimens from 2009, comprising GQ aggregate and comparison to four creep models.

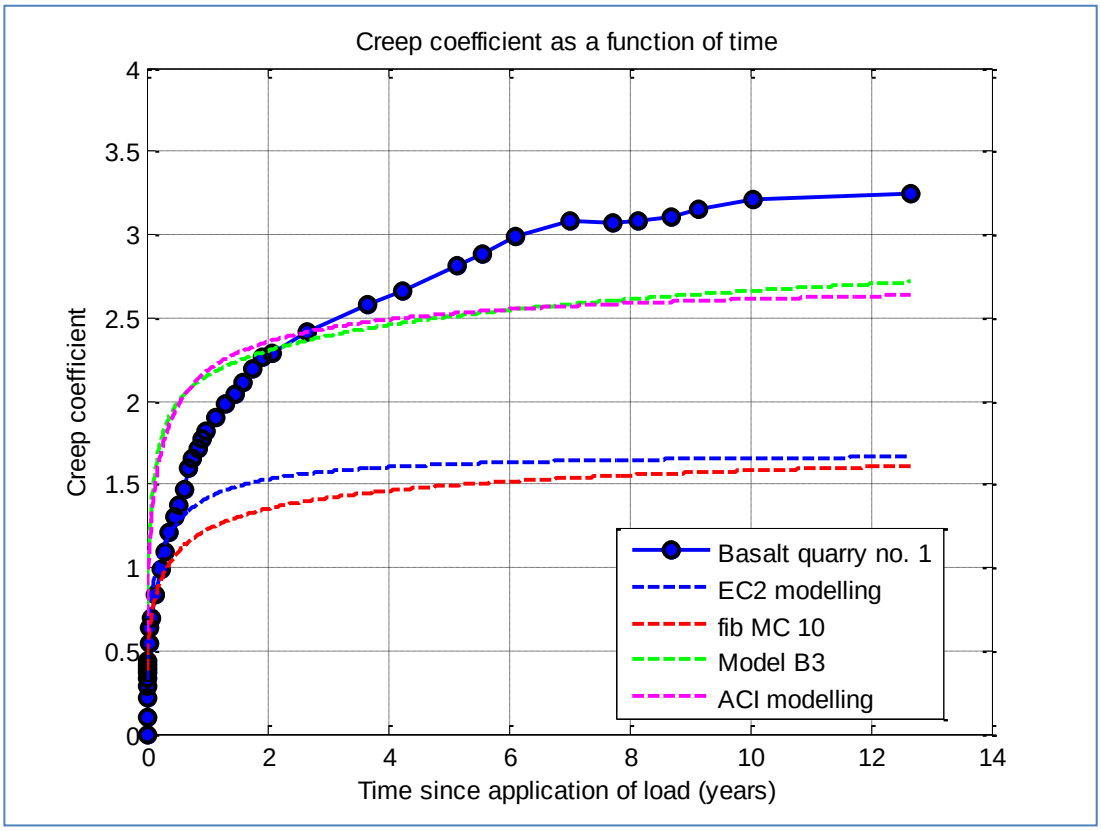

Figure 5-21: Measured creep coefficient for the CVC_2 specimens from 2002, comprising BQ1 aggregate and comparison to four creep models.

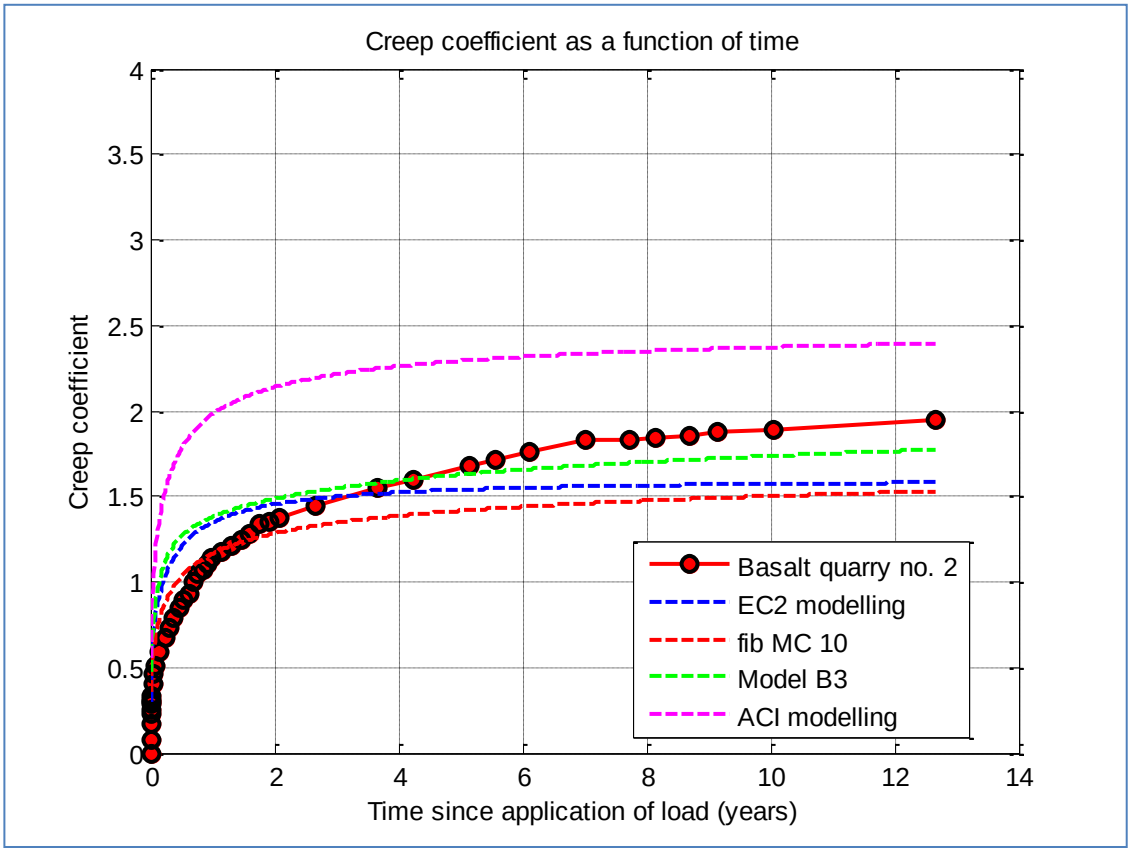

Figure 5-22: Measured creep coefficient for the CVC_2 specimens from 2002, comprising BQ2 aggregate and comparison to four creep models.

Figure 5-22 shows experimental development of creep coefficient for CVC_2 and aggregate from BQ2 in comparison with four mathematical creep models. The EC2; fib MC 10 and Model B3 underestimate the creep coefficient, but the ACI modelling overestimates the creep coefficient.

Figure 5-23 and Figure 5-24 show experimental development of creep coefficient for CVC_4 and aggregates from BQ1 and BQ2 in comparison with four mathematical creep models.

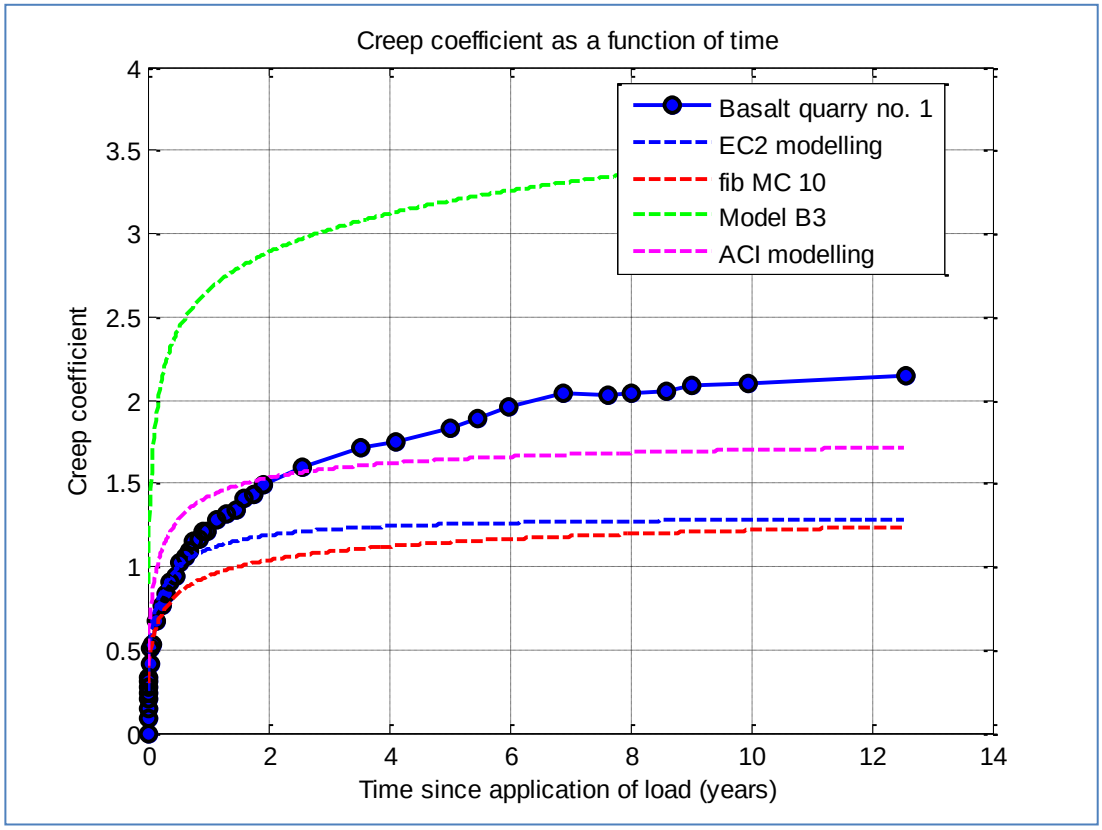

Figure 5-23: Measured creep coefficient for the CVC_4 specimens from 2002, comprising BQ1 aggregate and comparison to four creep models.

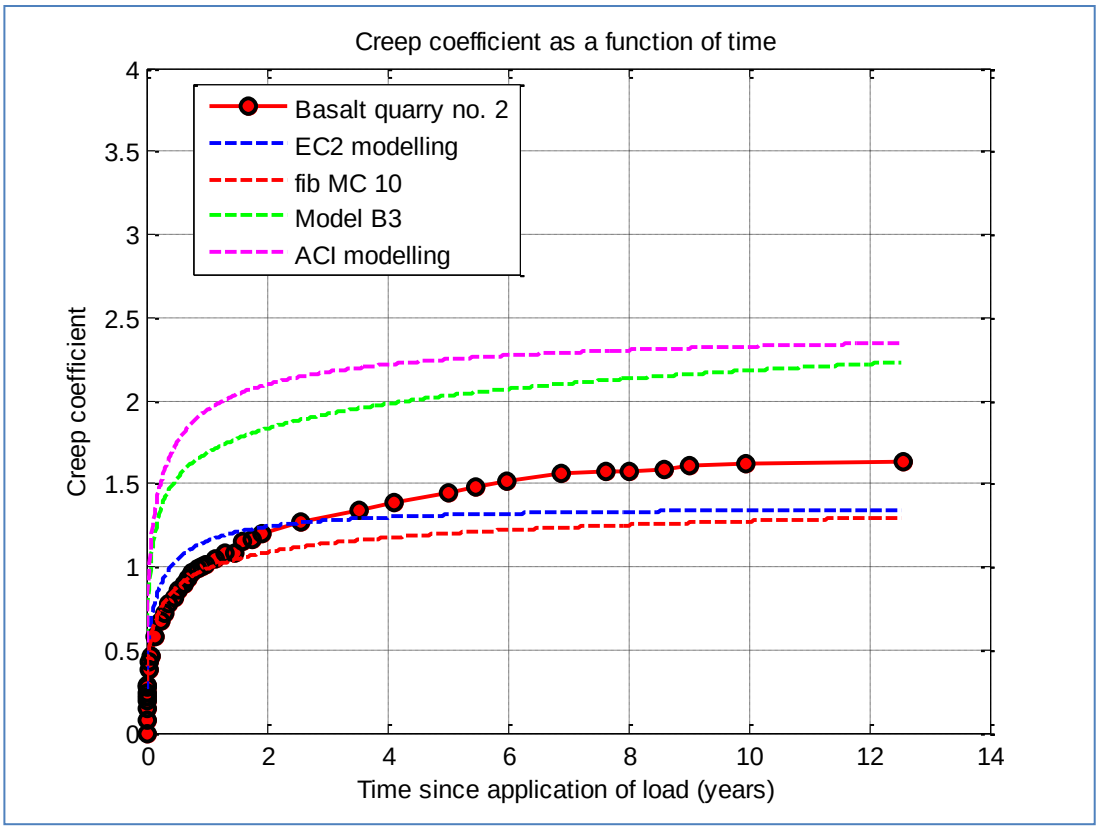

Figure 5-24: Measured creep coefficient for the CVC_4 specimens from 2002, comprising BQ2 aggregate and comparison to four creep models.

The comparison between experimental development of creep coefficient to well accepted mathematical models indicate that concrete made of porous basalt aggregate generally exhibits greater creep than expected.

5.3 Phase III

5.3.1 Deflection Calculations

Section 3.4 describes the slab in question; relevant theories; assumptions of load on the structure; relevant codes and the governing equation for comparison.

Figure 5-25 shows detailed deflection estimation based on material properties and model assumptions according to EC2 and INA. The deflection due to creep and shrinkage (δ_{QP}) is 38.3 mm and the elastic deflection (δ_{rare}) is 30.5 mm. The total deflection of 41.9 mm is calculated according to eq. (5.3)

$$\delta_{tot} = \delta_{QP} + \delta_{rare}\frac{M_{rare} - M_{QP}}{M_{rare}} \tag{5.3}$$

where M_{rare} is the bending moment due to maximum service limit load and M_{QP} bending moment due to quasi-permanent load.

TABLE CALCULATOR - DEFLECTION FOR UNIT STRIP

This program returns values for deflection for unit strip of slab.

Slab parameters

h	Thickness of slab	200 mm
d	Effective depth of tension reinforcement	160 mm
d´	Depth to compression reinforcement	40 mm
f_{ck}	Characteristic cylinder strength of concrete	50 MPa
A_s	Cross-sectional area of tension reinforcement	452.4 mm²
A'_s	Cross-sectional area of compression reinforcement	452.4 mm²
M_{QP}	Design value of bending moment (Quasi-permanent)	26,338 Nm
M_{rare}	Design value of bending moment (Rare)	29,938 Nm
t	Adjusted age of concrete	12.7 yr
t_0	Adjusted age of concrete at loading	28 days
RH	Ambient relative humidity	50%
	K-constant for deflection calculations	0.1042
	Span length	5.0 m

Other values

Non-porous aggregate from INA Characteristic tensile strength	0.90

Derived values

	Material properties				For deflection (Quasi-permanent)		
E_{cm}	33,550 MPa	f_{ctk} / f_{ctm}	2.9 MPa	α_1	0.7022	x_u	100.0 mm
f_{cm}	58.0 MPa	$\alpha_{e,rare}$	5.961	α_2	0.9039	x_c	40.0 mm
$E_{c,efl}$	13,583 MPa	$\alpha_{e,QP}$	14.724	α_3	0.7768	S_u	0 mm³
E_s	200,000 MPa	ε_{cd}	3.224E-04	h_0	200 mm	S_c	54,298 mm³
$\varepsilon_{cd,0}$	3.793E-04	$\varepsilon_{ca}(\infty)$	1.000E-04	ϕ_{RH}	1.4466	I_u	7.11E+08 mm^4
ε_{cs}	4.224E-04	α_{ds2}	0.12	$\beta(f_{cm})$	2.2059	I_c	1.17E+08 mm^4
α_{ds1}	4	ξ_{max}	0.6932	$\beta(t_0)$	0.4749	M_{cr}	20,630 Nm
	For deflection (rare)			ϕ_0	1.5155	ξ	0.6932
x_u	100.0 mm	x_c	27.7 mm	β_H	494.24	$1/r_n$	1.2E-05 (1/mm)
I_u	6.83E+08 mm^4	I_c	5.46E+07 mm^4	β_c	0.9700	β_{RH}	1.3563
M_{cr}	19,802 Nm	ξ	0.5625	$\phi(t,t_0)$	1.4700	$1/r_{CS}$	2.0E-06 (1/mm)
1/r	1.2E-05 (1/mm)			k_h	0.8500	$1/r_{t,QP}$	1.4E-05 (1/mm)

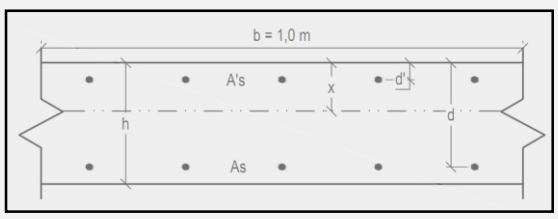

δ_{QP}	Deflection due to creep and shrinkage (Quasi-permanent):	**38.3 mm**
δ_{rare}	Elastic deflection (rare):	**30.5 mm**
δ_{tot}	Total deflection:	**41.9 mm**

Figure 5-25: Deflection calculations based on material properties and model assumptions according to EC2 and INA.

Figure 5-26 shows deflection estimation based on the creep compliance from figure 5-6 in conjunction with equation (3.10) and using BQ1 aggregate. The deflection due to creep and shrinkage is 40.8 mm and the elastic deflection is 30.6 mm, nearly the same as in previous deflection estimation (see Figure 5-25). The total deflection is 44.5 mm, 6.2% increase from the calculations based on EC2 parameters.

The modest increase in elastic deflection, despite significant decrease in E-modulus, is due to the drop in maximum distribution coefficient (ζ_{max}) (see section 3.4). The distribution coefficient is the ratio of uncracked and fully cracked conditions allowing for tension stiffening where the unit strip is uncracked. Once an arbitrary section cracks it will remain cracked and consequently, deflection estimations are based on the maximum distribution coefficient or eq. (5.4)

$$\zeta_{max} = \max\left[\zeta_{QP}\,;\,\zeta_{rare}\right] \tag{5.4}$$

where ζ_{QP} is the distribution coefficient based on quasi permanent loading and ζ_{rare} is the distribution coefficient based on the total SLS loading.

TABLE CALCULATOR - DEFLECTION FOR UNIT STRIP

This program returns values for deflection for unit strip of slab.

Slab parameters

h	Thickness of slab	200 mm
d	Effective depth of tension reinforcement	160 mm
d´	Depth to compression reinforcement	40 mm
f_{ck}	Characteristic cylinder strength of concrete	50 MPa
A_s	Cross-sectional area of tension reinforcement	452.4 mm²
$A´_s$	Cross-sectional area of compression reinforcement	452.4 mm²
M_{QP}	Design value of bending moment (Quasi-permanent)	26,338 Nm
M_{rare}	Design value of bending moment (Rare)	29,938 Nm
t	Adjusted age of concrete	12.7 yr
t_0	Adjusted age of concrete at loading	28 days
RH	Ambient relative humidity	50%
	K-constant for deflection calculations	0.1042
	Span length	5.0 m

Other values

Non-porous aggregate from INA Characteristic tensile strength	0.90

δ_{QP}	Deflection due to creep and shrinkage (Quasi-permanent):	**40.8 mm**
δ_{rare}	Elastic deflection (rare):	**30.6 mm**
δ_{tot}	Total deflection:	**44.5 mm**

Derived values

Material properties				For deflection (Quasi-permanent)			
E_{cm}	**27,303 MPa**	f_{ctk} / f_{ctm}	2.9 MPa	α_1	0.7022	x_u	100.0 mm
f_{cm}	58.0 MPa	$\alpha_{e,rare}$	7.325	α_2	0.9039	x_c	47.2 mm
$E_{c,eff}$	8,595 MPa	$\alpha_{e,QP}$	23.269	α_3	0.7768	S_u	0 mm³
E_s	200,000 MPa	ε_{cd}	3.224E-04	h_0	200 mm	S_c	47,760 mm³
$\varepsilon_{cd,0}$	3.793E-04	$\varepsilon_{ca}(\infty)$	1.000E-04	ϕ_{RH}	1.4466	I_u	7.39E+08 mm^4
ε_{cs}	4.224E-04	α_{ds2}	0.12	$\beta(f_{cm})$	2.2059	I_c	1.70E+08 mm^4
α_{ds1}	4	ξ_{max}	0.6688	$\beta(t_0)$	0.4749	M_{cr}	21,437 Nm
For deflection (rare)				ϕ_0	1.5155	ξ	0.6688
x_u	100.0 mm	x_c	30.3 mm	β_H	494.24	$1/r_n$	1.3E-05 (1/mm)
I_u	6.87E+08 mm^4	I_c	6.53E+07 mm^4	β_c	0.9700	β_{RH}	1.3563
M_{cr}	19,931 Nm	ξ	0.5568	$\phi(t,t_0)$	**2.1764**	$1/r_{CS}$	1.9E-06 (1/mm)
1/r	1.2E-05 (1/mm)			k_h	0.8500	$1/r_{t,QP}$	1.5E-05 (1/mm)

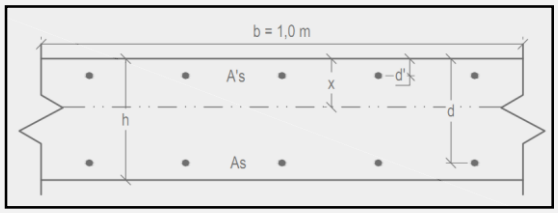

Figure 5-26: Deflection calculations based on the creep compliance according to figure 5-6 in conjunction with equation (3.10) and using BQ1 aggregate.

Figure 5-27 shows deflection estimation based on the creep compliance from figure 5-6 in conjunction with equation (3.10) and using BQ2 aggregate. The deflection due to creep and shrinkage is 42.3 mm and the elastic deflection is 32.5 mm. The total deflection is 46.5 mm or 10.3% increase from the calculations based on EC2 parameters.

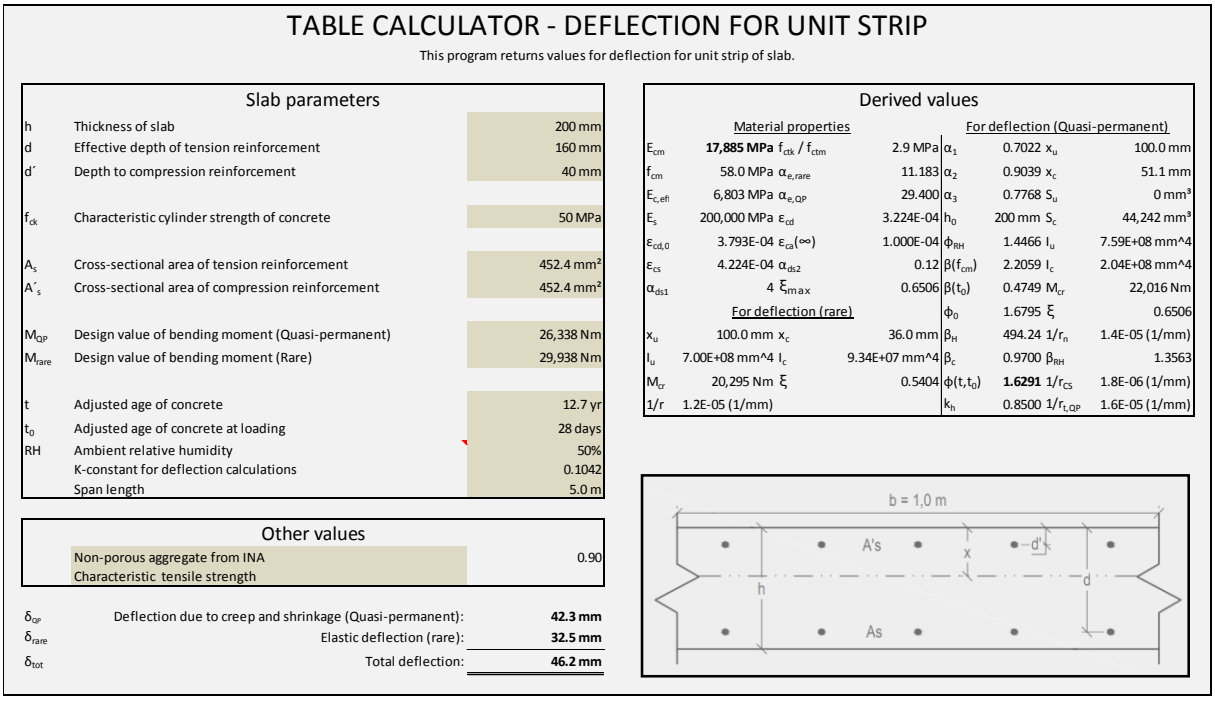

TABLE CALCULATOR - DEFLECTION FOR UNIT STRIP

This program returns values for deflection for unit strip of slab.

Slab parameters

h	Thickness of slab	200 mm
d	Effective depth of tension reinforcement	160 mm
d´	Depth to compression reinforcement	40 mm
f_{ck}	Characteristic cylinder strength of concrete	50 MPa
A_s	Cross-sectional area of tension reinforcement	452.4 mm²
$A´_s$	Cross-sectional area of compression reinforcement	452.4 mm²
M_{QP}	Design value of bending moment (Quasi-permanent)	26,338 Nm
M_{rare}	Design value of bending moment (Rare)	29,938 Nm
t	Adjusted age of concrete	12.7 yr
t_0	Adjusted age of concrete at loading	28 days
RH	Ambient relative humidity	50%
	K-constant for deflection calculations	0.1042
	Span length	5.0 m

Other values

Non-porous aggregate from INA Characteristic tensile strength	0.90

δ_{QP}	Deflection due to creep and shrinkage (Quasi-permanent):	**42.3 mm**
δ_{rare}	Elastic deflection (rare):	**32.5 mm**
δ_{tot}	Total deflection:	**46.2 mm**

Derived values

Material properties				For deflection (Quasi-permanent)			
E_{cm}	**17,885 MPa**	f_{ctk} / f_{ctm}	2.9 MPa	α_1	0.7022	x_u	100.0 mm
f_{cm}	58.0 MPa	$\alpha_{e,rare}$	11.183	α_2	0.9039	x_c	51.1 mm
$E_{c,efl}$	6,803 MPa	$\alpha_{e,QP}$	29.400	α_3	0.7768	S_u	0 mm³
E_s	200,000 MPa	ε_{cd}	3.224E-04	h_0	200 mm	S_c	44,242 mm³
$\varepsilon_{cd,0}$	3.793E-04	$\varepsilon_{ca}(\infty)$	1.000E-04	ϕ_{RH}	1.4466	I_u	7.59E+08 mm^4
ε_{cs}	4.224E-04	α_{ds2}	0.12	$\beta(f_{cm})$	2.2059	I_c	2.04E+08 mm^4
α_{ds1}	4	ξ_{max}	0.6506	$\beta(t_0)$	0.4749	M_{cr}	22,016 Nm
For deflection (rare)				ϕ_0	1.6795	ξ	0.6506
x_u	100.0 mm	x_c	36.0 mm	β_H	494.24	$1/r_n$	1.4E-05 (1/mm)
I_u	7.00E+08 mm^4	I_c	9.34E+07 mm^4	β_c	0.9700	β_{RH}	1.3563
M_{cr}	20,295 Nm	ξ	0.5404	$\phi(t,t_0)$	**1.6291**	$1/r_{CS}$	1.8E-06 (1/mm)
1/r	1.2E-05 (1/mm)			k_h	0.8500	$1/r_{t,QP}$	1.6E-05 (1/mm)

Figure 5-27: Deflection calculations based on the creep compliance according to figure 5-6 in conjunction with equation (3.10) and using BQ2 aggregate.

Note: The estimated deflection is based on creep coefficient after little over twelve years. Figure 5-6 shows that the concrete is still deforming and thus the deflection is expected to increase, not least because concrete is known to deform for twenty to thirty years (see section 2.5).

5.3.2 Prestress Losses

Section 3.5 describes the post tensioned structure; exposure conditions; load on structure and the governing equation for comparison. The additional parameters needed for calculating the prestress force losses are:

Characteristic concrete strength $f_{ck} = 50\ MPa$
Coefficient of friction $\mu = 0.19$
Wobble factor $k = 0.01/m$
E-modulus from EC2 in conjunction with INA $E'_{cm} = 0.9\ E_{cm} = 33.55\ GPa$
Elastic modulus of steel tendon $E_s = 205\ GPa$
Creep coefficient, according to EC2 $\phi(t, t_0) = \phi(4626 + 28\ , 28) = 1.04$
Autogenous shrinkage strain from EC2 $\varepsilon_{ca} = 1.00 \cdot 10^{-4}$
Drying shrinkage strain from EC2 $\varepsilon_{cd} = 1.51 \cdot 10^{-4}$

Table 5-3 shows the estimated losses of initial prestress force, based on EC2 and INA and after the load has been moved to a single bridge beam, based on the resulting torque (see Appendix B for the area moment of inertia).

Additional abbreviations for tables containing estimations of prestress losses are as follows:

A	Cross-sectional area of concrete
A_p	Cross-sectional area of tendon
C	$y = C \cdot x^2$
e_{av}	Average eccentricity of tendon
h_0	Notional size
I	Area moment of inertia
k_h	Coefficient depending on the notional size h_0
P_0	Initial prestress force
u	Parameter of that part of the concrete cross-section which is exposed to drying
x	x- pos. at mid-span
y	y- pos. at mid-span (max. eccentricity of tendon)
α_e	Modular ratio
θ	The gradient at ends

Friction		*Elastic shortening*		*Creep*		*Shrinkage*		*Relaxation at anchor*	
μ	0.19	A_p	1.56 E+04 mm²	u	1.03 E+04 mm	ε_{cd}	1.51 E-04		2.5
k	0.01 /m	A	2.45 E+06 mm²	h_0	477 mm	k_h	0.7057		
x	20.0 m	α_e	6.11	$\varphi(t,t_0)$	**1.04**	ε_{ca}	1.00 E-04		
y	1.25 m	e_{av}	0.783 m	E_s	205 GPa	ε_{cs}	2.51 E-04		
C	0.00313 /m	I	1.32 E+12 mm^4	E'_{cm}	**33.6 GPa**				
θ	0.125 rad	P'	16.8 MN	ΔP	1.31 MN	ΔP	803 kN	ΔP	988 kN
	5.99%		**1.91%**		**7.62%**		**4.68%**		**5.76%**
				P_0 = 17.2 MN		Total estimated losses	**26.0%**	of P_0	

Table 5-3: Estimated losses of initial prestress force, based on EC2 and INA.

Table 5-4 shows the estimated losses of initial prestress force, based on the creep compliance from figure 5-6 in conjunction with equation (3.10) and using BQ1 aggregate. The total estimated losses are 36.6%, exceeding those values based on EC2 and INA by 10.6%.

Friction		*Elastic shortening*		*Creep*		*Shrinkage*		*Relaxation at anchor*	
μ	0.19	A_p	1.56 E+04 mm²	u	1.03 E+04 mm	ε_{cd}	1.51 E-04		2.5
k	0.01 /m	A	2.45 E+06 mm²	h_0	477 mm	k_h	0.7057		
x	20.0 m	α_e	7.51	$\varphi(t,t_0)$	**2.00**	ε_{ca}	1.00 E-04		
y	1.25 m	e_{av}	0.783 m	E_s	205 GPa	ε_{cs}	2.51 E-04		
C	0.00313 /m	I	1.32 E+12 mm^4	E_{cm}	**27.3 GPa**				
θ	0.125 rad	P'	16.8 MN	ΔP	3.07 MN	ΔP	803 kN	ΔP	983 kN
	5.99%		**2.34%**		**17.89%**		**4.68%**		**5.73%**

P_0 = 17.2 MN Total estimated losses **36.6%** of P_0

Table 5-4: Estimated losses of initial prestress force, based on the creep compliance from figure 5-6 in conjunction with equation (3.10) and using BQ1 aggregate.

Table 5-5 shows the estimated losses of initial prestress force, based on the creep compliance from figure 5-6 in conjunction with equation (3.10) and using BQ2 aggregate. The total estimated losses are 36.2%, little less than the losses using the BQ1 aggregate. The elastic shortening is greater using concrete containing the BQ2 aggregate, but the creep shortening is less.

Friction		*Elastic shortening*		*Creep*		*Shrinkage*		*Relaxation at anchor*	
μ	0.19	A_p	1.56 E+04 mm²	u	1.03 E+04 mm	ε_{cd}	1.51 E-04		2.5
k	0.01 /m	A	2.45 E+06 mm²	h_0	477 mm	k_h	0.7057		
x	20.0 m	α_e	11.46	$\varphi(t,t_0)$	**1.21**	ε_{ca}	1.00 E-04		
y	1.25 m	e_{av}	0.783 m	E_s	205 GPa	ε_{cs}	2.51 E-04		
C	0.00313 /m	I	1.32 E+12 mm^4	E_{cm}	**17.9 GPa**				
θ	0.125 rad	P'	16.6 MN	ΔP	2.80 MN	ΔP	803 kN	ΔP	983 kN
	5.99%		**3.53%**		**16.32%**		**4.68%**		**5.73%**

P_0 = 17.2 MN Total estimated losses **36.2%** of P_0

Table 5-5: Estimated losses of initial prestress force, based on the creep compliance from figure 5-6 in conjunction with equation (3.10) and using BQ2 aggregate.

Note: The estimated losses of initial prestress force are based on creep coefficient after little over twelve years. Figure 5-6 shows that the concrete is still deforming and thus the prestress losses are expected to increase further, but concrete is known to deform for twenty to thirty years (see section 2.5).

6 Conclusions and Final Remarks

This chapter summarizes the main findings of the thesis and lists recommendations for further research, to answer questions that arose during the work on the thesis.

6.1 Main Findings

Within the limitations of the work here conducted, these are the main findings:

- The results indicate substantial discrepancies in measured E-modulus for concrete made from limestone aggregates, compared to estimates based on mean concrete cylinder strength according to EC2.
- The measured E-modulus from concrete with Icelandic aggregates, basalt 1-4 from phase I, fairly agrees with the EC2 values if the correction factors from INA, based on aggregate porosity, are applied. However, experimental results from phase II show that the E-modulus drops well below the EC2 values, using correction factors from INA, if the porosity is increased.
- If the values obtained from granite and limestone aggregates are ignored, a fairly good correlation can be seen between aggregate porosity and E-modulus of concrete.
- Concrete containing porous basalt aggregate shows greater creep than concrete with granite aggregate.
- The oldest creep specimens, referred to in the thesis, are still deforming after twelve years.
- The Eco-SCC mixes, containing less cement but higher water-binder ratio, shows greater creep than conventional SCC.
- Addition of air entraining admixture seems to have limited effect on the specific creep of Eco-SCC mixes.
- Higher cement content, while maintaining constant water-cement ratio, is likely to increase creep-strain.
- The concrete containing basalt aggregates appears to increase its rate of creep after few months.
- Findings indicate that concrete made of porous basalt aggregate exhibits greater creep than predicted by well accepted mathematical models.
- A case study, for a post tensioned highway bridge, shows a 10% increase in initial prestress force losses when using experimental results for concrete with porous aggregate, compared to values from Eurocode 2.
- A case study of a slab of concrete with porous aggregate, 200 mm thick and spanning 5.0 m, shows a 6.2 and 10.3% increase in deflection using experimental results for concrete with BQ1 and BQ2 aggregates, compared to values predicted by Eurocode 2.

Note: When the E-modulus is critical to the performance of a structure, tests on the E-modulus should be conducted. In practice a structural designer has little control over aggregate composition in the concrete, thus it is best to specify the E-modulus to be used for structures sensitive to variations.

6.2 Recommendations for Further Research

This section reflects on unanswered questions that arose during the work on the thesis and could be the subjects of further research.

- Flexural strength of concrete is important in deflection calculations. When determining distribution coefficient for uncracked and fully cracked conditions, the tensile strength, determined in accordance with EC2, is normally used. In case of concrete made of porous aggregate, tensile strength might be overestimated, since it is strongly dependant on the interfacial transition zone (see section 2.1). Possible discrepancies in tensile strength between predictions according to EC2, and experimental results would be an interesting research subject.
- The Icelandic National Annex to EC2 suggests two reduction factors for E-modulus, based on aggregate porosity, but gives no guidance for what porosity range the reduction factor should be used. This ambiguity is unfortunate and might serve as a central point in a practical research topic. Experimental results, based on porosity, could then be compared to the EC2 model to find a suitable conversion factors or models.
- Accuracy in mathematical models is essential and the discrepancies, such as those depicted in phase II, are excessive. It would be worthwhile to fit the experimental results to EC2 or fib MC 10 model. By using some least squares regression method it should be possible to find a parameter that minimizes the differences between models and test data.

Finally

The thesis ends, but creep goes on [21].

References

[1] "How Portland Cement is Made | Portland Cement Association (PCA)," *Portland Cement Association*, 2014. [Online]. Available: http://www.cement.org/basics/howmade.asp. [Accessed: 21-Jul-2014].

[2] Ari Trausti Guðmundsson and Flosi Ólafsson, *Steinuð hús - Varðveisla, viðgerðir, endurbætur og nýsteining*. Lyngási 7, 210 Garðabær: Húsafriðunarnefnd ríkisins, 2003.

[3] *ASTM C512 / C512M - 10 Standard Test Method for Creep of Concrete in Compression1*. West Conshohocken: ASTM.

[4] *EN 1991-2:2003: Actions on structures - Part 2: Traffic loads on bridges*. Brussels: CEN, 2003.

[5] W. H. Mosley, J. H. Bungey, and R. Hulse, *Reinforced Concrete Design: to Eurocode 2*, 6th edition. Houndmills, Basingstoke, Hampshire ; New York, N.Y: Palgrave Macmillan, 2007.

[6] "Hooke's law (physics)," *Encyclopedia Britannica*. [Online]. Available: http://www.britannica.com/EBchecked/topic/271336/Hookes-law. [Accessed: 21-May-2014].

[7] A. M. Neville and J. J. Brooks, *Concrete Technology*, Second Edition. England: Pearson Education Limited, 2010.

[8] "Young's modulus (physics)," *Encyclopedia Britannica*. [Online]. Available: http://www.britannica.com/EBchecked/topic/654186/Youngs-modulus. [Accessed: 21-May-2014].

[9] B. Paul, "Prediction of Elastic Constants of Multiphase Materials," *Trans. Metall. Soc. AIME*, vol. 218, pp. 36–41, 1960.

[10] P. Simeonov and S. Ahmad, "Effect of transition zone on the elastic behavior of cement-based composites," *Cem. Concr. Res.*, vol. 25, no. 1, pp. 165–176, Jan. 1995.

[11] J. Weiss, "Stress-Strain Behaviour of Concrete." [Online]. Available: http://www.theconcreteportal.com/cons_rel.html. [Accessed: 24-May-2014].

[12] "Byggingarreglugerð nr. 112/2012," *Mannvirkjastofnun*, 2012. [Online]. Available: http://www.mannvirkjastofnun.is/library/Skrar/Byggingarsvid/Byggingarreglugerd/Bygg.regluger%C3%B0_skj%C3%A1.pdf.

[13] P. Bamforth, D. Chisholm, J. Gibbs, and T. Harrison, "Properties of concrete for use in Eurocode 2," *The Concrete Centre*, Jan-2008.

[14] *EN 1992-1-1:2004: Eurocode 2: Design of concrete structures - Part 1-1: General rules and rules for buildings*. Brussels: CEN, 2004.

[15] Guðni Jónsson, "Formbreytingar í steinsteypu - fjaðurstuðull og skrið - (e. Deformations of Concrete - E-modulus and Creep)," The Icelandic Building Research Institute, Reykjavik, 93, Dec. 2006.

[16] *Icelandic National Annexes to Eurocodes*, 1st ed. Staðlaráð Íslands (e. Icelandic Council for Standardization), 2010.

[17] "Building Code Requirement for Structural Concrete and Commentary (ACI 318M-05)," 2004. [Online]. Available: http://netedu.xauat.edu.cn/jpkc/netedu/jpkc/hntjg/site/jxzy/wlkt/ACI318M-05%20%E7%BE%8E%E5%9B%BD%E8%A7%84%E8%8C%83%20Building%20Code%20Requirement%20For%20Structural%20Concrete.pdf.

[18] *fib Model Code 2010, Final draft, fib bulletin 66*, vol. 1, 2 vols. Switzerland: International Federation for Structural Concrete, 2012.

[19] S. H. Kosmatka, B. Kerkhoff, and W. C. Panarese, *Design and Control of Concrete Mixtures*, 14th edition. Portland Cement Association, 2003.
[20] I. E. Shkolnik, "Effect of nonlinear response of concrete on its elastic modulus and strength," *Cem. Concr. Compos.*, vol. 27, no. 7–8, pp. 747–757, Aug. 2005.
[21] A. M. Neville, W. H. Dilger, and J. J. Brooks, *Creep of plain and structural concrete*. London, New York: Construction Press, 1983.
[22] Z. P. Bažant, Y. Xi, and I. Carol, "New test Method to Separate Microcracking from Drying Creep: Curvature Creep at Equal Bending Moments and Various Axial Forces," in *The Fifth International RILEM Symposium*, Barcelona, Spain, 1993, pp. 77–82.
[23] G. E. Troxell, J. M. Raphael, and R. E. Davis, "Long-Time Creep and Shrinkage Tests of Plain and Reinforced Concrete," *Proc. ASTM 58*, pp. 1101–1120, 1958.
[24] A. M. Neville, *Properties of Concrete*, 5 th edition. Harlow, England ; New York: Trans-Atlantic Publications, Inc., 2012.
[25] T. C. Holland, *Silica Fume User's Manual*. Lovettsville, VA 22180: Silica Fume Association, 2005.
[26] K. H. Khayat, "Lecture on Concrete Technology at Innovation Center Iceland," 15-May-2014.
[27] M. Farah, F. Grondin, M. Matallah, A. Loukili, and J. Saliba, "Multi-scales Characterization of the Early-age Creep of Concrete," in *Mechanics and Physics of Creep, Shrinkage, and Durability of Concrete*, American Society of Civil Engineers, pp. 211–218.
[28] Z. P. Bažant, "Solidification theory for aging creep," *Civ. Environ. Eng. Northwest.*, 1988.
[29] J. Saliba, F. Grondin, M. Matallah, A. Loukili, and H. Boussa, "Relevance of a mesoscopic modeling for the coupling between creep and damage in concrete," *Mech. Time-Depend. Mater.*, vol. 17, no. 3, 2013.
[30] E. L. Sveinsdóttir and B. J. Wigum, "Aggregate production in Iceland," *Vegagerðin*.
[31] Guðni Jónsson, "Aggregates - Presentation in material science at Reykjavik University," Reykjavik University, 2011.
[32] U. Bolmstedt, "About rheology," *Instituto de Química*. [Online]. Available: http://www.iq.usp.br/mralcant/About_Rheo.html.
[33] H. A. Barnes, J. F. Hutton, and F. R. S. Walters, *An Introduction to Rheology*, Third impression. Amsterdam: Elesvier science publishers B.V., 1993.
[34] E. G. Nawy, *Concrete Construction Engineering Handbook*, Second Edition. Boca Raton, FL: Taylor & Francis Group, 2008.
[35] K.-K. Choi, S. L. Lissel, and M. M. R. Taha, "Rheological modelling of masonry creep," *Can. J. Civ. Eng.*, vol. 34, no. 11, pp. 1506–1517, 2007.
[36] "Structural Eurocodes - Institution of Civil Engineers," *Institution of Civil Engineers*. [Online]. Available: http://www.ice.org.uk/topics/structuresandbuildings/Eurocodes. [Accessed: 08-Aug-2014].
[37] *EN 1097-6:2000: Tests for mechanical and physical properties of aggregates - Part 6: Determination of particle density and water absorption*. Brussels: CEN, 2000.
[38] F. Mola and L. M. Pellegrini, "The New Model for Creep of Concrete in fib Model Code 2010," presented at the 37th Conference on Our World in Concrete & Structures, Singapore, 2012.
[39] "Model B3 for Predicting Concrete Creep and Shrinkage." [Online]. Available: https://mech.fsv.cvut.cz/homeworks/student/PPMA/ae.pdf.

[40] Z. P. Bažant and S. Baweja, “Creep and Shrinkage Prediction Model for Analysis and Design of Concrete Structures: Model B3,” presented at the Adam Neville Symposium: Creep and Shrinkage—Structural Design Effects, pp. 1–83.
[41] *ACI 209.2R-08: Guide for Modeling and Calculating Shrinkage and Creep in Hardened Concrete*. Farmington Hills, MI 48331: American Concrete Institute.
[42] *ACI 209R-92: Prediction of Creep, Shrinkage, and Temperature Effects in Concrete Structures*. Farmington Hills, MI 48331: American Concrete Institute.
[43] B. M. Das, *Fundamentals of Geotechnical Engineering*, 3rd ed. CL-Engineering.
[44] *EN 933-1:1997: Tests for geometrical properties of aggregates. Determination of particle size distribution. Sieving method*. Brussels: CEN, 1997.
[45] *EN 932-2:1999: Tests for general properties of aggregates. Methods for reducing laboratory samples*. Brussels: CEN, 1999.
[46] *EN 12350-2:2000: Testing fresh concrete. Slump test*. Brussels: CEN, 2000.
[47] “Concrete slump test - Wikipedia, the free encyclopedia,” *Wikipedia, the free encyclopedia*. [Online]. Available: http://en.wikipedia.org/wiki/Concrete_slump_test. [Accessed: 16-Nov-2013].
[48] P. Domone, “The Slump Flow Test for High-Workability Concrete,” *Cem. Concr. Res.*, vol. 28, no. 2, pp. 177–182, Feb. 1998.
[49] J. E. Wallevik, “Relationship between the Bingham parameters and slump,” *Cem. Concr. Res.*, vol. 36, no. 7, pp. 1214–1221, Jul. 2006.
[50] O. H. Wallevik and J. E. Wallevik, “Rheology as a tool in concrete science: The use of rheographs and workability boxes,” *Cem. Concr. Res.*, vol. 41, no. 12, pp. 1279–1288, Desember 2012.
[51] O. H. Wallevik and B. Hjartarson, “A novel field instrument to measure rheological properties of self-compacting concrete,” presented at the 3rd North America Conference on Self-Compacting Concrete, USA, 2008, p. 6.
[52] *EN 12350-7:2000: Testing fresh concrete. Air content. Pressure methods*. Brussels: CEN, 2000.
[53] *ISO 1920-10:2010: Testing of concrete — Part 10: Determination of static modulus of elasticity in compression*. Geneva: ISO, 2010.
[54] *EN 12390-3:2009: Testing hardened concrete - Part 3: Compressive strength of test specimens*. Brussels: CEN, 2009.
[55] *EN 206-1:2000: Concrete - Part 1: Specification, performance, production and conformity*. Brussels: CEN, 2000.
[56] A. Chowdhury, A. S. M. Z. Hasan, M. Z. Alam, and A. A. Masum, “Effect of Size on Compressive Strength of Concrete Cylinder Specimens using Sand and Sulfur Cap,” *Glob. J. Res. Eng. Civ. Struct. Eng.*, vol. 13, no. 8, 2013.
[57] C. M. Wang, “Timoshenko Beam-Bending Solutions in Terms of Euler-Bernoulli Solutions,” *J. Eng. Mech.*, vol. 121, no. 6, pp. 763–765, Jun. 1995.
[58] *EN 1990: 2002: Basis of structural design*. Brussels: CEN, 2002.
[59] *EN 1991-1:2002: Actions on structures*. Brussels: CEN, 2002.
[60] “Serviceability Limit States,” Mineral Products Association - The Concrete Centre, London, Informative.
[61] H. D. Hernandez and W. L. Gamble, “Time-dependent prestress losses in Pretensioned concrete construction,” University og Illinois, Illinois, Issued as a Documentation Report on The Field Investigation of Prestressed Reinforced Concrete Highway Bridges UILU-ENG-75-2005, May 1975.

[62] Hákon Ólafsson and Jón Baldvinsson, *Eiginleikar íslensk sements 2004*, vol. Sementseftirlit Rb. Reykjavik: Rannsóknastofnun byggingariðnaðarins, 2005.
[63] *EN 197-1:2000: Cement - Part 1: Composition, specifications and conformity criteria for common cements*. Brussels: CEN, 2000.
[64] K.-R. Wu, B. Chen, W. Yao, and D. Zhang, "Effect of coarse aggregate type on mechanical properties of high-performance concrete," *Cem. Concr. Res.*, vol. 31, no. 10, pp. 1421–1425, Oct. 2001.
[65] *Properties of Rock Materials*. Lausanne, Swiss: Ecole Polytechnique Fédérale de Lausanne, EPFL.
[66] W. Navidi, *Statistics for Engineers and Scientists*, Third Edition. New York: McGraw-Hill, 2011.
[67] G. Giaccio and R. Zerbino, "Failure Mechanism of Concrete: Combined Effects of Coarse Aggregates and Strength Level," *Adv. Cem. Based Mater.*, vol. 7, no. 2, pp. 41–48, Mar. 1998.
[68] Z. P. Bažant, *Mathematical Modeling of Creep and Shrinkage of Concrete*. Wiley-Interscience Publication.
[69] Z. P. Bažant, "Theory of Creep and Shrinkage in 'Concrete Structures: A ·Précis of Recent Developments," *Mech. Today*, vol. 2, pp. 1–93, 1975.
[70] J. Kováčik, "Correlation between Young's modulus and porosity in porous materials," *J. Mater. Sci. Lett.*, vol. 18, no. 13, pp. 1007–1010, Jul. 1999.
[71] B. V. Rangan and A. E. McMullen, "A rational approach to control of slab deflection," *ACI J.*, no. 75, pp. 256–62, 1978.
[72] Johann A. Hardarson, Thordur I. Kristjansson, and Olafur H. Wallevik, "Discrepancies in Measured and Modelled E-modulus due to Porous Aggregates. Some Experiences from tests on Icelandic Concrete," in *Proceedings of the XXII Nordic Concrete Research Symposium*, Reykjavik, Iceland, 2014, pp. 179–182.
[73] B. C. Jensen, *Teknisk Ståbi*, 21. udgave. Valby: Nyt Teknisk Forlag, 2011.
[74] *ACI E1-99: Education Bulletin - Aggregates for Concrete*. Farmington Hills, MI 48331: American Concrete Institute.

Appendix A

Discrepancies in Measured and Modelled E-modulus due to Porous Aggregates. Some Experiences from tests on Icelandic Concrete [72]

Johann A. Hardarson
B.Sc.
ICI Rheocenter, Reykjavik University & Innovation Center Iceland
Arleynir 2-8
IS-112 Reykjavik
E-mail: johann09@ru.is

Thordur I. Kristjansson
B.Sc., M.Sc.
ICI Rheocenter, Reykjavik University & Innovation Center Iceland
Arleynir 2-8
IS-112 Reykjavik
E-mail: thordur.k@nmi.is

Olafur H. Wallevik
Dr. Ing., Prof.
ICI Rheocenter, Reykjavik University & Innovation Center Iceland
Arleynir 2-8
IS-112 Reykjavik
E-mail: wallevik@ru.is

ABSTRACT

Six concrete mixes were made containing: granite, limestone and porous basalt aggregates. Compressive strength and E-modulus tests were carried out. The results show discrepancies in E-modulus compared to those obtained from models, especially when using limestone aggregate and reduction of E-modulus with increasing porosity.

Key words: Elastic Modulus of Concrete, Aggregate, Porous Aggregates, Saturated Surface Dry.

1. INTRODUCTION

Elastic modulus (E-modulus) describes a linear relationship between stress and strain i.e. where Hook's law applies ("Hooke's law (physics)," n.d.). Concrete however exhibits a non-linear relationship between stress and strain. To simplify calculations engineers attempt to define its E-modulus, using various models. The most common definition of E-modulus for concrete, used in this article, is known as the secant modulus (Neville & Brooks, 2010).

In practice, E-modulus of concrete is measured and empirical equations then fitted to the results. Eurocode 2 (EC2) presents a formula to calculate the E-modulus of concrete (E_{cm}) from the mean value of concrete cylinder compressive strength (f_{cm}), or from equation (1) (EN 1992-1-1, 2004),

$$E_{cm} = 22\left(\frac{f_{cm}}{10}\right)^{0.3}. \quad (1)$$

The research presented in this paper is intended to elucidate the effect of porosity in aggregates on the E-modulus of concrete. The difference in porosity will be quantitated by the moisture content (MC) of aggregates in saturated surface dry (SSD) condition.

2. MATERIALS AND METHODS

Six mixes were made using different combination of aggregates. The mass-ratio of fine aggregates (< 4.0 mm) was the same in all mixes, 47% of total aggregates. This made the accumulative particle size distribution fairly homogeneous, except maybe for the basalt mix no. 4 (see fig. 1). Abbreviations and aggregate composition can be seen below.

Granite: Norwegian granite aggregates.
Limestone: Dune sand and limestone aggregates from Abu Dhabi (United Arab Emirates).
Basalt no. 1: Basalt aggregates from Harðikambur, Icelandic inland quarry.
Basalt no. 2: Basalt from Björgun, Icelandic seabed quarry + sand from Rauðimelur.
Basalt no. 3: Basalt aggregates from Björgun, Icelandic seabed quarry.
Basalt no. 4: Basalt aggregates from Vatnsskarð, Icelandic inland quarry.

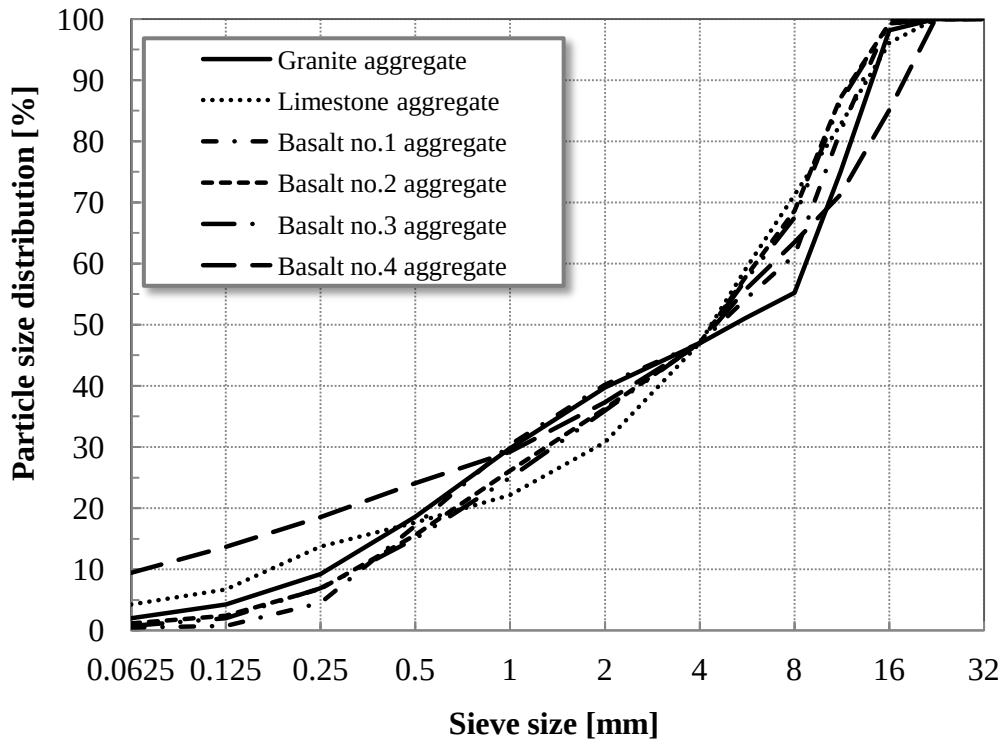

Figure 1 – Cumulative particle size distribution of mixes containing various aggregates.

Required mass content was calculated for the six mixes by maintaining a constant volume of 25 litres. Cement content in all the mixes was 315 kg/m^3 and water content 174 kg/m^3, maintaining a water-to-cement ratio of 0.55 and a paste volume of 27.7%. The amount of superplasticizer in each mix was arrived at with acceptable workability in mind. E-modulus tests were done according to the standard (ISO 1920-10, 2010). Additional info for mixes can be seen in table 1.

Table 1 – Various values, measured prior to casting

	SPC-25 [a] (kg/m^3)	Air (%)	Slump (mm)	G-yield (A)	H-plastic [b] (A·s)	SSD [c] (%)
Granite	1.0	4.1	215	0.68	1.87	0.3
Limestone	1.5	3.3	190	0.73	2.10	0.6
Basalt no. 1	1.0	4.3	235	0.64	1.50	1.7
Basalt no. 2	2.2	5.5	185	-	-	2.9
Basalt no. 3	2.0	4.2	185	-	-	3.0
Basalt no. 4	1.9	3.2	170	0.92	5.21	4.8

a . Omnicon SPC 25 (polycarboxylic ether)
b. Plastic viscosity
c. Weighted average MC in SSD condition

3. RESULTS AND DISCUSSION

Table 2 shows the results from both 7th and 28th day compressive strength as well as E-modulus. Calculated values, using equation from EC2, are based on 28th day compressive strength.

Table 2 – Measured values, after casting, and compared to calculated E-modulus

	7th day [c] Compressive st. (MPa)	7th day E-modulus (GPa)	28th day [d] Compressive st. (MPa)	28th day E-modulus (GPa)	E-modulus [e] from EC2 (GPa)
Granite	30.9	29.4	40.5	29.4	33.5
Limestone	31.4	35.9	41.7	39.4	33.8
Basalt no. 1	31.5	28.9	42.0	30.8	33.8
Basalt no. 2	37.9	27.9	47.0	28.3	35.0
Basalt no. 3	38.8	27.8	51.0	29.6	35.9
Basalt no. 4	41.8	19.2	54.6	22.3	36.6

d. Mean value of concrete cylinder compressive strength.
e. Value calculated according to equation (1) and without modification factor.

Article 3.1.3 in EC2 states that equation (1) is valid for quartzite aggregates, but the outcome should be reduced by 10% for limestone and increased by 20% for basalt (EN 1992-1-1, 2004). It is clear from table 2 that the EC2 model drastically underestimates the E-modulus with respect to limestone aggregates, especially if the reduction factor is used. There is a known discrepancy between EC2 values for E-modulus and measured results, using Icelandic aggregates. This is attributed to the prevailing porosity of Icelandic aggregates, MC in SSD condition from 3 to 8% (Jónsson, 2006). In fact the Icelandic National Annex (INA) to EC2 suggests a correction factors to multiply the values obtained from (1), 0.9 for non-porous

aggregates and 0.6 for porous aggregates (INA to EN 1992-1-1, 2010). The measured results, for basalt 1-4, fairly agrees with the EC2 model if the correction factors from INA are used.

Figure 2 shows the measured E-modulus plotted as a function of MC in SSD condition. If the values obtained from granite and limestone aggregates (values with low MC) are ignored, a fairly good linear correlation emerges between porosity and E-modulus.

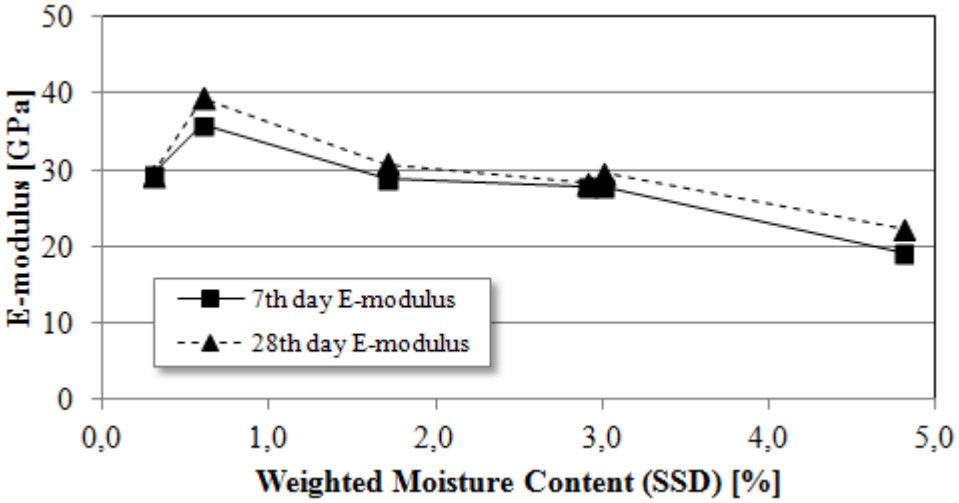

Figure 2 – E-modulus of concrete as a function of aggregate MC in SSD condition

4. CONCLUSIONS

The results indicate substantial discrepancies in measured E-modulus for concrete made from limestone aggregates, compared to estimates based on mean concrete cylinder strength according to EC2.

The measured results from concrete with Icelandic aggregates, basalt 1-4, fairly agrees with the EC2 values if the correction factors from INA, based on aggregate porosity, are applied.

If the values obtained from granite and limestone aggregates are ignored, a fairly good correlation can by seen between aggregate porosity and E-modulus of concrete.

REFERENCES

EN 1992-1-1:2004: Eurocode 2: Design of concrete structures - Part 1-1: General rules and rules for buildings. (2004). Brussels: CEN.

Hooke's law (physics). (n.d.). Encyclopedia Britannica. Retrieved May 21, 2014, from http://www.britannica.com/EBchecked/topic/271336/Hookes-law

Icelandic National Annexes to Eurocodes. (2010) (1st ed.). Staðlaráð Íslands (e. Icelandic Council for Standardization).

ISO 1920-10:2010 - Testing of concrete -- Part 10: Determination of static modulus of elasticity in compression. (2010). Geneva: ISO.

Jónsson, G. (2006). Formbreytingar í steinsteypu - fjaðurstuðull og skrið - (e. Deformations of Concrete - E-modulus and Creep) (No. 93). Reykjavik: The Icelandic Building Research Institute.
Neville, A. M., & Brooks, J. J. (2010). Concrete Technology (Second Edition.). England: Pearson Education Limited.

Appendix B

B.1. Obtaining the Final Value of Creep Coefficient According to EC2

This annex includes a worked example of obtaining the final value of creep coefficient according to annex B in EN 1992-1-1: 2004 or EC2.

Determine the final value of creep coefficient for a 200 mm thick slab that spans in one direction given the following parameters:

- Slab strip, 1.0 m wide and exposed to drying from above and below.
- The slab is exposed to inside conditions with relative humidity of 50%.
- The characteristic strength of the concrete is C30/37.
- The formwork is allowed to support the slab until the concrete has reached equivalent of 28 days strength development at 20°C, therefore the age at loading (t_0) is 28 days.
- The type of cement is Class N.

$$f_{cm} = f_{ck} + 8 = 30 + 8 = 38\ MPa\ ; \quad h_0 = \frac{2 \cdot A_c}{u} = \frac{2 \cdot 200\ mm \cdot w}{2 \cdot w} = 200\ mm$$

$$\alpha_1 = \left(\frac{35}{f_{cm}}\right)^{0.7} = 0.944\ ; \quad \alpha_2 = \left(\frac{35}{f_{cm}}\right)^{0.2} = 0.984\ ; \quad \alpha_3 = \left(\frac{35}{f_{cm}}\right)^{0.5} = 0.960$$

$$f_{cm} > 35\ MPa \Rightarrow \phi_{RH} = \left[1 + \frac{1 - RH/100}{0.1 \cdot \sqrt[3]{h_0}} \cdot \alpha_1\right] \cdot \alpha_2 = \left[1 + \frac{1 - 50/100}{0.1 \cdot \sqrt[3]{200}} \cdot 0.944\right] \cdot 0.984$$

$$= 1.78\ , \quad \beta(f_{cm}) = \frac{16.8}{\sqrt{f_{cm}}} = 2.73\ ; \ \beta(t_0) = \frac{1}{0.1 + {t_0}^{0.2}} = \frac{1}{0.1 + 28^{0.2}}$$

$$= 0.488\ , \quad \phi_0 = \phi_{RH} \cdot \beta(f_{cm}) \cdot \beta(t_0) = 1.78 \cdot 2.73 \cdot 0.488 = 2.37$$

$$\beta_c(\infty, t_0) = \lim_{t \to \infty}\left[\frac{t - t_0}{\beta_H + t - t_0}\right]^{0.3} = 1$$

$$\phi(\infty, t_0) = \phi_0 \cdot \beta_c(\infty, t_0) = \phi_0 = \underline{\underline{2.37}}$$

B.2. Derivation of Equation (2.20)

Since the creep coefficient is equal to the ratio of creep strain to elastic strain we have

$$\phi(t,t_0) = \frac{\varepsilon_{cc}}{\varepsilon_{cE}} => \varepsilon_{cc} = \phi(t,t_0) \cdot \varepsilon_{cE}$$

where ε_{cE} is the elastic strain, ε_{cc} is the creep strain and $\phi(t,t_0)$ the creep coefficient.

The total strain (ε_c) is the sum of elastic strain and creep strain, or

$$\varepsilon_c = \varepsilon_{cE} + \varepsilon_{cc}$$

The effective modulus of elasticity is the compressive stress (σ_c) divided by the total strain or

$$E_{c,eff} = \frac{\sigma_c}{\varepsilon_c} = \frac{\sigma_c}{\varepsilon_{cE} + \varepsilon_{cc}}$$

By substituting the first equation into the second, we get

$$E_{c,eff} = \frac{\sigma_c}{\varepsilon_{cE} + \varepsilon_{cc}} = \frac{\sigma_c}{\varepsilon_{cE} + \phi(t,t_0) \cdot \varepsilon_{cE}} = \frac{\sigma_c}{\varepsilon_{cE}\left(1 + \phi(t,t_0)\right)} = \frac{\sigma_c}{\varepsilon_{cE}} \frac{1}{\left(1 + \phi(t,t_0)\right)}$$

$$= \frac{E_{c(28)}}{\left(1 + \phi(t,t_0)\right)} = \underline{\underline{\frac{1.05\, E_{cm}}{\left(1 + \phi(t,t_0)\right)}}}$$

B.3. Derivation of Equation (3.3)

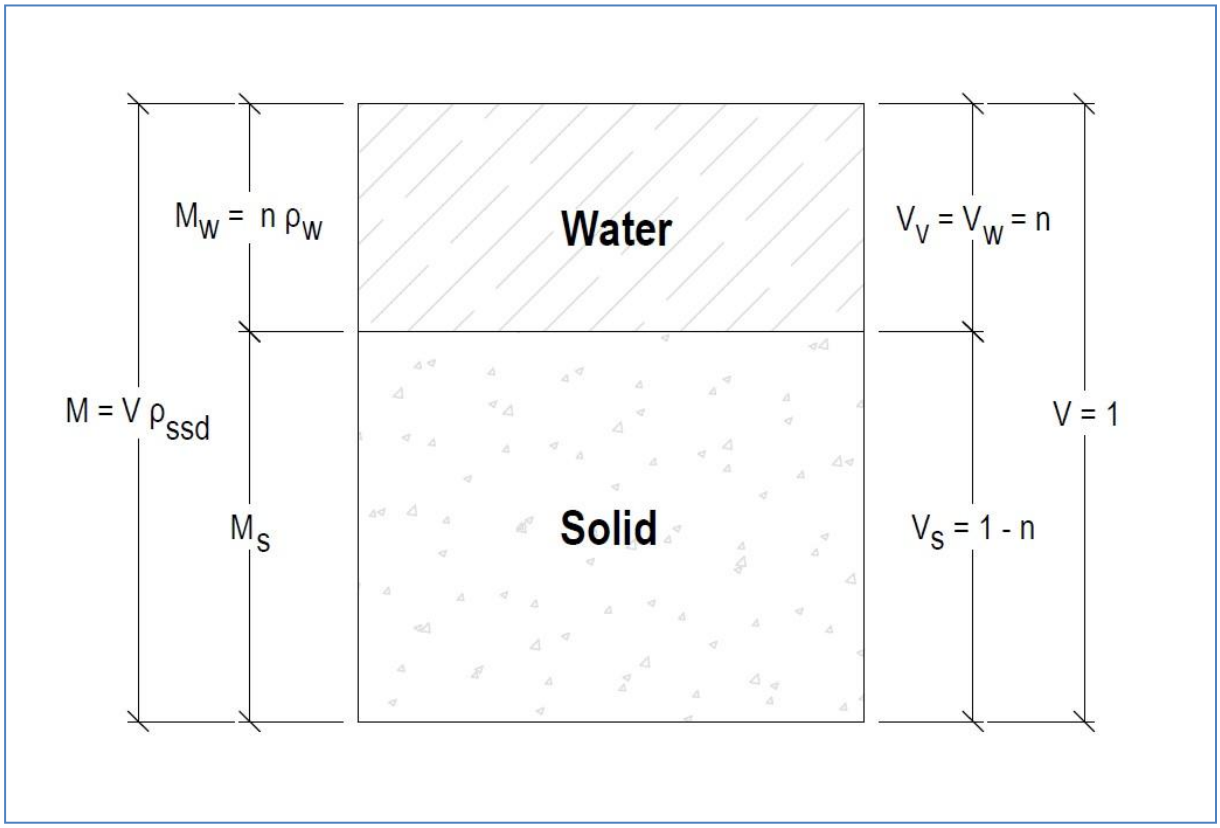

Figure B-1: Saturated aggregate element (SSD) with total volume equal to 1. Mass to the left and volume to the right.

Formal definition of porosity from geotechnical engineering

$$n = V_v/V$$

The moisture content of a saturated aggregate sample can be expressed as

$$w = M_w/M_s \Rightarrow M_w = w\,M_s$$

Since the element is saturated and by writing the voids as mass divided by density, porosity becomes

$$n = \frac{V_v}{V} = \frac{V_w}{V} = \frac{M_w/\rho_w}{(M_w + M_s)/\rho_{ssd}} = \frac{w\,M_s/\rho_w}{(w\,M_s + M_s)/\rho_{ssd}} = \frac{w\,M_s/\rho_w}{M_s(w+1)/\rho_{ssd}} = \frac{w/\rho_w}{(w+1)/\rho_{ssd}}$$

$$= \frac{w}{(1+w)}\frac{\rho_{ssd}}{\rho_w} = \underline{\underline{\frac{(WA_{24}/100\%)}{\left(1 + (WA_{24}/100\%)\right)}\frac{\rho_{ssd}}{\rho_w}}}$$

B.4. Derivation of K for Simply Supported Beam

The following is a derivation of K-constant for simply supported beam, based on equations from Teknisk Ståbi (see Figure B-2) and used in deflection calculations.

Curvature $(1/r)$ can be written so

$$1/r = \frac{M}{EI},$$

where M is the mending moment, E the elastic modulus and I the area moment of inertia. The maximum deflection at the centre is (see Figure B-2)

$$\delta = \frac{5}{384} \cdot \frac{ql^4}{EI} = \frac{5}{48} \cdot \left(\frac{1}{8} ql^2\right) \cdot \frac{1}{EI} \cdot l^2$$

The value in the bracket is the same as the maximum bending moment (see Figure B-2) or

$$\delta = \frac{5}{48} \cdot M \cdot \frac{1}{EI} \cdot l^2 = \frac{5}{48} \cdot {}^1\!/_r \cdot l^2 \Rightarrow \underline{\underline{K = \frac{5}{48} \approx 0.104}}$$

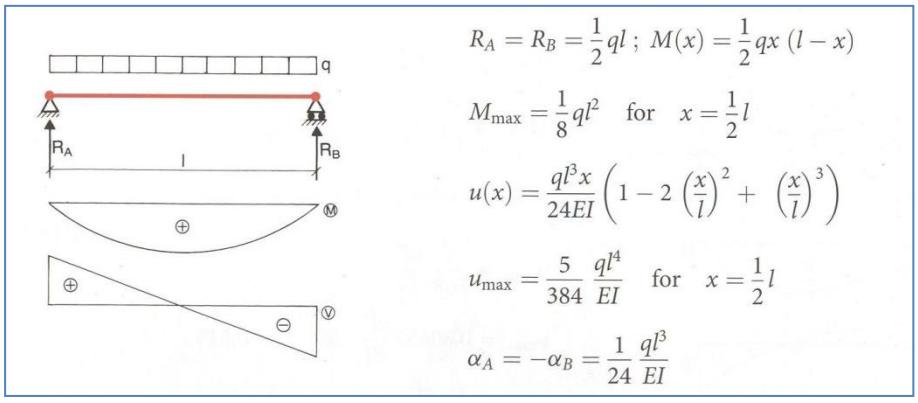

$$R_A = R_B = \frac{1}{2} ql \; ; \; M(x) = \frac{1}{2} qx\,(l - x)$$

$$M_{max} = \frac{1}{8} ql^2 \quad \text{for} \quad x = \frac{1}{2} l$$

$$u(x) = \frac{ql^3 x}{24EI} \left(1 - 2\left(\frac{x}{l}\right)^2 + \left(\frac{x}{l}\right)^3\right)$$

$$u_{max} = \frac{5}{384} \frac{ql^4}{EI} \quad \text{for} \quad x = \frac{1}{2} l$$

$$\alpha_A = -\alpha_B = \frac{1}{24} \frac{ql^3}{EI}$$

Figure B-2: Simply supported beam [73].

B.5. Area Moment of Inertia for Bridge Beam

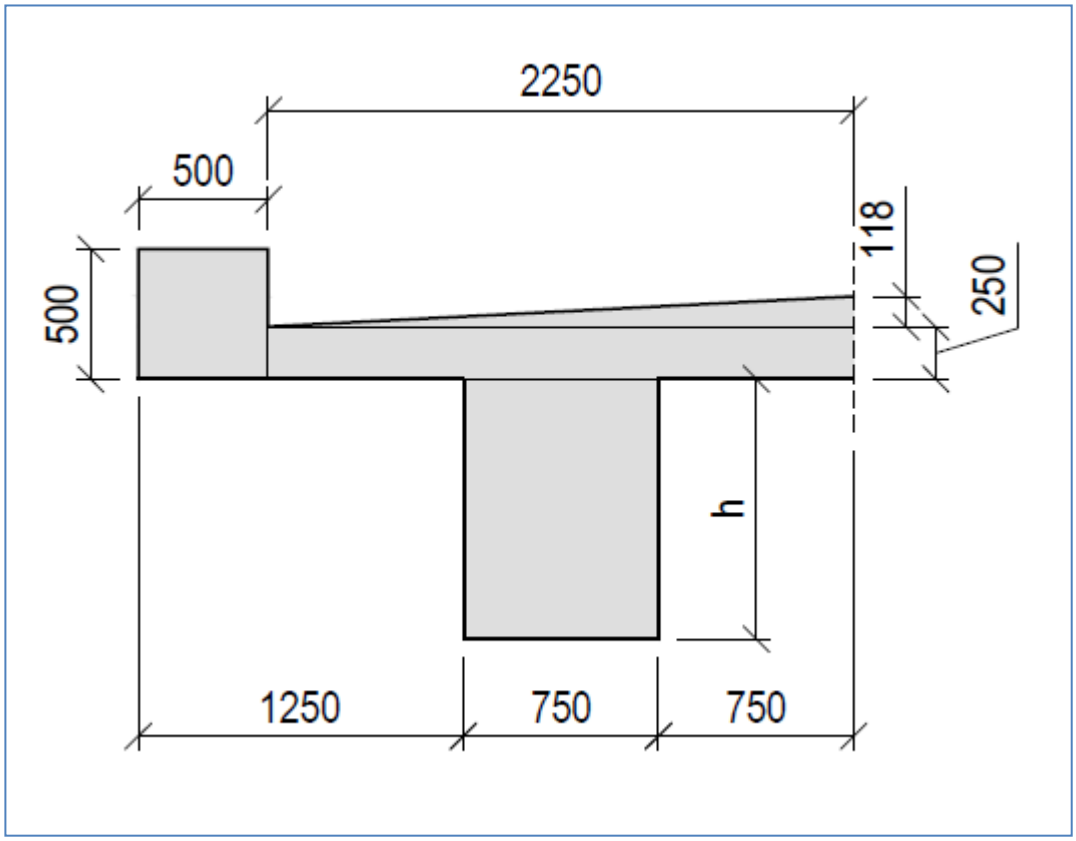

Figure B-3: Bridge Beam.

Area Moment of Inertia for Bridge Beam h = 2000 mm

	h	b	A	S	I_o	d	d^2	$I_{o,c}$
	[mm]	[mm]	[mm^2]	[mm^3]	[mm^4]	[mm]	[mm^2]	[mm^4]
Edge	500	500	250000	5.63E+08	5.21E+09	793	629555	1.63E+11
Slab	250	2250	562500	1.20E+09	2.93E+09	668	446819	2.54E+11
Slope	118	2250	132657	3.04E+08	1.02E+08	833	693474	9.21E+10
Beam	2000	750	1500000	1.50E+09	5.00E+11	457	208442	8.13E+11
			2445157	3.56E+09				**1.32E+12**

	[mm]		[mm^3]
$y_N=\Sigma S/\Sigma A$	1457	$W_N=I_{o,c}/y_N$	9.07E+08
$y_E=H-y_N$	1043	$W_E=I_{o,c}/y_E$	1.27E+09

Table B-1: Area Moment of Inertia for Bridge Beam.

Appendix C

C.1. MatLab Function that Calculates the Creep Coefficient According to EC2

```
function phi = EC2_CreepCo(f_ck,h_0,RH,Type,t_0_T,t)
%Syntax: phi = EC2_CreepCo(f_ck,h_0,RH,Type,t_0_T,t);
%
% This is a program that calculates the creep coefficient according to
% annex B in EN 1992-1-1: 2004 or EC2.
%
% Example of usage
% phi = EC2_CreepCo(30,200,50,'N',28,'inf')
% Calculates the creep coefficient with the following parameters:
% f_ck = 30 MPa; h_0 = 200 mm; RH = 50%; Type 'N'; t_0 = 28 days; t ='inf'
%
% Input
%   f_ck: Characteristic cylinder strength of concrete at 28 days in MPa
%   h_0:  Notional size of the member in mm
%   RH:   Relative humidity of the ambient environment in %
%   Type: Cement type: 'S' (slow); 'N' (normal); 'R' (rapid)
%   t_0:  The age of concrete at the time of loading in days
%   t:    Time being considered in days or 'inf' for infinite
%
% Output
%   phi:  Creep coefficient according to EC2

% Creep Coefficient According to EC2
% Date: 18th of November 2014
% Programmed by : Jóhann Albert Harðarson

% f_cm is the mean compressive strength af concrete in MPa at the age of 28
% days [Table 3.1]:
f_cm = f_ck + 8;

% α1/ α2/ α3 are coefficients to consider the influence of the concrete
% strength [B.8c]:
alpha_1 = (35/f_cm)^0.7;
alpha_2 = (35/f_cm)^0.2;
alpha_3 = (35/f_cm)^0.5;

% t_0_T takes into account the type of cement used by modifying the age of
% loading t_0 [B.9]
if     Type == 'S'
    alpha = -1;
elseif Type == 'N'
    alpha = 0;
elseif Type == 'R'
    alpha = 1;
else
    error('Unknown cement type')
end
t_0 = t_0_T * (9 / (2 + t_0_T^1.2) + 1)^alpha;

% ϕ_RH is a factor to allow for the effect of relative humidity on the
```

```
% notional creep coefficient [B.3a] & [B.3b]:
if f_cm <= 35
    phi_RH = 1 + (1 - RH/100) / (0.1*(h_0)^(1/3));
else
    phi_RH = (1 + (1 - RH/100) / (0.1*(h_0)^(1/3)) * alpha_1) * alpha_2;
end

% β(f_cm) is a factor for the effect of concrete strength on the notional
% creep coefficient (ϕ_0) [B.4]:
beta_f_cm = 16.8 / sqrt(f_cm);

% β(t_0) is a factor for the effect of concrete age at loading on the
% notional creep coefficient (ϕ_0) [B.5]:
beta_t_0 = 1/(0.1 + t_0^0.20);

% ϕ_0 is Notional creep coefficient [B.2]:
phi_0 = phi_RH * beta_f_cm * beta_t_0;

% β_H is a coefficient depending on the relative humidity (RH in %) and the
% notional member size (h_0 in mm) [B.8a] & [B.8b]:
if f_cm <= 35
    beta_H = 1.5 * (1 + (0.012 * RH)^18) * h_0 + 250;
    if beta_H > 1500
        beta_H = 1500;
    end
else
    beta_H = 1.5 * (1 + (0.012 * RH)^18) * h_0 + 250 * alpha_3;
    if beta_H > (1500 * alpha_3)
        beta_H = 1500 * alpha_3;
    end
end

% β_c(t,t_0) is a coefficient to describe the development of creep with
% time after loading [B.7]:
if t == 'inf'
    beta_c = 1;
else
    beta_c = ((t - t_0) / (beta_H + t - t_0))^(0.3);
end

% ϕ(t,t_0 ) is the creep coefficient, defining creep between times t and
% t_0, related to elastic deformation at 28 days [B.1]
phi = phi_0 * beta_c;
```

Published with MATLAB® R2013a

C.2. MatLab Function that Calculates the Creep Coefficient According to fib MC 10

```
function phi = fib_CreepCo(f_ck,h,RH,Type,t_0_T,t)
%Syntax: phi = fib_CreepCo(f_ck,h,RH,Type,t_0_T,t);
%
% This is a program that calculates the creep coefficient according to
% paragraph 5.1.9.4.3 in fib Model Code 2010, Final draft, fib bulletin 66.
%
% Example of usage
% phi = fib_CreepCo(30,200,50,'N',28,365)
% Calculates the creep coefficient with the following parameters:
% f_ck = 30 MPa; h = 200 mm; RH = 50%; Type 'N'; t_0 = 28 d; t = 365 d
%
% Input
%   f_ck: Characteristic cylinder strength of concrete at 28 days in MPa
%   h:    Notional size of the member in mm
%   RH:   Relative humidity of the ambient environment in %
%   Type: Cement type: 'S' (slow); 'N' (normal); 'R' (rapid)
%   t_0:  The age of concrete at the time of loading in days
%   t:    Time being considered in days
%
% Output
%   phi:  Creep coefficient according to fib Model Code 2010

% Creep Coefficient According to fib Model Code 2010
% Date: 8th of Desember 2014
% Programmed by : Jóhann Albert Harðarson

% f_cm is the mean compressive strength af concrete in MPa at the age of 28
% days according to eq. 5.1-1:
f_cm = f_ck + 8;

% t_0_T takes into account the type of cement used by modifying the age of
% loading t_0 (5.1-73)
if     Type == 'S'
    alpha = -1;
elseif Type == 'N'
    alpha = 0;
elseif Type == 'R'
    alpha = 1;
else
    error('Unknown cement type')
end
t_0_adj = t_0_T * (9 / (2 + t_0_T^1.2) + 1)^alpha;

% The basic creep coefficient % (5.1-64)
beta_bc_1 = 1.8 / (f_cm)^0.7;                                  % (5.1-65)
beta_bc_2 = log( (30 / t_0_adj + 0.035)^2 * (t - t_0_T) + 1); % (5.1-66)
phi_bc = beta_bc_1 * beta_bc_2;                                % (5.1-64)

% The drying creep coefficient % (5.1-67)
beta_dc_1 = 412 / (f_cm)^1.4;                                  % (5.1-68)
beta_RH = (1-RH/100) / (0.1*h/100)^(1/3);                      % (5.1-69)
beta_dc_2 = 1 / (0.1 + (t_0_adj)^0.2);                         % (5.1-70)
```

```
gamma = 1 / (2.3 + 3.5 / sqrt(t_0_adj));                    % (5.1-71b)
alpha_fcm = (35/f_cm)^0.5;                                  % (5.1-71d)
if 1.5 * h + 250 * alpha_fcm <= 1500 * alpha_fcm            % (5.1-71c)
    beta_h = 1.5 * h + 250 * alpha_fcm;
else
    beta_h = 1500 * alpha_fcm;
end
beta_dc_3 = ( (t - t_0_T) / (beta_h + (t - t_0_T)) )^gamma;  % (5.1-71a)
phi_dc = beta_dc_1 * beta_RH * beta_dc_2 * beta_dc_3;       % (5.1-67)

% The total creep coefficient % (5.1-63)
phi = phi_bc + phi_dc;                                      % (5.1-63)
```

Published with MATLAB® R2013a

C.3. MatLab Function that Calculates the Creep Comp. According to Model B3

```
function J = B3_CreepCompliance(f_bar,w,c,a_c,t_0,t_d,t,v_s,h,k_s,Type)
%Syntax: J = B3_CreepCompliance(f_bar,w,c,a_c,t_0,t_d,t,v_s,h,k_s,Type);
%
% This is a program that calculates the creep compliance (note: not the
% creep coefficient) according to model B3 and curing at 100% RH.
%
% Input
%   f_bar: Mean value of 28th day cylinder compressive strength in MPa
%   w:     Water content of concrete (kg/m^3)
%   c:     Cement content of concrete (kg/m^3)
%   a_c:   Aggregate-cement ratio, by weight
%   t_0:   Age at loading, in days
%   t_d:   Age when drying begins, in days (only t_d < t_0 is considered)
%   t:     Time being considered in days
%   v_s:   Volume-to-surface ratio in inches
%   h:     Relative humidity of the environment (expressed as a decimal
%          number, not as percentage) 0 < h < 1;
%   k_s:   Cross-section shape factor
%               1.00 for an infinite slab
%               1.15 for an infinite cylinder
%               1.25 for an infinite square prism
%               1.30 for a sphere
%               1.55 for a cube
%   Type:  Cement type: I, II or III
%
% Output
%   J:  Creep compliance according to model B3 in 10E-6/MPa,

% Creep compliance according to model B3
% Date: 12th of Desember 2014
% Programmed by : Jóhann Albert Harðarson

E_28 = 4734 * sqrt(f_bar); % E-modulus at 28 days
w_c = w / c; % Water-cement ratio

%  Alpha_1 Coefficient Taking into Account the Type of Cement.
if     Type == 'I'
    alpha_1 = 1;
elseif Type == 'II'
    alpha_1 = 0.85;
elseif Type == 'III'
    alpha_1 = 1.1;
else
    error('Unknown cement type')
end

% Shrinkage Parameter used for Evaluation of Drying Creep
epsilon = -alpha_1 * 1.0 * (1.9E-2 * w^2.1 * f_bar^(-0.28) + 270);

% Various Parameters
q1 = 0.6E6 / E_28;
q2 = 185.4 * sqrt(c) * f_bar^(-0.9);
```

```
q3 = 0.29 * (w_c)^4 * q2;
q4 = 20.3 * (a_c)^(-0.7);
q5 = 7.57E5 * f_bar^(-1) * (abs(epsilon))^(-0.6);

% Size Dependence
k_t = 8.5 * t_d^(-0.08) * f_bar^(-1/4);
D = 2 * v_s;
tau = k_t * (k_s * D)^2;

% Time Dependence
t_max = max(t_0,t_d);
S = tanh( sqrt( (t - t_d)/tau ) );
S_max = tanh( sqrt( (t_max - t_d)/tau ) );

% Additional Creep Due to Drying (Drying Creep)
H = 1 - (1 - h) * S;
H_max = 1 - (1 - h) * S_max;
C_d = q5 * (exp(-8 * H) - exp(-8 * H_max))^0.5;

% Basic Creep (Material Constitutive Property)
C_0 = q2 * Q(t,t_0) + q3 * log(1 + (t - t_0)^0.1) +q4 * log(t / t_0);

% Creep Compliance
J = q1 + C_0 + C_d;
```

Published with MATLAB® R2013a

C.4. MatLab Function, Approximating the Value for $Q(t,t_0)$, Needed for Model B3

```
function Result = Q(t,t_0)
%Syntax: Result = Q(t,t_0);
%
% This is a program that calulates an approximate value for Q(t,t_0) for
% model B3
%
% Input
%   t:    Time being considered in days
%   t_0:  The age of concrete at the time of loading in days
%
% Output
%   Result:  Approximate value for Q(t,t_0)

% Approximate value for Q(t,t_0)
% Date: 12th of Desember 2014
% Programmed by : Jóhann Albert Harðarson

n = 0.1; % Empirical parameter
m = 0.5; % Empirical parameter

% Equations 1.36
r = 1.7 * t_0^0.12 + 8;
Z = t_0^(-m) * log(1 + (t - t_0)^n);
Q_f = (0.086 * t_0^(2/9) + 1.21 * t_0^(4/9))^(-1);

Result = Q_f * (1 + (Q_f / Z)^r)^(-1/r);
```

Published with MATLAB® R2013a

C.5. MatLab Function that Calculates the Creep Coefficient According to ACI 209

```
function phi = ACI_CreepCo(t_0,h,V_S,s,psi,alpha,t)
%Syntax: phi = ACI_CreepCo(t_0,h,V_S,s,psi,alpha,t);
%
% This is a program that calculates the creep coefficient according to
% annex A.1 in ACI 209.2R-08: Guide for Modeling and Calculating Shrinkage
% and Creep in Hardened Concrete. The function-model is based on moist
% curing and relative humidity higher than 40%.
%
% Input
%   t_0:   The age of concrete at the time of loading in days
%   h:     Relative humidity expressed as a decimal
%   V_S:   Volume-surface ratio in mm
%   s:     Slump in mm
%   psi:   Ratio of fine aggregate to total aggregate by mass expressed as %
%   alpha: Air content expressed as percentage
%   t:     Time being considered in days
%
% Output
%   phi:  Creep coefficient according to ACI 209

% Creep Coefficient According to ACI 209
% Date: 15th of Desember 2014
% Programmed by : Jóhann Albert Harðarson

% Constants for a member shape and size
d = 10; P = 0.6;

% Ultimate creep coefficient (A-19)
phi_u = 2.35;

% Age of loading factor (A-22)
gamma_t0 = 1.25 * t_0^(-0.118);

% Ambient relative humidity factor (A-24)
if h < 0.4 || h > 1.0
    error('The value of relative humidity is not valid')
end
gamma_RH = 1.27 - 0.67 * h;

% Size of the member factor, in terms of the volume-surface ratio (A-25)
gamma_VS = 2 / 3 * (1 + 1.13 * exp(-0.0213 * V_S));

% Slump (composition) factor (A-28)
gamma_s = 0.82 + 0.00264 * s;

% Fine aggregate factor (A-29)
if psi < 1.0 || psi > 100
    error('The value of fine aggregate factor is not valid')
end
gamma_psi = 0.88 + 0.0024 * psi;

% Air content factor (A-30)
```

```
if alpha < 1.0 || alpha > 100
    error('The value of air content factor is not valid')
end
if 0.46 + 0.09 * alpha < 1
    gamma_alpha = 1;
else
    gamma_alpha = 0.46 + 0.09 * alpha;
end

% Correction factor (A-21)
gamma = gamma_t0 * gamma_RH * gamma_VS * gamma_s * gamma_psi * gamma_alpha;

% Creep coefficient according to ACI 209 (A-18)
phi = (t - t_0)^P / (d + (t - t_0)^P) * phi_u * gamma;
```

Published with MATLAB® R2013a

Appendix D

This appendix tabulates the parameters used in creep models. Some material parameters have been lost. In the case of missing material parameter, tables will indicate a dash symbol (-) and either default value selected or true value approximated. Creep specimens are listed in the same order as in Table 4-4 to Table 4-7.

D.1. Parameters used in the EC2 creep model

The design value for the CVC from 2004 was C40 and in the absent of correct value it will be used for f_{ck}.

	Aggregate Quarry	$f_{ck} = f_{cm} - 8$ *(MPa)*	h_0 *(mm)*	*RH (%)*	*Cement type*	t_0 *(Days)*
CVC_2 2002	BQ1	51.33	75.04	50	R	28
	BQ2	54.40	75.13			
	BQ3	48.35	76.38			
CVC_3 2002	BQ1	69.50	75.98	50	R	28
	BQ2	62.40	74.75			
	BQ3	68.00	74.80			
CVC_4 2002	BQ1	68.90	75.01	50	R	28
	BQ2	65.50	74.74			
	BQ3	83.40	76.54			
CVC_0 2004	GQ	-	74.50	50	R	28
	GQ	-	75.00			
	BQ1	-	76.50			
CVC_1 2009	BQ1	26.10	75.00	50	R	28
	BQ2	30.37	75.13			
	GQ	28.04	75.00			
SCC 2010	GQ	49.60	75.00	50	R	33
	GQ	50.00	75.00			
	GQ	40.40	75.50			

Table D-1: Parameters used in the EC2 creep model.

D.2. Parameters used in the fib MC 10 creep model

The design value for the CVC from 2004 was C40 and in the absence of correct value it will be used for f_{ck}.

	Aggregate Quarry	$f_{ck} = f_{cm} - 8$ *(MPa)*	*h (mm)*	*RH (%)*	*Cement type*	t_0 *(Days)*
CVC_2 2002	BQ1	51.33	75.04	50	R	28
	BQ2	54.40	75.13			
	BQ3	48.35	76.38			
CVC_3 2002	BQ1	69.50	75.98	50	R	28
	BQ2	62.40	74.75			
	BQ3	68.00	74.80			
CVC_4 2002	BQ1	68.90	75.01	50	R	28
	BQ2	65.50	74.74			
	BQ3	83.40	76.54			
CVC_0 2004	GQ	-	74.50	50	R	28
	GQ	-	75.00			
	BQ1	-	76.50			
CVC_1 2009	BQ1	26.10	75.00	50	R	28
	BQ2	30.37	75.13			
	GQ	28.04	75.00			
SCC 2010	GQ	49.60	75.00	50	R	33
	GQ	50.00	75.00			
	GQ	40.40	75.50			

Table D-2: Parameters used in the fib MC 10 creep model.

D.3. Parameters used in the B3 creep model

The design value for the CVC from 2004 was C40 and in the absence of correct value 48 MPa will be used for f_{cm}. Type I cement was thought to best represent the cement used in the mixes.

	Aggreg. Quarry	f_{cm} *(MPa)*	w *(kg/m^3)*	c *(kg/m^3)*	a/c *(-)*	t_0 *(Days)*	t_d *(Days)*	V/S *(in)*	h *(-)*	k_s *(-)*	*Cem. type*
CVC_2 2002	BQ1	59.33	164.52	440.00	3.66	28	28	1.48	0.5	1.15	I
	BQ2	62.40	168.67	452.00	3.35			1.48			
	BQ3	56.35	169.06	454.00	3.73			1.50			
CVC_3 2002	BQ1	77.50	159.64	512.00	3.28	28	28	1.50	0.5	1.15	I
	BQ2	70.40	157.77	505.00	3.00			1.47			
	BQ3	76.00	158.98	513.00	3.34			1.47			
CVC_4 2002	BQ1	76.90	159.88	549.00	3.13	28	28	1.48	0.5	1.15	I
	BQ2	73.50	156.31	539.00	2.83			1.47			
	BQ3	91.40	162.13	555.00	3.15			1.51			
CVC_0 2004	GQ	-	167.20	440.00	3.67	28	28	1.47	0.5	1.15	I
	GQ	-	138.10	360.00	5.04			1.48			
	BQ1	-	141.61	359.00	5.22			1.51			
CVC_1 2009	BQ1	34.10	176.49	321.00	5.56	28	28	1.48	0.5	1.15	I
	BQ2	38.37	161.36	317.00	5.39			1.48			
	GQ	36.04	176.71	322.00	5.57			1.48			
SCC 2010	GQ	57.60	186.66	549.00	2.64	33	33	1.48	0.5	1.15	I
	GQ	58.00	192.76	316.00	5.81			1.48			
	GQ	48.40	183.28	316.00	5.53			1.49			

Table D-3: Parameters used in the B3 creep model.

D.4. Parameters used in the ACI 209 creep model

According to ACI, fine aggregate or sand is that portion of an aggregate passing through the 4.75 mm (No. 4) sieve [74]. The exact percentage of fine aggregate are unknown and the values are based on best estimation.

	Aggregate Quarry	t_0 *(Days)*	*h (-)*	*V/S (mm)*	*s (mm)*	ψ *(%)*	α *(%)*
CVC_2 2002	BQ1	28	0.5	37.52	210	48	7.1
	BQ2			37.56	130	48	8.0
	BQ3			38.19	190	48	6.0
CVC_3 2002	BQ1	28	0.5	37.99	80	50	4.7
	BQ2			37.38	100	50	6.2
	BQ3			37.40	90	48	4.7
CVC_4 2002	BQ1	28	0.5	37.50	60	50	4.0
	BQ2			37.37	170	50	6.6
	BQ3			38.27	160	50	3.8
CVC_0 2004	GQ	28	0.5	37.25	190	50	8.4
	GQ			37.50	140	50	5.3
	BQ1			38.25	30	52	3.5
CVC_1 2009	BQ1	28	0.5	37.50	110	50	5.6
	BQ2			37.56	130	48	5.5
	GQ			37.50	150	48	4.9
SCC 2010	GQ	33	0.5	37.50	> 260	60	7.2
	GQ			37.50	> 260	62	1.3
	GQ			37.75	> 260	62	5.7

Table D-4: Parameters used in the ACI 209 creep model.

Appendix E

E.1. Calibration of Strain Gauge

Rannsóknastofnun byggingariðnaðarins
Keldnaholti, 112 Reykjavík - Sími 91-676000 - Fax 91-678811

Rannsókn nr. V-360
Dags. 1994.12.12
Framkv. af KI

Kalibrering

Fyrir:
Rb
Vegna:
Demac No. 2933 - Lengdarbreytingamælir

Aflestur á mælir	Lengd mm	*) mm
0	0,00	0,00
5	0,78	0,78
10	1,60	1,56
15	2,37	2,34
20	3,13	3,12
25	3,90	3,90

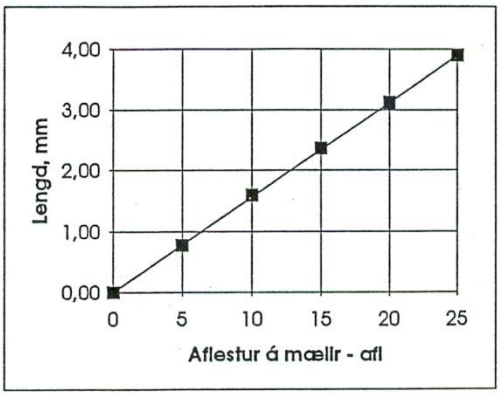

*)
Lengd = 0,156*Aflestur á mælir

minnsta eining á mælir = 0,00156 mm

Lengd á milli mælipúnktar L.o = 200 mm

Dæmi: Lengdarbreyting á milli 2 aflestur -	1. aflestur	14,32
	2. aflestur	11,35
	Mismun	2,97
	2,97*0,156 =	0,4633 mm
Lengdarbreyting í o/oo	0,4633/200*1000 =	**2,317 o/oo**
eða	2,97 * 0,78	**2,317 o/oo**

1994.12.12 - Sheet2/ki

bls. 1

E.2. Construction details for post tensioned bridge

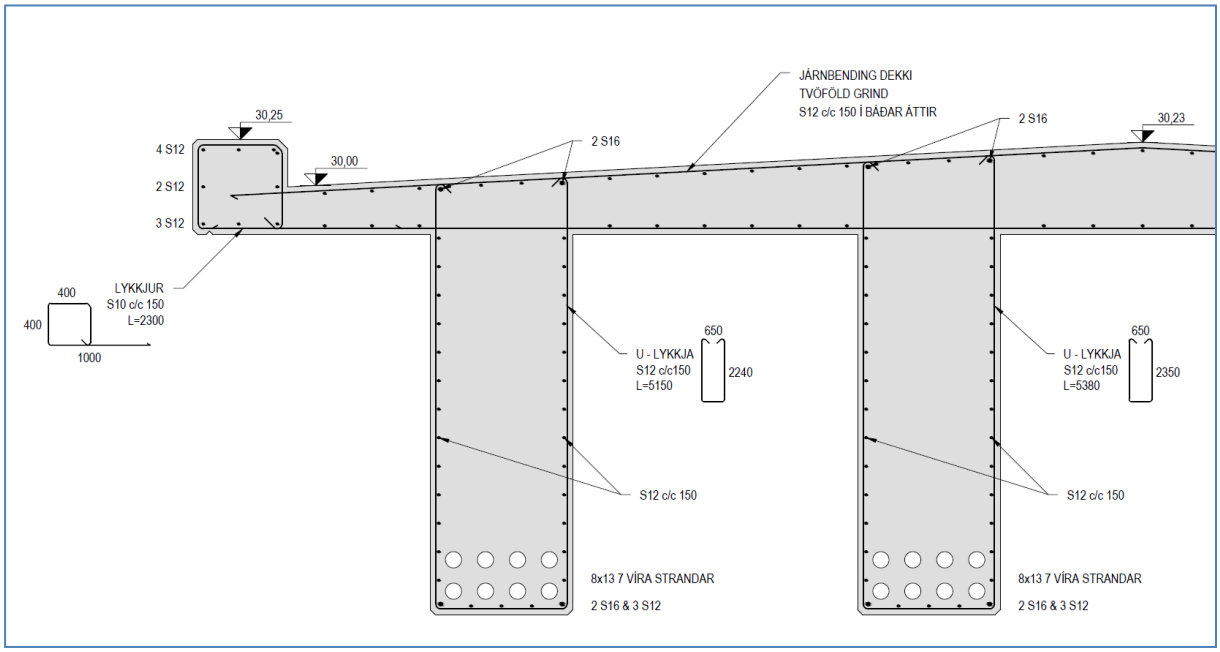

Figure E-1: Construction details at mid-span for post tensioned bridge.

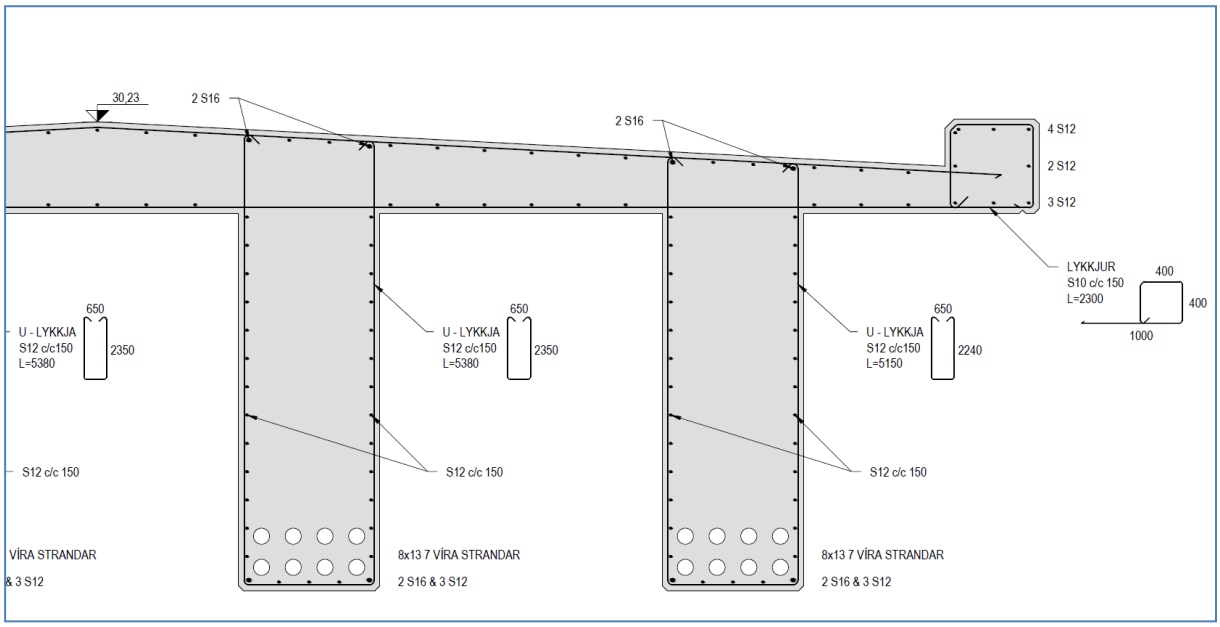

Figure E-2: Construction details at mid-span for post tensioned bridge.